Investigation of a Novel Hydrogel Anion Exchange Material for the Capture and Purification of Baculovirus

by

Jian Xiong

A thesis

presented to the University of Waterloo

in fulfillment of the

thesis requirement for the degree of

Master of Applied Science

in

Chemical Engineering

Waterloo, Ontario, Canada, 2014

AUTHOR'S DECLARATION

I hereby declare that I am the sole author of this thesis. This is a true copy of the thesis, including any required final revisions, as accepted by my examiners.

I understand that my thesis may be made electronically available to the public.

Abstract

Baculoviruses are versatile viruses that can be used as biopestisides, or for the production of recombinant protein and vaccines. Baculoviruses have also been found to be able to transfer genes to mammalian cells. This finding opened the door for the application of baculovirus vectors in human gene therapy. However, the mass production of clinical grade baculovirus vectors is challenging. Downstream processing has now become the bottle-neck of the manufacturing process.

In this work, an anion exchange chromatography-based process was investigated for the purification of recombinant baculovirus vectors using a novel hydrogel based membrane (Natrix Separations Ltd.). Crude recombinant baculovirus supernatant from infected insect cell cultures was first subjected to a clarification process consisting of centrifugation and filtration. The pH of the viral solution was adjusted and then passed through a fast protein liquid chromatography system consisting of the ion exchange membrane. After washing weakly bound impurities, the captured baculoviruses are recovered by an elution step. Overall, baculoviruses strongly associated with the membrane; however, this interaction which was much physical as it was chemical, could not be entirely reversed and baculovirus was lost in the process. Product purity has also been evaluated and up to 85 % of total protein reduction was determined. The significant losses of baculovirus observed have indicated major limitations in using this membrane for the purification of baculovirus.

Acknowledgements

I would express my sincere gratitude to my supervisor, Prof. Marc Aucoin, for providing me the opportunity to conduct interesting master research. I deeply acknowledge his guidance, training, and support throughout my master's career.

I would thank Prof. Xianshe Feng and Prof. Christine Moresoli for being my thesis readers. Their advices greatly broaden my scope towards this research topic.

Special thanks to Prof. Maud Gorbet, for providing access to her lab for flow cytometry experiments.

I would thank past and present group members in the Aucoin's lab: Joon, Shahab, Cameron, Steve, Eric, Stan, Andreas, Nada, Bhavik, Valerie, Jann, Sandi, Altamash, Megan, Valya, Steffen, and Simon. My master's study in the Aucoin group is one of the most memorable experiences in my life.

I wouldn't be able to start my master study in Canada without my parents' unconditional love and support.

Finally, special appreciation to Boya Zhang, for your love and confidence in me, for making my everyday special.

Dedication

献给我的家人

To My Family

Table of Contents

Chapter 1 Introduction 1

1.1 Hypotheses 2

1.2 Objectives 2

1.3 Thesis organization 3

Chapter 2 Literature Review 4

2.1 Recombinant baculovirus (rBV) 4

2.2 Baculovirus purification 5

2.2.1 Challenges and requirements 5

2.2.2 Ultracentrifugation 6

2.2.3 Chromatography process 6

Chapter 3 Materials and Methods 16

3.1 Fast protein liquid chromatography 16

3.2 Reverse-flow operation 18

3.3 Production of baculovirus 19

3.4 Buffer preparation 19

3.5 Virus stock treatment 20

3.6 Dilution factor 20

3.7 Anion exchange membrane 21

3.8 Virus quantitation 21

3.8.1 Flow cytometry 21

3.8.2 Real time quantitative polymerase chain reaction (RT-qPCR) 23

3.9 Virus breakthrough and recovery 24

3.10 Protein analysis 24

3.10.1 Micro BCA assay 24

3.10.2 SDS-PAGE and silver staining 25
3.10.3 Western blotting 27
3.11 Statistical analysis 29
3.12 Experimental conditions summary 30
Chapter 4 Purification of Baculovirus Through Linear Gradient Elution Using a Novel Strong Anion (Q) Exchange Membrane 31
4.1 Overview 31
4.2 Results and discussion 32
4.2.1 Pilot loading and recovery study 32
4.2.2 Linear gradient NaCl operation 34
4.2.3 Step gradient NaCl operation 40
4.2.4 Membrane cleaning at extreme conditions 44
Chapter 5 Reverse-Flow Elution Operations for the Process Development of Baculovirus Purification using a Novel Strong Anion Exchange Membrane Chromatography 46
5.1 Overview 46
5.2 Materials and methods 47
5.2.1 Reverse-flow 47
5.3 Results and discussion 47
5.3.1 Linear gradient reverse-flow elution 47
5.3.2 Step gradient elution 51
Chapter 6 Conclusions and Recommendations 57
6.1 Conclusions 57
6.2 Recommendations 58
References 59
Appendix A Calibration and Optimization of BD FACSCalibur Flow Cytometer for In-House Virus Quantitation 64

A.1 Overview 64
A.2 Materials and methods 65
A.2.1 Flow cytometry 65
A.3 Results and discussion 66
A.3.1 Instrument parameters 66
A.3.2 Detection of fluorospheres 68
A.3.3 Finding baculovirus using the flow cytometer 70
A.3.4 Negative control 73
A.3.5 Dilution test 74
A.3.6 RT-PCR vs. Flow Cytometry Linearity Validation 75
A.3.7 Virus production 76
A.3.8 Benzonase® Digestion Study 77
A.4 Summary 81
Appendix B Characterization of the hydrogel material's microstructure using scanning electron microscopy 82
Appendix C Sample calculation for Micro BCA assay 93

List of Figures

Figure 2-1 Diagram of baculovirus structure including envelope glycoprotein (gp64), and capsid protein (p39 and p87). Obtained copyright clearance from publisher (Rohrmann, 1992). 4

Figure 2-2. Comparison of solute transport in packed-bed chromatography and membrnae-based chromatography. Copyright clearance obtained from Elsevier (Ghosh, 2002). 7

Figure 2-3 Schematic of the principle of binding and eluting using affinity mechanism. Only the target molecules possessing affinity specificity can couple with the affinity ligand. No interaction occurs between the contaminant and immobilized ligand. Obtained copyright from Elsevier (Denizli & Pişkin, 2001). 9

Figure 2-4 Sample distribution across a size exclusion column over different courses of the process with corresponding concentration profile. Obtained copyright clearance from publisher (Striegel, Yau, Kirkland, & Bly, 2009). 9

Figure 2-5 Four phases associated with the anion exchange process: A) Negatively charged target material flows through the anion-exchange matrix with contaminants. B) Negatively charged macromolecules bind to the anion exchanger while contaminants flow through. C) Elution buffer competes in the electrostatic binding between bound material and ligands. D) Buffer ions displace the target molecule and screen the binding sites from the eluting molecule. . 10

Figure 2-6 Four phases associated with cation exchange process: A) Positively charged target material flow through cation-exchange matrix with contaminants. B) Positively charged macromolecules bind to Cation exchanger while contaminants flow through. C) Elution buffer competes in the electrostatic binding between bound material and ligands. D) Buffer ions displace the target molecule and screen the binding sites from the eluted molecule.... 11

Figure 3-1 Diagram of the Äktaprime FPLC system (GE Healthcare Bio-Sciences, 2009). B: base elution buffer; V1: loading, washing, and equilibration buffer valve; SW: base buffer switch; P: pump; M: mixer; V2: sample loading valve; UV: UV absorbance sensor; C: conductivity

sensor; pH: optional pH sensor; F: fractionator; W: waste reservior. The arrows indicates dead-end flow direction. 17

Figure 3-2 Partial view of the flow path across a 50 mm Natrix *Quantum* Q anion exchange membrane in different operations during baculovirus purification process: a) loading process with normal flow: upstream virus solution moves into the membrane device from the inlet and exits at the outlet. b) eluting process with reverse-flow: upstream elution buffer moves into the membrane from the outlet and exits at the inlet. c) elution process with normal flow: upstream elution buffer moves into the membrane from the inlet and exits at the outlet. Dot pattern fill represents the relative virus titre in various phases. 18

Figure 3-3 Membrane blotting assembly. Copyright clearance obtained from Elsevier (Kurien & Scofield, 2006). 28

Figure 4-1 Virus recoveries from anion exchange purifications using different loading conductivities..... 33

Figure 4-2 UV absorbance and conductivity profile and virus yield. 20 mL 5X diluted virus loading solution followed by 20 mL wash and 40 mL elution with NaCl concentration increasing from 0.2 M to 1.5 M using a 50 mM Natrix *Quantum* Q anion exchange membrane and Äktaprime FPLC system, exported from PrimeView™ 5.0 (GE Health Care, Mississauga, ON, Canada). Data points represent virus recovery (n=2) in individual fractions collected over the course of the process, obtained using BD FACSCalibur flow cytometry, CellQuest Pro and Flowjo software..... 37

Figure 4-3 Virus recovery (n=2) versus average NaCl concentration over the course of fraction 5 (200 mM to 330 mM), fraction 6 (330 mM to 680 mM NaCl), fraction 7 (680 mM to 1000 mM NaCl) and fraction 8 (1000 mM to 1500 mM NaCl) in elution step of 20mL 5X diluted virus loading purification with linear gradient elution using 50mm Natrix *Quantum* Q anion exchange membrane and Äktaprime FPLC system. 39

Figure 4-4 Online UV absorbance and conductivity profile of 20 mL 5X diluted virus loading purification with 20 mL wash and 80 mL step gradient elution at 330 mM NaCl, 590 mM NaCl, 850 mM NaCl, and 1500 mM NaCl using a 50mM Natrix *Quantum* Q anion exchange membrane and Äktaprime FPLC system, exported from PrimeView™ 5.0 (GE Health Care, Mississauga, ON, Canada). Data points represent virus recovery (n=2) in pooled fractions during loading and wash, 330 mM NaCl elution step, 590 mM elution step, 850 mM elution step and 1500 mM NaCl, respectively, obtained using BD FACSCalibur flow cytometry, CellQuest Pro and Flowjo software. 41

Figure 4-5 A: Silver stained gel after SDS-PAGE, loaded with molecular weight marker (lane 1 and 7), virus loading solution (lane 2), loading fractions (lane 3 and 4), wash fractions (lane 5 and 6), 330 mM, 590 mM, 850 mM, and 1.5 M NaCl Elutions (lane 8 – 11). B: Western blot of virus loading solution and flow-through. C: Western blot of virus loading solution, 330 mM, 590 mM, 850 mM, and 1.5 M NaCl Elutions. The arrows indicate the location of gp64 protein. 43

Figure 4-6 Virus titration from fractions collected during the cleaning process using flow cytometric assay. Fractions were collected 5mL each. Error bars indicate standard error for n=2. 45

Figure 5-1 UV absorbance and conductivity profile of 20mL 5X diluted virus loading purification process operated with reverse-flow linear gradient NaCl elution from 200mM to 1500mM NaCl over a length of 80mL at flow rate of 4mL/min using 50mM Natrix *Quantum* Q anion exchange membrane with Äktaprime FPLC system exported from PrimeView™ 5.0 (GE Health Care, Mississauga, ON, Canada). Data points reflect virus recovery (n=2) in pooled fraction during loading and wash, and individual fractions during elution, obtained using BD FACSCalibur flow cytometry, CellQuest Pro and Flowjo software. 49

Figure 5-2 “Reverse” represents virus yield achieved in linear gradient NaCl elution during salt ranges of 200 mM NaCl to 330 mM NaCl, 330 mM NaCl to 680 mM NaCl, 680 mM NaCl

to 1000 mM NaCl and 1000 mM NaCl to 1500 mM NaCl, respectively, from 20 mL 5 X diluted virus loading purification process using reverse-flow linear gradient elution process. "Normal" represents virus yield achieved in linear gradient NaCl elution during salt ranges of 200 mM NaCl to 330 mM NaCl, 330 mM NaCl to 680 mM NaCl, 680 mM NaCl to 1000 mM NaCl and 1000 mM NaCl to 1500 mM NaCl respectively from the 20 mL 5X diluted virus loading purification process using normal flow linear gradient elution process.Step gradient elution with reverse-flow operation. Error bars indicate standard error for n=2. ... 50

Figure 5-3 UV absorbance and conductivity profile exported by PrimeView 5.0 from 20 mL 5 X diluted virus loading purification process operated with reverse-flow step gradient elution using 50 mm Natrix *Quantum* Q anion exchange membrane and ÄKTAPrime FPLC system. Data points reflect virus recovery from pooled fractions during loading and wash, 330 mM NaCl elution, 590 mM NaCl elution, 850 mM NaCl elution and 1500 mM NaCl elution, respectively (n=2). 52

Figure 5-4 "Reverse" represents virus yield achieved in elution step at salt levels of 330 mM, 590 mM, 850 mM and 1500 mM NaCl, respectively, from 20 mL 5 X diluted virus loading purification process using reverse-flow elution process. "Normal" represents virus yield achieved in the elution step at salt levels of 330 mM, 590 mM, 850 mM and 1500 mM NaCl, respectively, from 20 mL 5 X diluted virus-loading purification process using normal flow elution process. Error bars indicate standard error for n=2. 53

Figure 5-5 Comparison of recoveries at different NaCl levels from linear gradient and step gradient operations (n=2). The recoveries of linear gradient correspond to the fractions collected at salt ranges of 200 – 330 mM, 3330 – 680 mM, 680 – 850 mM, and 850 – 1500 mM. Error bars indicate standard error for n=2. 54

Figure 5-6 Silver-stained SDS-PAGE gel loaded with (from left to right): molecular weight marker (lane 1), virus loading solution (lane 2), loading and wash fractions pool (lane 3), 330 mM

NaCl elution fractions pool (lane 4), 590 mM NaCl elution fractions pool (lane 5), 850 mM NaCl elution fractions pool (lane 6), and 1.5 M NaCl elution fractions pool (lane 7). 55

Figure A-1 Data processing of flow cytometer. The laser strikes single partcles to generate emissions at different wavelenghts. The emitted lights are directed by bypass band filters into corresponding detectors and coverted into voltage pulses. Then data processor transforms the voltage signals into digital values and plots the particles as a point with its singal values. . 66

Figure A-2 A. Forward scatter and side scatter generated from a typical cell. B. Forward scatter and side scatter from a baculovirus. 67

Figure A-3 2-D dot plots during detection of Flow Set in SSC vs. FSC and SSC vs. FL1 scales 69

Figure A-4 A. 2-D dot plot at SSC and FL1 scale. An aliquote of 900X diluted baculovirus stock solution was subjected to sample preparation procedure and put through the flow cytometry for 30s. B. Histogram of particle count versus SSC form the same sample in A. "SSC-H^-" is the gate covering the particles with a fluorescence intensity less than 1. "SSC-H^+" is the gate that summrizes the total particle number outside "SSC-H^-". 70

Figure A-5 2-D dot plot at SSC vs. FL1 scale of an aliquote of 900 X diluted baculovirus stock solution. The fluorospheres were mixted with the aliquote..... 72

Figure A-6 2-D dot plot with SSC vs. FSC scale at instrument setting of SSC 660 and FL1 480 of the stock recombinant baculovirus. 73

Figure A-7 2-D dot plot of a blank solution: a mixture of 20 μL of 2 % (v/v) paraformaldehyde, 10 μL of 10 % (v/v) Triton-X 100, 20 μL of 200 X diluted SYBR Green I, and 950 μL of PBS. 74

Figure A-8 Particle count of gated regions of diluted baculovirus samples. "Gated Count" refers to the particle number in the virus region and "Noise" refers to the total partcle number outside the virus region. 75

Figure A-9 Comparison analysis of RT-PCR and flow cytometry acquired data. (n=4 for RT-PCR; n=2 for flow cytometry) 76

Figure A-10 Production kinetics of the recombinant baculoviru in Sf9 cells and Gibco® Sf-900™ III serum free media in a 30 mL shake-flask experiment. 77
Figure A-11 The effect of Benzonase® treatment on flow cytomtric data acquisition. The left graph depicts the distribution change in FL1 scale and the right graph shows the distribution change in SSC scale 78
Figure A-12 Effect of Benzonase® treatment on stock virus samples for different incubation times in two fluorescnece regions. 79
Figure A-13 Effect of Benzonase® treatment in eluted samples (n=2). 80
Figure B-1 Membrane column assembly 82
Figure B-2 SEM image of "top" side of a untreated membrane 83
Figure B-3 SEM image of the "bottom" side of a untreated membrane 84
Figure B-4 SEM image of the "top" side of layer 1 from a membrane used in normal flow purifcation. 85
Figure B-5 SEM image of the "bottom" side of layer 1 from a membrane used in normal flow purifcation. 86
Figure B-6 SEM image of the "top" side of layer 2 from a membrane used in normal flow purifcation. 87
Figure B-7 SEM image of the "bottom" side of layer 2 from a membrane used in normal flow purifcation. 88
Figure B-8 SEM image of the "top" side of layer 1 from a membrane used in reverse flow purifcation. 89
Figure B-9 SEM image of the "bottom" side of layer 1 from a membrane used in reverse flow purifcation. 90
Figure B-10 SEM image of the "top" side of layer 2 from a membrane used in reverse flow purifcation. 91

Figure B-11 SEM image of the “bottom” side of layer 2 from a membrane used in reverse flow purifcation. 92

Figure C-1 Caliburation curve for absorbance at 562 nm. BSA samples over a linearge range from 2.5 – 200 μg/mL. the trendline shows a second order polynomial approximation to the date point. Error bars indicate standard error at n=2. 93

List of Tables

Table 2-1 Summary of ion exchange media for baculovirus purification. 13

Table 3-1 Buffer types and compositions used for the anion exchange baculovirus purification processes using 50 mm Natrix *Quantum* Q anion exchange membranes. 20

Table 3-2 Recipe for making polyacrylamide gel for SDS-PAGE. All the chemicals were purchased from Bio-Rad Laboratories Ltd. (Missisauga, ON, Canada). 27

Table 3-3 Experiment summary. 30

Table 4-1 Dilution factors and the corresponding solution conductivity 32

Table A-1 Instrument settings for fluorosphere detection. 69

Table A-2 Instrument settings for virus detection. 71

Table A-3 Instrument settings 72

List of Abbreviations

Roman Letters

Q	Quaternary Ammonium
S	Sulfonic Acid

Other Abbreviations

2-D	Two Dimensional
$AgNO_3$	Silver Nitrate
aIEXc	Anion Exchange Chromatography
APS	Ammonium Persulfate
BCA	Bicinchoninic Acid
cGMP	Current Good Manufacturing Practice
cIEXc	Cation Exchange Chromatography
DEAE	Diethylaminoethyl
DF	Dilution Factor
DI	Deionized
dsDNA	Double-stranded DNA
EPDA	End-point Dilution Assay
FPLC	Fast Protein Liquid Chromatography
FSC	Forward Scatter
FL	Fluorescence
gfp	Green Fluorescent Protein
HCHO	Formaldehyde
HCl	Hydrogen Chloride
HEPES	4-(2-hydroxyethyl)-1-piperazineethanesulfonic acid
hpi	Hours Post Infection
HRP	Horseradish Peroxidase
HPLC	High Performance Liquid Chromatography
IEXc	Ion Exchange Chromatography
kDa	Kilodalton

mAu	Milli-absorbance-unit
MOI	Multiplicity of Infection
NaCl	Sodium Chloride
Na_2CO_3	Sodium Carbonate
$Na_2S_2O_3$	Sodium Thiosulfate
OD	Outer Diamater
PCR	Polymerase Chain Reaction
PBS	Phosphate Buffered Saline
PES	Polyethersulfone
pI	Isoelectric Point
PE	Polyethylene
PVDF	Polyvinylidene Fluoride
qPCR	Quantitative Polymerase Chain Reaction
qRT-PCR	Quantitative Real-time Polymerase Chain Reaction
rBV	Recombinant Baculovirus
RC	Reinforced Cellulose
SDS	Sodium Dodecyl Sulfate
SDS-PAGE	Sodium Dodecyl Sulfate Polyacrylamide Gel Electrophoresis
SEC	Size Exclusion Chromatography
SEM	Scanning Electron Microscopy
SP	Sulfopropyl
SSC	Side Scatter
TBS	Tris Buffered Saline
TBST	Tris Buffered Saline with Tween 20
TCID	Tissue Culture Infectious Dose
TEMED	Tetramethylethylenediamine

Chapter 1

Introduction

Viral vectors have great potential to benefit human society through their versatile applications including agricultural pest control, recombinant protein production, vaccine production, and recent uses in gene transfer to mammalian cells for cancer therapy (Chen, Chen, Chang, Matsuura, & Hu, 2009). Given the potential of viral vectors, enormous efforts have been put into viral vector production, while downstream processing has gradually become a bottleneck in the process (Vicente, Mota, Peixoto, Alves, & Carrondo, 2011).

Baculoviruses have, in particular, recently been recognized as a powerful tool for expressing foreign genes in mammalian cells (Hu, 2005). But so far, it is underrepresented in purification process research (Segura, Kamen, & Garnier, 2011). Thus, this study evaluates membranes as devices to purify baculovirus vectors.

Membranes, as novel chromatographic media, present advantageous features such as lower pressure drop, less buffer consumption, and better scalability compared to traditional packed-bed chromatography. Successful development of virus purification through ion exchange membrane chromatography has been reported (Grein, Michalsky, Vega López, & Czermak, 2012; Vicente, Peixoto, Carrondo, & Alves, 2009; Wu, Soh, & Wang, 2007). A hydrogel-based anion exchange membrane (Natrix *Quantum* Q) was recently developed and its usefulness in virus purification was anticipated due to its large binding capacity and its ability to be used for direct capture of virus without a clarification step. This current study focuses on establishing a baculovirus purification process based on the Natrix *Quantum* Q anion exchange membranes.

1.1 Hypotheses

Given that:

1. the baculovirus should possess sufficient negative charge at a pH that is higher than its isoelectric point (pH 5.4, Yang et al. 2009), to bind to the anion exchange membrane; and
2. bound baculoviruses can be recovered from the membrane by either lowering the operating pH or strengthening the buffer's ionic strength;

the driving hypothesis of this work is that all traditional downstream processing steps can be eliminated and replaced by one step using a novel anion exchange membrane (Natrix *Quantum* Q).

1.2 Objectives

1. Design a one-step baculovirus purification process using the Natrix *Quantum* Q membranes and a fast protein liquid chromatography system.
2. Determine initial operating conditions allowing for virus capture, including loading solution pH and conductivity.
3. Attempt to recover the captured baculovirus by lowering operating pH and introducing NaCl in elution buffer.
4. Evaluate the feasibility of using this current membrane for anion exchange baculovirus purification by investigating irreversible binding, physical hindrance, and reliability of the current virus assay.

1.3 Thesis organization

Chapter 2 reviews the nature of the baculovirus and existing baculovirus purification techniques.

Chapter 3 presents general materials and methods used throughout this work.

Chapter 4 presents the investigation of binding conditions in terms of dilution factor and pH. Membrane breakthrough of the baculovirus was tested to evaluate binding efficacy. The eluting condition was estimated using a linear NaCl gradient experiment with a NaCl buffer. Further development of the process has been done using a step gradient approach. Membrane regeneration was also evaluated in this chapter.

Chapter 5, a reverse-flow operation mode is investigated to overcome mass transfer hindrance through the membrane.

Finally, Chapter 6 summarizes the results and conclusions and gives recommendations for future works related to this project.

Chapter 2

Literature Review

2.1 Recombinant baculovirus (rBV)

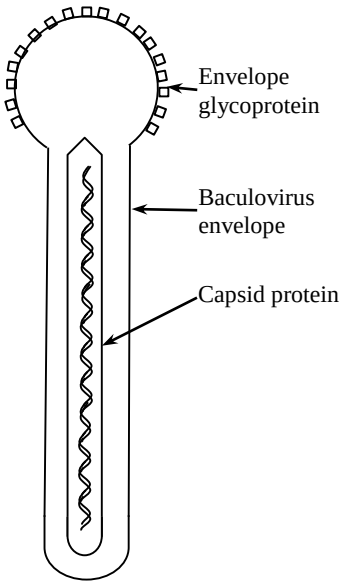

Figure 2-1 Diagram of baculovirus structure including envelope glycoprotein (gp64), and capsid protein (p39 and p87). Obtained copyright clearance from publisher (Rohrmann, 1992).

Baculoviruses form a family of large double-stranded deoxyribonucleic acid (DNA) viruses whose hosts are mainly insects (Rohrmann, 1992). The structure of a budded baculovirus (Figure 2-1) consists of a protein coat that encapsulates its genome, surrounded by a membrane obtained from the host cell (Guarino, 2011). The gp64 proteins cover the apex region, and are responsible for cell membrane fusion during infection (Blissard & Wenz, 1992). A budded baculovirus is roughly 250 – 300 nm in length and 30 – 60 nm in diameter (Guarino, 2011). With the development of an arsenal of molecular biology tools, uses of baculovirus have gone from agricultural pest control (McCutchen et al., 1991; Moscardi, 1999; Wood & Granados, 1991), recombinant protein production (Caron, Archambault, & Massie, 1990; Hensler & Agathos, 1994; Maiorella, Inlow, Shauger, & Harano, 1988;

Wickham & Nemerow, 1993) to the expression of foreign genes in mammalian cells for gene therapy development (Boyce & Bucher, 1996; Carinhas et al., 2009; Hofmann, 1995; Kost & Condreay, 1999).

2.2 Baculovirus purification

For most of the current applications, purification of baculovirus has not been required. However, with successful application of recombinant baculovirus in gene delivery to mammalian cells, and the prospect of curing human diseases by gene therapy through *in vivo* applications of baculovirus vectors, there has been growing attention to downstream processing (DSP). Over the past decade, challenges in recombinant baculovirus vector (rBV) based bioprocessing have shifted from upstream to DSP and point to a need for the development of robust, cost-effective and scalable processes to produce pure, efficient, and safe rBV for human gene therapy applications (Aucoin, Mena, & Kamen, 2010; Morenweiser, 2005; Roldão, Vicente, Peixoto, Carrondo, & Alves, 2011; Segura et al., 2011).

2.2.1 Challenges and requirements

The production of virus requires a simple, robust and cost-effective process for both upstream and downstream development that conforms to current Good Manufacturing Practices (cGMP) regulation (Lesch et al., 2011). To date, most research has focused on efficient production of rBV-related bioproducts, virus-like particles and viral vectors (Ikonomou, Schneider, & Agathos, 2003; Negrete & Kotin, 2008; Shuler et al., 1990). Much less effort has been put into development of essential DSP for such complex biopharmaceutical particles leading to a major bottleneck in the path of final virus product creation (Vicente, Mota, et al., 2011). As viruses are distinct from therapeutic proteins in terms of size and molecular weight, current protein purification strategies are not always transferable to virus systems. Thus, the design and validation of DSP often requires a greater appreciation of the physical, chemical and biological characteristics of the virus (Morenweiser, 2005). The major purpose of a virus purification process is the removal of host cells and culture media derived contaminants,

during large-scale production of active viruses at high titres (Morenweiser, 2005). The appropriate design often relies on the nature of the viral particle, such as its isoelectric point, surface hydrophobicity, integrity of the viral envelope, stability under proposed process conditions, and hydrodynamic diameters (Negrete & Kotin, 2008).

2.2.2 Ultracentrifugation

For applications of recombinant baculovirus *in vitro*, harvested virus solutions are usually ready for use, and little to no purification is required (Aucoin et al., 2010). Ultracentrifugation is one of the earliest methods proposed for recovering virus. Viruses can be pulled out of solution by centrifuging at 96,000 × g for three hours at 4℃ (O'Reilly, Miller, & Luckow, 1993). The main drawbacks associated with this method include limited scalability and low recovery (Vicente, Peixoto, Mota, Carrondo, & Alves, 2011), extended processing time, potential to produce infectious aerosols (Segura et al., 2011), and formation of irreversible virus aggregation (Vicente, Mota, et al., 2011).

2.2.3 Chromatography process

Chromatography is a preferred technology for selective separation of bioproducts in industrial-scale processes, as it offers excellent reproducibility and ensures final product quality in continuous operations. Current chromatography systems can be automated, minimizing human-associated procedures. Additionally, chromatography enables a closed-system process for virus purification, which favors sanitization and overall aseptic operation (Segura et al., 2011).

Traditional chromatography processes are largely based on the use of packed beds of resin. A significant limitation associated with this technology is the column fouling caused by accumulation of colloidal loading material (Ghosh, 2002). Transport of target molecules to binding sites, which relies essentially on pore diffusion into the packing particles, can also be a major impediment. These limitations can lead to a lengthy process and increase elution buffer consumption. Other molecule

transport concerns include channeling and heterogeneity in axial and radial movement, as shown in Figure 2-2 (Ghosh, 2002).

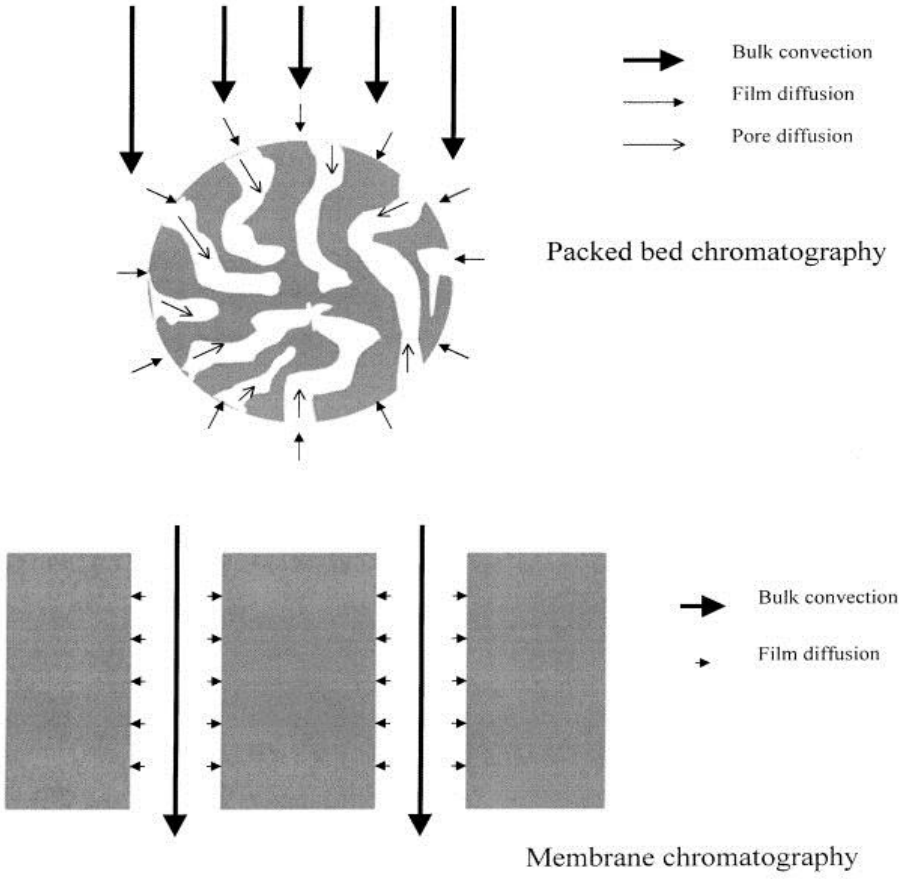

Figure 2-2. Comparison of solute transport in packed-bed chromatography and membrnae-based chromatography. Copyright clearance obtained from Elsevier (Ghosh, 2002).

Novel membrane based chromatography techniques have been developed to overcome some of the problems associated with packed beads (Brandt, Goffe, Kessler, O'Connor, & Zale, 1988; Briefs & Kula, 1992; Champluvier & Kula, 1991). The most significant improvement brought by application of membrane processes lies in the transport of solutes to binding ligands, where convection becomes the dominating transfer mechanism instead of diffusion in the packed-bed chromatographic media. As a result, process time, buffer consumption, and pressure drop reduces, with a resultant increase in scalability and economy. Moreover, the ease in membrane manufacture also benefits optimization of

the process cost (Ghosh, 2002). Nevertheless, further developments are still in need for membrane based processes due to existing disadvantages, such as low binding capacities, inefficient membrane design, and irregular physical properties including pore size distribution, membrane thickness, and ligand density (Orr, Zhong, Moo-Young, & Chou, 2013).

The design of chromatography processes for virus purification relies on surface characteristics of the virus particles and/or their size. Several chromatography-based strategies for baculovirus purification have been developed and are introduced next.

2.2.3.1 Affinity chromatography

Affinity chromatography is a type of chromatography-based purification technology that utilizes the highly selective and reversible interactions between immobilized affinity ligands and target molecules in the mobile phase to separate species of interest from contaminants (Urh, Simpson, & Zhao, 2009), as shown in Figure 2-3. However, to date, the only published work in baculovirus purification using affinity membranes was done by Chen et al. (2009). In the study, a Concanavalin A (Con A) functionalized membrane was used to separate the baculoviruses from insect cell culture. Con A is a type of lectin that binds glycoproteins containing D-mannopyranosyl or D-glucopyranosyl residues in the presence of Mn^{2+} and Ca^{2+} (Andujar-Sánchez, Cámara-Artigas, & Jara-Pérez, 2003). In the structure of a baculovirus, the gp64 protein is the major envelope protein containing N-linked mannose which potentially binds to Con A. Here Chen et al. reported a 21.3 % recovery of the total virus the Con A functionalized membrane. The procedure also allowed for reduction of 99 % of protein impurities.

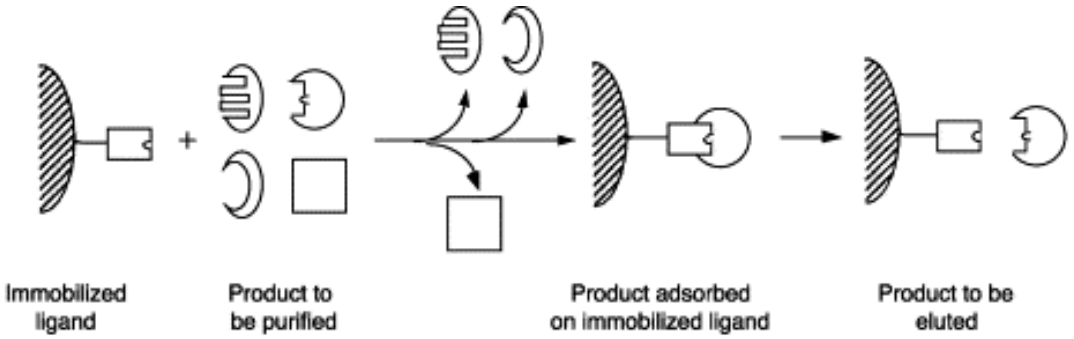

Figure 2-3 Schematic of the principle of binding and eluting using affinity mechanism. Only the target molecules possessing affinity specificity can couple with the affinity ligand. No interaction occurs between the contaminant and immobilized ligand. Obtained copyright from Elsevier (Denizli & Pişkin, 2001).

Though total protein reduction was deemed satisfactory, the poor yield and the cost of using affinity chemistry (Klein, 2000) hampers the spreading of its use.

2.2.3.2 Size exclusion chromatography (SEC)

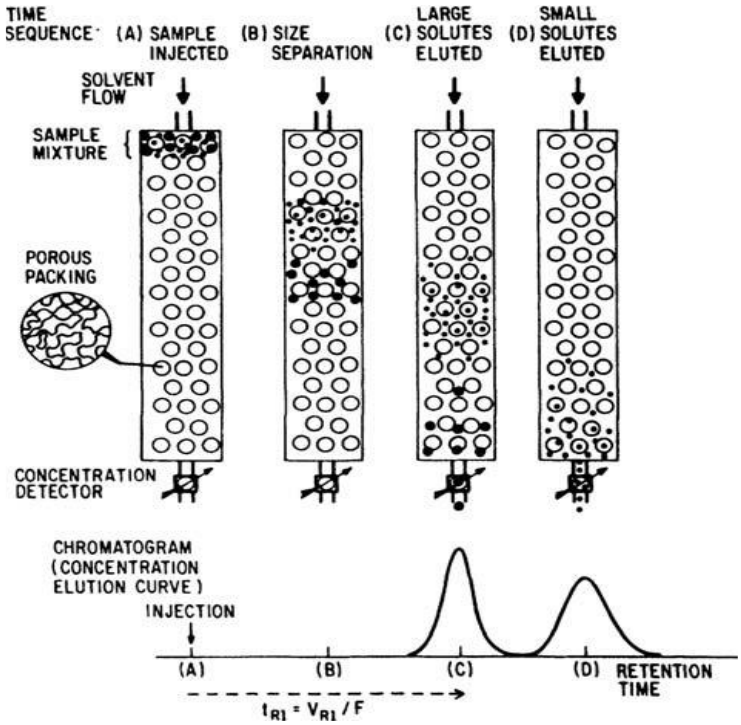

Figure 2-4 Sample distribution across a size exclusion column over different courses of the process with corresponding concentration profile. Obtained copyright clearance from publisher (Striegel, Yau, Kirkland, & Bly, 2009).

Size exclusion chromatography separates species based on their sizes, where different sized components penetrate the column at different retention times (Harrison, Todd, Rudge, & Petrides, 2003) (Figure 2-4). Transfiguracion et al. (2007) developed a baculovirus purification process based on SEC-HPLC, using Sepharose CL-4B resin (Amersham Biosciences, Pistacaway, NJ). The recovery from the SEC was 24 % and western blot analysis revealed good selectivity for baculovirus in the recovered fractions.

2.2.3.3 Ion exchange chromatography (IEXc)

Being the most frequently exploited chromatographic technique for separation and purification of charged biomolecules, successful applications of IEXc have expanded from proteins, polypeptides, nucleic acids (Bonnerjea, Oh, Hoare, & Dunnill, 1986), and plasmid DNA (Zhong et al., 2011) to baculovirus (Gerster et al., 2013; Grein et al., 2012; Vicente et al., 2009; Wu et al., 2007).

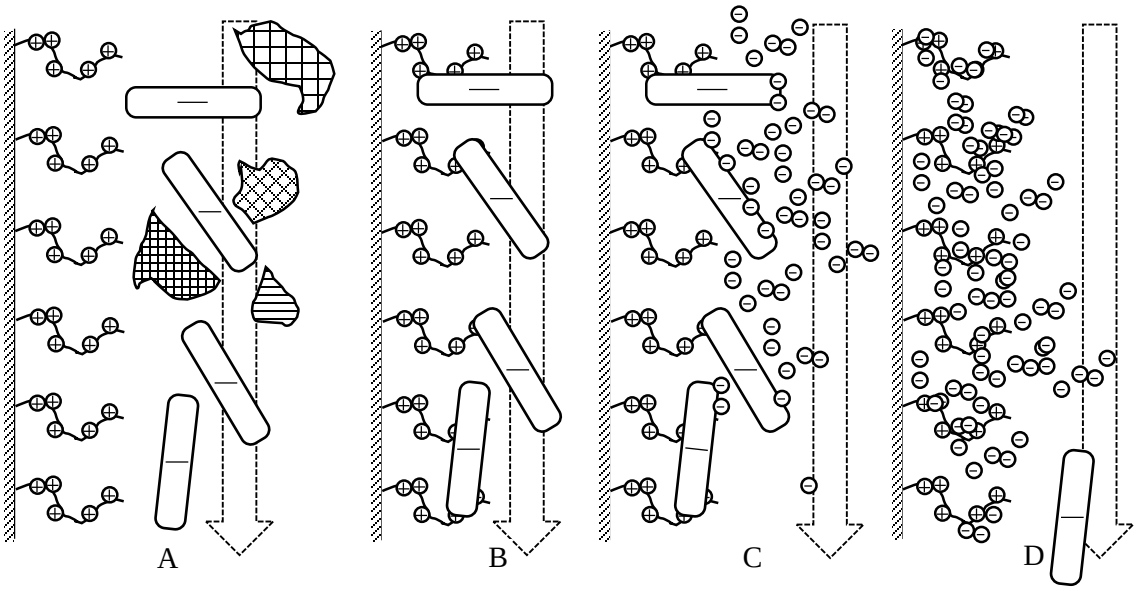

Figure 2-5 Four phases associated with the anion exchange process: A) Negatively charged target material flows through the anion-exchange matrix with contaminants. B) Negatively charged macromolecules bind to the anion exchanger while contaminants flow through. C) Elution buffer competes in the electrostatic binding between bound material and ligands. D) Buffer ions displace the target molecule and screen the binding sites from the eluting molecule.

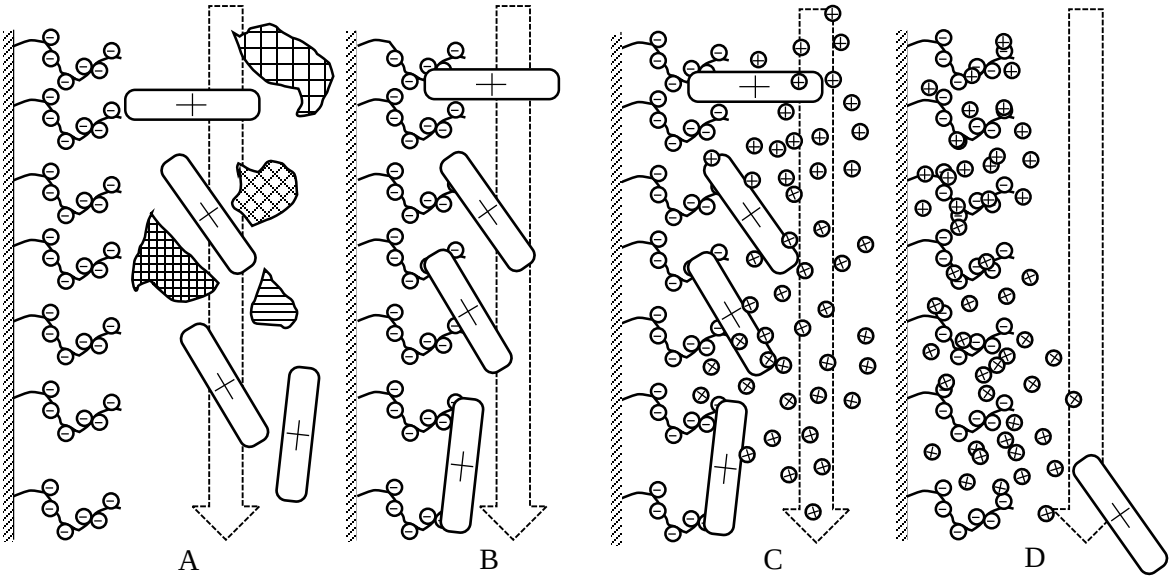

Figure 2-6 Four phases associated with cation exchange process: A) Positively charged target material flow through cation-exchange matrix with contaminants. B) Positively charged macromolecules bind to Cation exchanger while contaminants flow through. C) Elution buffer competes in the electrostatic binding between bound material and ligands. D) Buffer ions displace the target molecule and screen the binding sites from the eluted molecule.

Ion exchange chromatography depends on electrostatic interaction between target molecules and immobilized ion exchange ligands (Figure 2-5 and Figure 2-6). A typical ion exchange chromatographic process for baculovirus purification consists of three stages including virus capture, contaminant removal, and virus recovery. First, negatively (or positively) charged virus particles bind to anion (or cation) exchangers while impurities flow through the ligand matrix (Figure 2-5A and 2-6A). Then a washing process removes weakly bound impurities (Figure 2-5B and 2-6B). Finally, bound viruses are recovered in an elution step using strong electrolytes (eg. NaCl) (Figure 2-5C, 2-5D and Figure 2-6C, 2-6D).

For industrial chromatography applications, Langmuir isotherm is often used to describe the adsorption mechanism (Harrison et al., 2003):

$$[CS]=\frac{K_{eq}S_{tot}[C]}{1+K_{eq}[C]}$$

Where

C = dissolved substances

CS = substance bound to the binding sites

K_{eq} = reaction equilibrium constant

S_{tot} = the total binding site concentration.

The applications of ion exchange chromatography for baculovirus purification is categorized into two types: anion exchange (Gerster et al., 2013; Grein et al., 2012; Vicente et al., 2009) and cation exchange (Barsoum, 1999; Wu et al., 2007). The chromatographic media for baculovirus purification includes resins (Barsoum, 1999; Vicente et al., 2009), membranes (Grein et al., 2012; Vicente et al., 2009; Wu et al., 2007), and monolith (Gerster et al., 2013). Common ion exchange chemistries are sulfonic acid (S), diethylaminoethyl (DEAE), sulfopropyl (SP) and quaternary ammine (Q) and their applications for baculoviruses are summarized in Table 2-1. Sulfonic acid and sulfopropyl are strong cation exchangers. DEAE is a weak anion exchanger and Q is a strong anion exchanger. Given that baculovirus is negatively charged at physiological condition (~ pH 7), anion exchange is the preferred process for baculovirus purification (Segura et al., 2011).

The majority of commercial membranes are based on organic support matrices, due to manufacturing economy and low non-specific binding of target molecules. Reinforced cellulose (RC) is commonly used for supporting material for ion exchange membranes. Another type of membrane support is synthetic organic polymers (eg. polyethersoulfone (PES) and polyethylene (PE)), featuring better physical properties than organic polymer support but presenting more non-specific adsorption to biomolecules (Orr et al., 2013).

A detailed review of current ion exchange applications in baculovirus purification is introduced next.

Table 2-1 Summary of ion exchange media for baculovirus purification.

Ion Exchange Media	Ion Exchange Chemistry	Pore size	Reference
Resin (Sepharose, GE Healthcare)	Sulfopropyl (SP)	n/a	(Barsoum, 1999)
RC (Sartobind, Sartorius)	Diethylaminoethyl (DEAE)	> 3 μm	(Vicente, Fáber, et al. 2011)
RC (Sartobind, Sartorius)	DEAE	> 3 μm	(Vicente et al. 2009)
RC (Sartobind, Sartorius)	Quaternary amine (Q)	> 3 μm	(Grein et al., 2012)
PES (Mustang, Pall)	Q	0.8 μm	(Grein et al., 2012)
PE (Chromasorb, Millipore)	Q	n/a	(Grein et al., 2012)
RC (Sartobind, Sartorius)	Sulfonic acid (S)	> 3 μm	(Wu et al., 2007)
PES (Mustang, Pall)	S	0.8 μm	(Wu et al., 2007)

2.2.3.3.1 Anion exchange chromatography (aIEXc) for baculovirus purification

Vicente et al.(2009) reported a complete downstream process for baculovirus purification. DEAE was chosen as the anion exchange ligand for chromatographic process development, as it features best adsorption kinetics among the four ligands tested (Capto DEAE (GE Healthcare), Capto ViralQ (GE Healthcare) and UNOSphere Q (Bio-Rad, California, USA), and a sulfate group resin. The virus loading solution was prepared by diluting virus supernatant in Tris-HCl buffer at pH 8.0. The performance of DEAE based anion exchange membrane Sartobind D (Sartorious Stedim Biotech) was analyzed against the Capto DEAE resin packed bed. Three elution steps (48 mS/cm, 73 mS/cm, and 120 mS/cm) were used for recovering the virus. The results indicated the virus recovery was 20 % higher with the membrane process. The dynamic binding capacity at 10 % breakthrough for the DEAE membrane was determined at 8.5×10^{8} Total Particles (TP)/cm^2. With addition of 0.6 M NaCl Dulbecco's phosphate-buffered saline (D-PBS) buffer, up to 70 % of the captured virus can be recovered. The end product showed endotoxin level lower than 10 EU ml^{-1} with dsDNA concentrations of 2 μg per 10^9 TP.

The application of strong anion exchange membranes to the baculovirus purification was also investigated (Grein et al., 2012). Cellulose-based (Sartobind Q, Sartorious, SQ), polyether-sulfone-based (Mustang Q, Pall, MQ), and an ultra-high weight polyethylene-based (ChromaSorb, Millipore, CS) membranes were tested in the study. Each membrane was equilibrated with 20 mM Tris buffer at pH 6.5 and then loaded with 3 mL of virus supernatant. A wash step using 20mM Tris buffer was used before elution step consisted of 0.15 M NaCl and 0.5 M NaCl. The three membranes were capable to retain most of the original virus (98.4 %, 99.0 %, and 89.4 % by the MQ, SQ, and CS). Elution with 0.15 M NaCl can only achieve minor virus recovery while 0.5 M NaCl recovered most of the virus with MQ and SQ membranes. This one-step anion exchange process also allowed for significant host cell protein reduction and DNA level reduction.

A recent baculovirus purification process using anion exchange monolith has been reported (Gerster et al., 2013). A strong (Q) and a weak (DEAE) monolith anion exchange devices were investigated in initial screening tests for further process development. Higher virus recovery (9.6 %) was observed with Q monolith. Virus loading solution was mixed with 200 mM NaCl for further linear gradient elution development and virus recovery increased to 26.0 % along with protein reduction up to 92.6 %.

The recovery was further increased to 68.2 % by using 50 mM HEPES buffer and a step gradient elution process which allows for extended contact between the captured virus and elution buffer. The interference from hydrophobic species (eg. lipids) in the loading solution was also investigated by implementing an Epoxy column at upstream for elimination of lipid fouling which further increased virus recovery to 97.0 %.

2.2.3.3.2 Cation exchange chromatography (cIEXc)

Barsoum et al. (1997) investigated the performance of an SP Sepharose® Fast Flow Column (Catalog No. 17-0729-01; Amersham Pharmacia Biotech, Piscataway, NJ, USA) for baculovirus purification using cation exchange mechanism. Virus particles were prepared in conditioned media at pH 5.8. A gravity-driven loading process loaded 40 mL of virus solution into the column. Then phosphate buffered saline (PBS) at pH 7.4 was used for elution, followed by another elution step using 0.5 M NaCl solution. Virus concentrations of 25-fold to 60-fold was routinely achieved, with virus recovery of up to 75 %. This study lacked the evaluation in product purity which rendered this process questionable for production of clinical-grade baculovirus.

Chapter 3

Materials and Methods

This chapter summarizes the material and methods commonly used in this study. Other methods and reagents, specifically modified for different experiments are described in the chapters where they are used.

3.1 Fast protein liquid chromatography

Fast protein liquid chromatography is a type of high-performance chromatography originally introduced for high-resolution separation of biomacromolecules in 1982, with a variety of features including large loading capacity, biocompatible buffer systems, high flow rates, and compatibility with common chromatography modes (Sheehan & O'Sullivan, 2004).

An ÄKTAprime FPLC system (GE Healthcare Canada, Mississauga, ON, Canada) was set up for the purification processes. The system comprises a digital control system, a pump, a fraction collector and a chart recorder, together with valves for buffer selection, sample injection, gradient formation and flow diversion (Figure 3-1). The pump delivers liquid with high precision over a wide flow rate range to ensure fast and reproducible purification. A switch valve and mixer are used for gradient formation and a pressure sensor prevents damage to columns. An eight-port buffer selection valve allows automated loading, washing, and eluting events to be programmed. Motorized valves ensure that buffer or sample selection, sample loading and fraction collection are performed automatically. The sensors provide on-line monitoring for UV (280nm), conductivity and pH for each run. The fractionator directs the flow to sample containers at programmable volumes. Fraction marks and fraction numbers are recorded during each run to allow for easy identification of fractions and peaks.

All of the experiments in this study have been operated at a flow rate of 4 mL/min over the course of the process, as suggested by the manufacturer. The membrane-permeating flow was collected in 16 (OD) × 100 mm (L) disposable borosilicate glass tubes (Fisher Scientific Company, Ottawa, Canada). The fractions were collected in 10 mL aliquots, each collected throughout the course of the purification, and sealed with Parafilm® M (American National Can, USA) and then stored at 4 ℃ for future use.

Various process lengths are investigated in the study and will be specified in the sections where they occur.

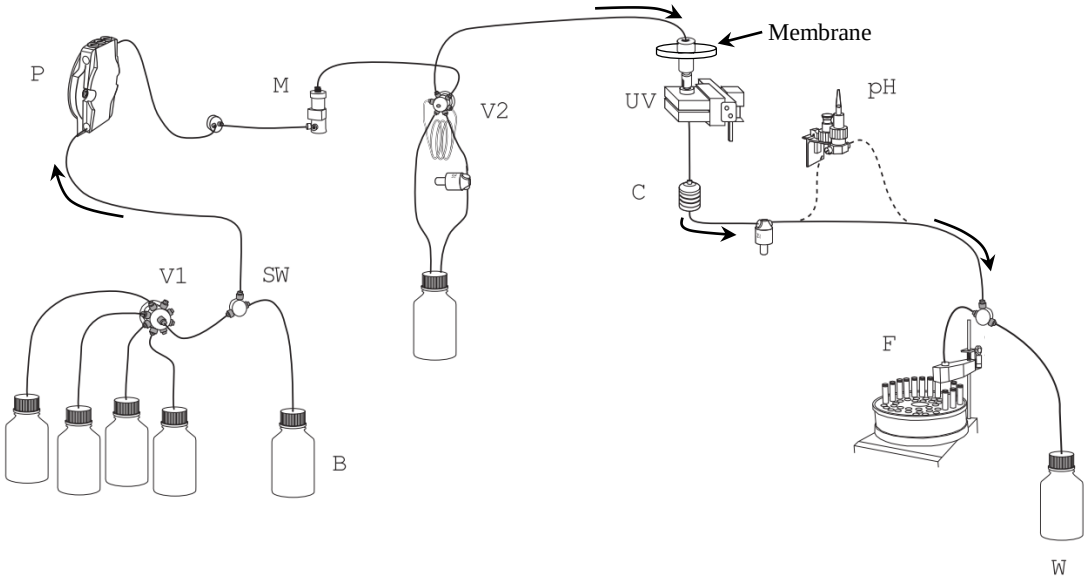

Figure 3-1 Diagram of the Äktaprime FPLC system (GE Healthcare Bio-Sciences, 2009). B: base elution buffer; V1: loading, washing, and equilibration buffer valve; SW: base buffer switch; P: pump; M: mixer; V2: sample loading valve; UV: UV absorbance sensor; C: conductivity sensor; pH: optional pH sensor; F: fractionator; W: waste reservior. The arrows indicates dead-end flow direction.

3.2 Reverse-flow operation

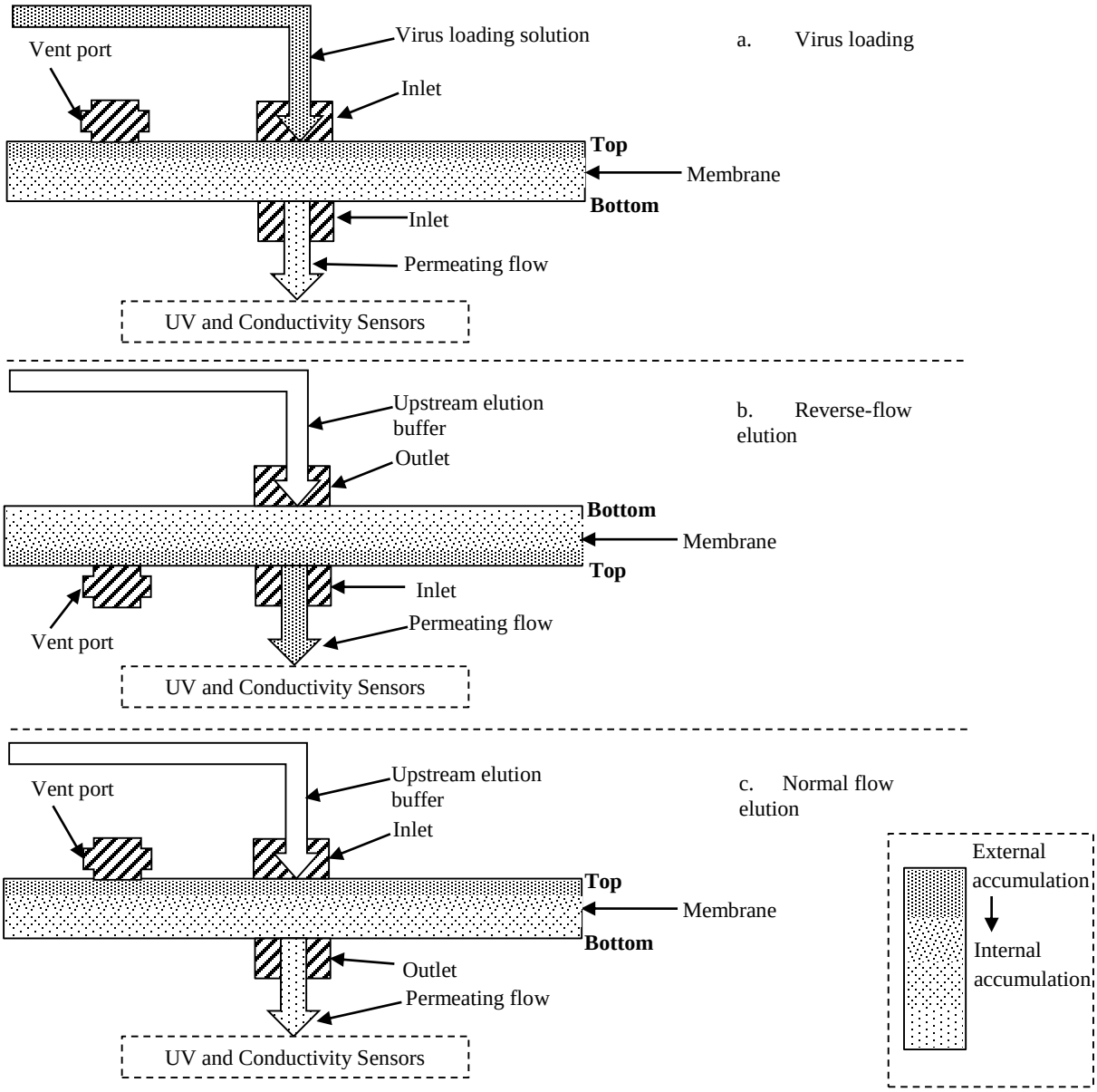

Figure 3-2 Partial view of the flow path across a 50 mm Natrix *Quantum* Q anion exchange membrane in different operations during baculovirus purification process: a) loading process with normal flow: upstream virus solution moves into the membrane device from the inlet and exits at the outlet. b) eluting process with reverse-flow: upstream elution buffer moves into the membrane from the outlet and exits at the inlet. c) elution process with normal flow: upstream elution buffer moves into the membrane from the inlet and exits at the outlet. Dot pattern fill represents the relative virus titre in various phases.

A reverse-flow operation is used in study, shown as Figure 3-2b. Compared to normal flow loading (Figure 3-2a) and normal flow elution (Figure 3-2c), where baculovirus can potentially blocked at near surface region of the membrane and is not able to be recovered using dead-end flow elution,

reverse flow is hypothesized as it is capable of recovering the trapped virus particles. Reverse-flow elution introduces NaCl buffer from the opposite side of the virus-blocking surface, releases virus from electrostatic interaction and carries the virus particles into permeating flow.

3.3 Production of baculovirus

Cell cultures of *Spodoptera frugiperda* Sf9 cells were routinely maintained in Gibco® SFF-900™ III serum-free media (Life Technologies Inc., Burlington, ON, Canada) at 27 ℃ and used for amplifying an in-house baculovirus stock. A 500 mL insect cell culture was infected at a density of 1 million cells/mL, with a multiplicity of infection (MOI) of 1 using the in-house virus stock and harvested when the cell viability reduced to 80 %. The culture was then centrifuged at 2500 × g for 15 minutes at room temperature using an Eppendorf Centrifuge 5804 R (Eppendorf Canada, Mississauga, ON, Canada). The supernatant was removed and filtered using a filtration system with 0.2 μm PES membrane (VWR International, Mississauga, ON, Canada) in a biosafety cabinet and stored at 4 ℃ for future use.

3.4 Buffer preparation

The different buffers used in the purification processes are shown in Table 3-1. HEPES powder and sodium chloride powder were purchased from Bio-Rad Laboratories Ltd., (Mississauga, ON, Canada). HCl solution was purchased from Thermo Fisher Scientific Inc., (Mississauga, ON, Canada) (Thermo Fisher Scientific Inc., Mississauga, ON, Canada). The solution's pH was measured using a Fisher Scientific™ accumet™ Excel XL20 pH meter (Thermo Fisher Scientific Inc., Mississauga, ON, Canada). The buffers were filtered through a 50 mm diameter 0.2 μm GELMAN Laboratory vent filter (Pall Canada Ltd., Mississauga, ON, Canada) for sterilization and removal of solids waste and stored in one-litre Pyrex® round media storage bottles (VWR International, Mississauga, ON, Canada) at room temperature. Before each purification trial, an aliquot was taken from each buffer stock to prepare

a single-use buffer solution and filtered again with a 32 mm diameter 0.2 μm pore size Acrodisc® Syringe Filter with Supor® Membrane (Pall Canada Ltd., Mississauga, ON, Canada) for temporary sterilization.

Table 3-1 Buffer types and compositions used for the anion exchange baculovirus purification processes using 50 mm Natrix *Quantum* Q anion exchange membranes.

Buffer Type	Composition
Equilibration	30 mM HEPES, 200 mM NaCl, pH 6.9
Wash #1	30 mM HEPES, 200 mM NaCl, pH 6.9
Wash #2	30 mM HEPES, 200 mM NaCl, pH 6.0
Elution Base	30 mM HEPES, 1500 mM NaCl, pH 6.0

3.5 Virus stock treatment

Successful baculovirus capture has been reported through the dilution of baculovirus supernatant in physiological buffers at pH 7.2 (Gerster et al., 2013). Here, the virus supernatant's pH and conductivity was adjusted by adding the equilibration buffer at various dilution factors. The diluted virus solution was again put through a 32 mm diameter 0.2 μm pore size Acrodisc® Syringe Filter with Supor® Membrane (Pall Canada Ltd., Mississauga, ON, Canada), for removal of virus aggregates, and stored in a 15 mL Nalgene™ Conical-Bottom Centrifuge Tube (Thermo Fisher Scientific Inc., Mississauga, ON, Canada) at room temperature.

3.6 Dilution factor

Dilution factors that applied to initial virus supernatant are calculated based on Equation 3-1:

$$DF = \frac{V_{tot}}{V_0} \qquad \text{(Equation 3-1)}$$

Where

DF = dilution factor

V_{tot} = volume of loading solution (mL)

V_0 = volume of the initial virus supernatant (mL)

3.7 Anion exchange membrane

50 mm Natrix *Quantum* Q anion exchange hydrogel membranes (50 mm in diameter, with crosslinking percentage ranged from 9 % to 12 %) (Natrix Separations Inc., Burlington, ON, Canada) were used in this study. The functional anion exchange ligand is 3-acrylamidopropyl-trimethylammonium chloride (ATPAC) providing cationic quaternary ammonium structure (Zhong et al., 2011). The 50 mm disk has a membrane volume of 0.75 mL (Natrix Separations, 2008).

3.8 Virus quantitation

Quantitation of the baculovirus is of great importance in evaluating process performance and assessing reproducibility.

3.8.1 Flow cytometry

The sample concentration for flow cytometry analysis should be 10^5 to 2×10^7 particles/mL. As described by Shen et al. (2002), samples were analyzed based on a cumulative count over 30 seconds. The detection limit of the FACS Calibur Flow Cytometer is 1000 particles/second (BD Bioscience, 2007), to prevent coincidence between individual particles. Thus, appropriate dilution was necessary to retain the counts below 3×10^4 particles/mL.

A methanol free paraformaldehyde solution (Thermo Fisher Scientific Inc., Mississauga, ON, Canada), 16 % (w/v), was first diluted to 2 % (v/v) using PBS for the ease of liquid handling for the following steps. Diluted samples were fixed by adding 2 % (v/v) formaldehyde to a final concentration of 0.04 % (v/v) and storing at 4 ℃ for 1 hour.

The formaldehyde incubated samples were freeze-thawed by freezing at -80 ℃ in a VWR® Symphony™ Ultra-Low Temperature Freezer and thawing at 37.5 ℃ for 10 minutes in a 20-well VWR® Digital Dry Block Heater with 0.2 μm PES membrane (VWR International, Mississauga, ON, Canada). A 10 % (v/v) Triton-X 100 (Bio-Rad Laboratories Ltd., Mississauga, ON, Canada) stock solution was further added to each of the samples to a final concentration of 0.1 % (v/v).

A stock SYBR® Green I Nucleic Acid Gel Stain, 10,000 X Concentrate in DMSO (Life Technologies Inc., Burlington, ON, Canada) reagent was diluted in the PBS buffer to 50-fold dilution and stored at -20 ℃. Samples were incubated with Triton-X 100 for 5 min before adding SYBR Green I solution to a final concentration of 0.2 % (v/v). Samples were transferred to a 20-well VWR® Digital Dry Block Heater with 0.2 μm PES membrane (VWR International, Mississauga, ON, Canada) and incubated at 80 ℃ for 10 minutes. Samples were cooled on ice for 5 minutes prior to passing then through the flow cytometer.

Flow-Set™ Pro 3 μm (nomial diameter) polystyrene fluorospheres (Beckman Coulter Canada, Missisauga, ON, Canada) at 1×10^6 fluorospheres/mL (nominal concentration) were used for day-to-day instrument calibration. The fluorosphere emits fluorescence between 515-800 nm when excited at 488 nm (Beckman Coulter, 2011).

The determination of virus quantity using flow cytometry assay relies on the conversion of detected particle to a true viral titre, using fluorescent beads as a standard reference. The count of viruses is firstly differentiated from background noises using a gating strategy based on a positive and negative control. Then the noise-corrected virus count was converted to an actual virus titre by

$$\text{Virus titre (viral paricles/mL)} = \frac{N_+ - N_-}{N_s} \times DF \times c_s \qquad \text{(Equation 3-2)}$$

Where

N_+ = detected particle number that appeared in the virus particle region

N_- = number of particles from a negative control that appeared in the virus particle region

N_s = number of detected particles using the fluorescent bead standards

DF = dilution factor of virus samples

c_s = dilution-factor corrected concentration of fluorescent bead standards (particles/mL)

The results obtained from flow cytometry are highly reproducible. However the accuracy of the quantitation relies heavily on proper resolution of virus particles and distinct differentiation from background noises.

3.8.2 Real time quantitative polymerase chain reaction (RT-qPCR)

The protocol used for quantifying baculovirus using real time PCR was based on the paper by George et al. (2012).

The standard plasmid used in this protocol is a single plasmid containing *Ie-1* and *Gp-64* sequences. Triton-X 100 treatment was done by adding in Triton-X 100 solution to desired final concentration of 0.1% (v/v). The freeze-thaw cycle was done by storing the samples in a -80 ℃ freezer for 30 min and then thawing them at room temperature. The reaction for each analysis consisted of 2 μL of the sample, 10 μL of 2 × Power SYBR® Green PCR Master Mix (Applied Biosystems, Burlington, ON, Canada), a forward and a reverse GP-64 protein segment targeted primer at a concentration of 900 nM each, and UltraPure™ DNase/RNase-Free Distilled Water (Life Technologies Inc., Burlington, ON, Canada) for a final volume of 20 μL for each well in a MicroAmp Fast Optical 96-well Reaction Plates (Applied Biosystems, Burlington, ON, Canada). Then the amplification cycles were carried out as follows: 10 min at 95 ℃, 45 denaturing cycles at 95 ℃ for 30 s and annealing/extension at 60 ℃ for 30 s. Data obtained from the reaction plate were transferred to and analyzed by StepOne™ Software v2.0.

3.9 Virus breakthrough and recovery

Virus loss during the loading and wash processes was defined as virus breakthrough.

Virus breakthrough and virus recovery were calculated according to (Equation 3-3):

$$\%\text{Breakthrough (or \%Recovery)} = \frac{\sum_{i=1}^{n} c_i \times V_i}{c_0 \times V_0} \times 100\% \qquad \text{(Equation 3-3)}$$

Where

c_i = virus titre in fraction (particles/mL)

V_i = volume of the fractions (mL)

c_0 = virus titre of the virus loading solution (particles/mL)

V_0 = volume of virus loading solution (mL)

n = number of fractions collected in each step

3.10 Protein analysis

Because of the sample concentration ranges, buffer compatibility, and instrument availability associated with this study, the BCA assay is the method of choice for protein quantification.

Qualitative analysis of the sample was done through gel electrophoresis and silver staining.

3.10.1 Micro BCA assay

The micro BCA assay relies on the formation of an intense purple complex with Cu^{+} by initiating a BCA reaction between proteins and alkaline Cu^{2+}. This water-soluble compound has a strong absorbance at 562 nm that is linearly associated with protein concentration.

3.10.1.1 Sample preparation and measurement

A commercially available Micro BCA™ Protein Assay Kit (Thermo Fisher Scientific Inc., Mississauga, ON, Canada) was used. A protein standard made with serial dilution to bovine serum albumin containing 0.9 % saline and 0.05 % sodium azide (Thermo Fisher Scientific Inc., Mississauga, ON, Canada) was prepared for generating a calibration curve for further total protein calculations. Samples from the purification processes were diluted in PBS buffer at proper ratios to be compatible with the linear range of the calibration curve, 0 – 200 μg/mL. Then reagents were mixed with the samples in a 96-well plate and heated at 37 ℃ for 2 hours to conduct the reaction. The final mixture was subjected to a plate reader at 562 nm for absorbance data collection. Blank samples containing diluting buffers were quantified as well to correct interfering absorbance from the buffers.

The absorbance value from the PBS blank was subtracted from the absorbance values of the protein standards, and a calibration curve was generated by a polynomial correlation between the absorbance and protein concentration of the standard samples using Microsoft® Excel software. Then, a buffer blank correction was also done to the process samples by subtracting the absorbance of the corresponding process buffer from the samples. Finally, the protein concentrations of the samples were calculated the polynomial approximation equation based on standard samples (sample calculation given in Appendix C).

3.10.2 SDS-PAGE and silver staining

For qualitative analysis of sample protein, electrophoresis technique is often used to differentiate mixture of various proteins in order to investigate detailed compositions. The underlying mechanism of this technique is the migration of protein when subjected to an electric field through pores within a polyacrylamide gel matrix and the difference in migration rates of various protein species due to specific characteristics, including size, charge and shape (Gallagher, 2006).

Prior to electrophoresis procedure, protein samples were subjected to denaturing treatment described by Laemmli (1970). Polyacrylamide gel with 15 wells at 15 % cross-linking was made according to Table 3-2 using a set of Mini-PROTEAN Tetra Cell Casting Modules (Bio-Rad Laboratories Ltd., Mississauga, ON, Canada). The gel consisted of two layers: a stacking layer, having lower percentage of 4 % (v/v), with a height of roughly 1.5 cm, which is responsible for compressing the sample to a narrow band before entering the "resolving layer"; and a resolving layer, which differentiates the compressed protein samples with regard to their sizes such that, at the end of electrophoresis multiple bands appear at different location in the gel. After the reaction mixture is injected into the glass casts, it is left at room temperature for 45 minutes to allow for polymerization. The experimental set-up for SDS-PAGE was based on a Mini-PROTEAN® Tetra Cell (Bio-Rad Laboratories Ltd., Mississauga, ON, Canada). The samples were mixed with 5 X Protein Loading Buffer (Fermentas, now Thermo Fisher Scientific Inc., Mississauga, ON, Canada) and β-mercaptoethanol (Sigma-Aldrich Canada Co., Oakville, ON, Canada). The mixture was then heated at 95 ℃ for 5 min using a 20-well VWR® Digital Dry Block Heater (VWR International, Mississauga, ON, Canada) in a fume hood. At this stage, 20 μL of denatured sample was loaded into each well in the stacking layer of the gel in a fume hood. 0.7 μL of PageRuler Unstained Protein Ladder (Thermo Fisher Scientific Inc., Mississauga, ON, Canada) was added to the two ends as a protein standard for determination of the sample's molecular weight. Then the electrophoresis was driven by a PowerPac™ Power Supply system (Bio-Rad Laboratories Ltd., Mississauga, ON, Canada) at 150 V for 1hour and 10 minutes.

Table 3-2 Recipe for making polyacrylamide gel for SDS-PAGE. All the chemicals were purchased from Bio-Rad Laboratories Ltd. (Missisauga, ON, Canada).

Materials	Quantity for 2 pieces of gel	
	4 % stacking gel	15 % resolving gel
Deionized water	3.05 mL	5.1 mL
1.5 M Tris-HCl, pH 8.8	n/a	3.75 mL
0.5 M Tris-HCl, pH 6.8	1.25 mL	n/a
10 % (w/v) SDS	50 µL	150 µL
30% Acrylamide/Bis-acrylamide	0.665 mL	7.5 mL
10 % (w/v) Ammonium Persulfate (APS)	50 µL	150 µL
Tetramethylethylenediamine (TEMED)	5 µL	15 µL

The resultant gel removed from the electrophoresis assembly was soaked in a fixing buffer (30 % (v/v) ethanol and 10 % (v/v) acetic acid) (Thermo Fisher Scientific Inc., Mississauga, ON, Canada) for 3 times 5 minutes each on a rocker table and followed with two 5-minute washes with 30 % (v/v) ethanol. The gel was then rehydrated in DI water for 20 minutes. Removal of background was done by soaking the gel for 2 minutes and 15 seconds in 2.5mM $Na_2S_2O_3$ (Sigma-Aldrich Canada Co., Oakville, ON, Canada) solution. After 10 minutes washing with DI water, the gel was soaked in a 20 % (w/v) $AgNO_3$ (Sigma-Aldrich Canada Co., Oakville, ON, Canada) solution for 20 minutes, on a rocker table. The gel was washed with DI water afterwards, and soaked in a developing reagent (3 g Na_2CO_3 (Sigma-Aldrich Canada Co., Oakville, ON, Canada), 115.625 µL 16 % (w/v) HCHO (Thermo Fisher Scientific Inc., Mississauga, ON, Canada), 800 µL $Na_2S_2O_3$ and 100 mL DI water to visualize protein bands. The developed gel was dried with glass paper and scanned for future analysis.

3.10.3 Western blotting

Western blot, a method for detecting specific proteins from sample mixture, based on immunological mechanisms, is extensively used as an analytical method in biotechnological works. It

is reported that western blot can be used for determination of baculoviruss with an antibody specific to gp64 envelop protein (Transfiguracion, Mena, Aucoin, & Kamen, 2011). Therefore, this mechanism is useful for validation of virus purification process development. The fundamental of this method relies on the specific binding of antibodies to a specific protein within the sample. The exposure of a sample to the specific molecular probe was done through a process termed "blotting", which refers to transferring protein to microporous membranes.

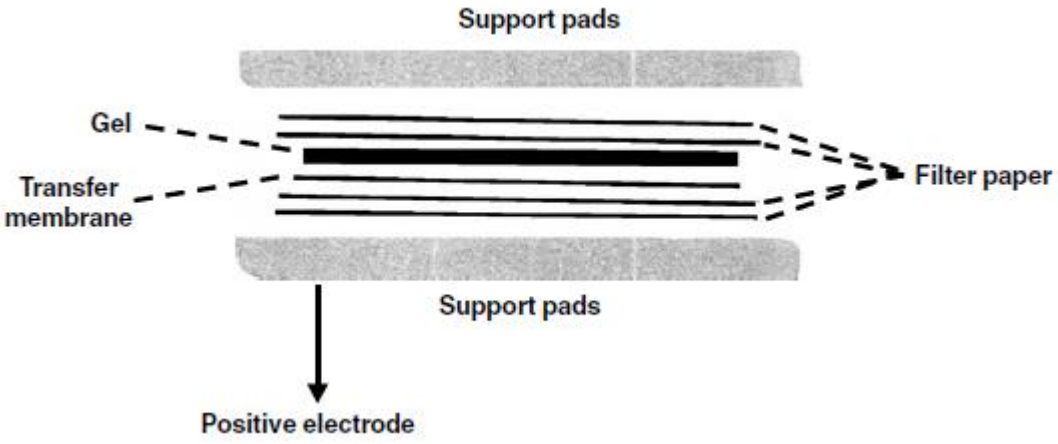

Figure 3-3 Membrane blotting assembly. Copyright clearance obtained from Elsevier (Kurien & Scofield, 2006).

Following a SDS-PAGE procedure, the resultant gel was washed in DI water 3 times for 5 min and the soaked in DI water. The resolved protein sample was transferred using a Trans-Blot® SD Semi-Dry Transfer Cell (Bio-Rad Laboratories Ltd., Missisauga, ON, Canada) at 20 V for 1 hour, with the assembly shown in Figure 3-3. The blotted PVDF membrane was then removed from the apparatus and incubated in Bløk Noise-Cancelling Reagent (EMD Millipore Corporation, Billerica, MA, USA) overnight at 4 ℃. Then, 2 µL of Anti-Baculovirus Envelope gp64 Protein Purified (eBioscience, Inc., San Diego, CA, USA) was 1000 times diluted in Bløk Noise-Cancelling Reagent. Next, 5 µL of Goat Anti-Mouse IgG Antibody, HRP conjugate (EMD Millipore Corporation, Billerica, MA, USA), which is the secondary antibody, was 5000 times diluted in Tris-buffered saline (TBS) (Bio-Rad Laboratories

Ltd., Missisauga, ON, Canada). The incubated membrane was soaked in an anti-gp64 antibody solution for 1 hour, on a rocking table, and then washed in TBS-Tween 20 (TBST) for 3 times 5 min each. Afterwards, the membrane was incubated in the secondary antibody solution for 1 hour. Afterwards, the membrane was washed 3 times 5 min each in TBST and 5 min in TBS. The imaging analysis was done using a BIS 303 PC bio-imaging system (DNR Bio-Imaging Systems Ltd., Jerusalem, Israel) with Luminata Forte Western HRP substrate (EMD Millipore Corporation, Billerica, MA, USA). The exposure time for the imaging process was set at 1 min 30 sec (with gain 25).

3.11 Statistical analysis

Comparison analysis between mean values of sample sets were carried out using t-test analyses. The test statistic t_0 obtained using (Equation 3-4) (Montgomery, 2009):

$$t_0 = \frac{\bar{y}_1 - \bar{y}_2}{S_p\sqrt{\frac{1}{n_1}+\frac{1}{n_2}}} \qquad \text{(Equation 3-4)}$$

Where

$\bar{y}$ = sample means

n = sample sizes

S_p = an estimate of the common variance given by

$$S_p^2 = \frac{(n_1-1)S_1^2+(n_2-1)S_2^2}{n_1+n_2-2} \qquad \text{(Equation 3-5)}$$

where S_1^2 and S_2^2 are the variances of two individual samples.

A 90 % confidence interval was used for comparative analysis. By comparing t_0 to the t distribution with n_1+n_2-2 degrees of freedom, the difference between the two samples can be tested.

3.12 Experimental conditions summary

Table 3-3 Experiment summary.

Operation mode	Feed volume (mL)	Dilution factor	Loading conductivity (mS/cm)	Loading pH	Elution volume (mL)	Elution NaCl concentration (M)	Elution pH
Dead-end	20	2	4.56	6.9	40	0.2, 0.3, 0.4, and 1.0	6.0
Dead-end	20	3	3.49	6.9	40	0.2, 0.3, 0.4, and 1.0	6.0
Dead-end	20	4	2.56	6.9	40	0.2, 0.3, 0.4, and 1.0	6.0
Dead-end	20	5	15.3	6.9	40	0.2 – 1.5	6.0
Dead-end	20	5	15.3	6.9	80	0.2, 0.33, 0.59, 0.85, and 1.5	6.0
Dead-end loading with reverse-flow elution	20	5	15.3	6.9	80	0.2 – 1.5	6.0
Dead-end loading with reverse-flow elution	20	5	15.3	6.9	80	0.2, 0.33, 0.59, 0.85, and 1.5	6.0

Chapter 4

Purification of Baculovirus Through Linear Gradient Elution Using a Novel Strong Anion (Q) Exchange Membrane

4.1 Overview

The investigation into the performance of the Natrix *Quantum* Q anion exchange membrane (Natrix Separations Inc., Burlington, ON, Canada) started with exploration in the effects of anion electrolyte concentrations on virus breakthrough and recovery. The process was broken down into four steps: 1) virus loading: the virus solution is driven through the membrane and contacts the anion exchange ligand, allowing capture of the baculovirus from solution; 2) membrane washing: the loading solution was removed by flushing the membrane with a wash buffer; 3) pH conditioning: the pH was adjusted by a second wash buffer at a lower pH; 4) elution: a strong electrolyte-containing buffer was applied to the membrane for virus recovery, as the high concentration electrolytes competes with virus-ligand binding, substitutes virus particles from the binding sites, and screens the free virus particles from the anion exchanger.

The virus loss during loading and wash steps are evaluated. Virus recovery is investigated using two operation modes: 1. Linear gradient NaCl elution, where the elution buffer's NaCl concentration is increasing over a certain range during the process; 2. Step gradient NaCl elution, where the elution buffer's NaCl concentration having stepwise increase over certain levels.

4.2 Results and discussion

4.2.1 Pilot loading and recovery study

4.2.1.1 Virus breakthrough at various loading conductivities

The anion exchange separation process depends on the successful binding interaction between negatively charged baculovirus and positively charged binding ligands. As this mechanism involves electrostatic interaction, the conductivity (ionic strength) of the virus solution plays a profound role in the binding process, because the free electrolyte ions can interact with binding ligands, screening the charged virus particles from the anion exchangers. A set of baculovirus loading solutions were prepared by diluting clarified virus supernatant in the equilibration buffer with dilution factors 2, 3, and 4. The conductivity of these solutions were determined and given in Table 4-1.

Table 4-1 Dilution factors and the corresponding solution conductivity

Dilution factor applied to stock virus solution	Solution conductivity (mS/cm)
2 X	4.56
3 X	3.49
4 X	2.89

The breakthrough results from the loading solutions were determined using the flow cytometric method. The minimal virus titres (accounted for less than ~ 0.5% of the viruses in loading solution) in the permeating flow suggested that most of the viruses were successfully captured by the anion exchange media, also indicating the limited effect of various loading conductivities on virus breakthrough at the given operating condition.

4.2.1.2 Virus recovery

The recovery of bound baculoviruses in ion exchange process is also subjected to the loading conductivity. When a small amount of free electrolyte ions is present in the virus loading solution, viral

particles are likely to be captured by multiple binding ligands when they are being transported through the anion exchange membrane, forming strong electrostatic bonds with the ligands. This potential multiple-binding mechanism hinders the virus recovery, as it requires much stronger anions to break the bonds. This rationale motivated further study on the virus recoveries from loading solutions at various conductivities, to determine the loading conductivity which satisfies both low breakthrough and instant virus recovery.

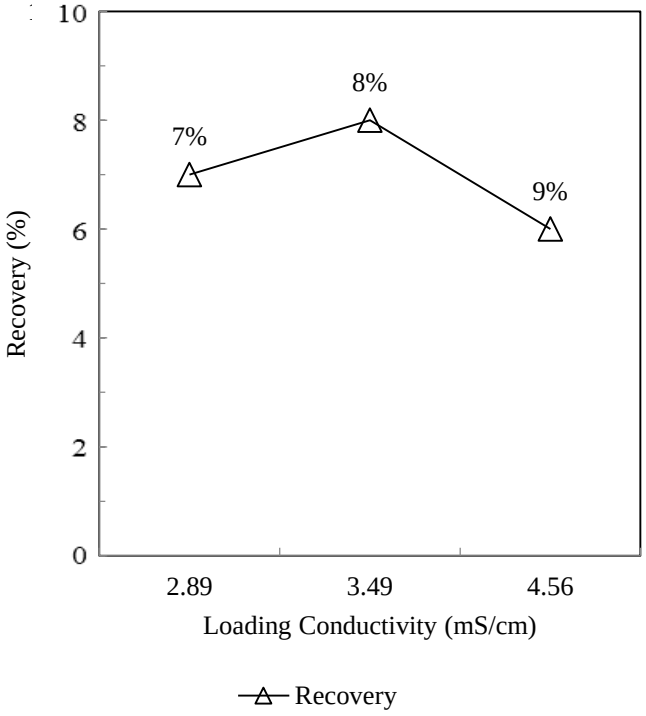

Figure 4-1 Virus recoveries from anion exchange purifications using different loading conductivities.

The virus loaded membranes from the previous experiments were eluted by buffer solutions with 200 mM, 300 mM, 400 mM, and 1 M NaCl to investigate how loading conductivity affect the virus recovery. The recovered virus titres at each salt stage were combined to reveal the total virus recovery. Based on further flow cytometry virus quantification, the average virus recovery of all these four trials was below 10 % (Figure 4-1).

One possible reason accounting for this unusual low yield was that the NaCl eluting solution failed to provide enough negative charged ions to replace the bound viruses. Increasing the salt's concentration can potentially address the issue. However, highly concentrated NaCl solution not only hampers the viruses' protein structure, but is also not compatible with the membrane material according to manufacturer's instruction.

While the approach to break the virus-ligand binding using high NaCl concentration seemed not practical, there is still a possible method to address the issue with lower salt content. If the binding strength can be lowered when viruses are being captured in the anion exchange media, then the amount of ions and charges to break the bond is accordingly decreased. High virus recoveries have recently reported in anion exchange process using loading conductivity around 15 mS/cm (Gerster et al., 2013). Therefore, sodium chloride was used to prepare the buffers. Using a dilution factor of 5, the loading solution conductivity can be appropriately adjusted to around 15.3 mS/cm and had been used for all of the following trials.

4.2.2 Linear gradient NaCl operation

4.2.2.1 Linear gradient elution

To identify the initial NaCl concentration ranges that favor virus recovery, a process with linearly increasing NaCl concentrations was established. The concentrations of NaCl in the flow path was adjusted by a solenoid valve that controls the time the wash buffer and NaCl buffer were connected to the system. The times were based on a programmed method. For example, for 10s during a process, given a NaCl concentration set at 30 %, the solenoid valve allows the wash buffer to enter the system for 7 seconds and then switches to the NaCl buffer for 3 seconds. As the flow enters the mixer, the two portions of buffer inside the flow path are homogenized before they pass through the membrane.

4.2.2.2 Purification process

20 mL of 5 × diluted virus stock was used as a loading solution (as suggested in Vicente et al., (2009). Then 20 mL of wash buffer was passed through the membrane to remove any residual loading solution. The elution phase started at conductivity of 17.2 mS/cm and gradually reached 100.2 mS/cm over 40 mL. The corresponding sodium chloride concentration varied from 200 mM to 1500 mM. UV absorbance and conductivity profiles are presented in Figure 4-2.

4.2.2.2.1 Equilibrating the membrane

As seen in the profile (Figure 4-2), the UV absorbance and conductivity curves formed a stable baseline near zero, reflecting the equilibration buffer flow in the system. The membranes were provided in a dry condition; therefore appropriate wetting was needed for the hydrogel base developing its pore structure (eg. pore sizes and macropore interconnections) (Zhong et al., 2011). The conductivity during wetting stabilized at 17.3 mS/cm.

4.2.2.2.2 Loading virus

After 30 mL of equilibration, virus capture was initiated by pumping the virus-loading solution through the anion exchange membrane. An increase in UV absorbance occurred, in the phase between 35 to 55 mL, (in Figure 4-2) because of the significant protein content in the virus solution.

4.2.2.2.3 Wash

Starting from 55mL of operation, a two-stage wash process started to remove any remaining loading solution and adjust the membrane pH for elution. Wash buffer #1 (30 mM/200 mM NaCl/pH 6.9) was first connected to the flow path to remove any unbound material associated with the loading step. Then, wash buffer #2 (30 mM/200 mM NaCl/pH 6.0) entered the system for a pre-treatment such that the macro environment's pH would favor virus eluting.

4.2.2.2.4 Elution

Recovery of the captured virus particles was achieved by passing the NaCl buffer through the membrane, allowing electrolyte ions to reach the anion exchangers and compete with bound viruses. As described in the previous section, the NaCl concentration of the buffer flow was increasing over the course of the elution from 200 mM (17.3 mS/cm) to 1.5 M NaCl (100.2 mS/cm).

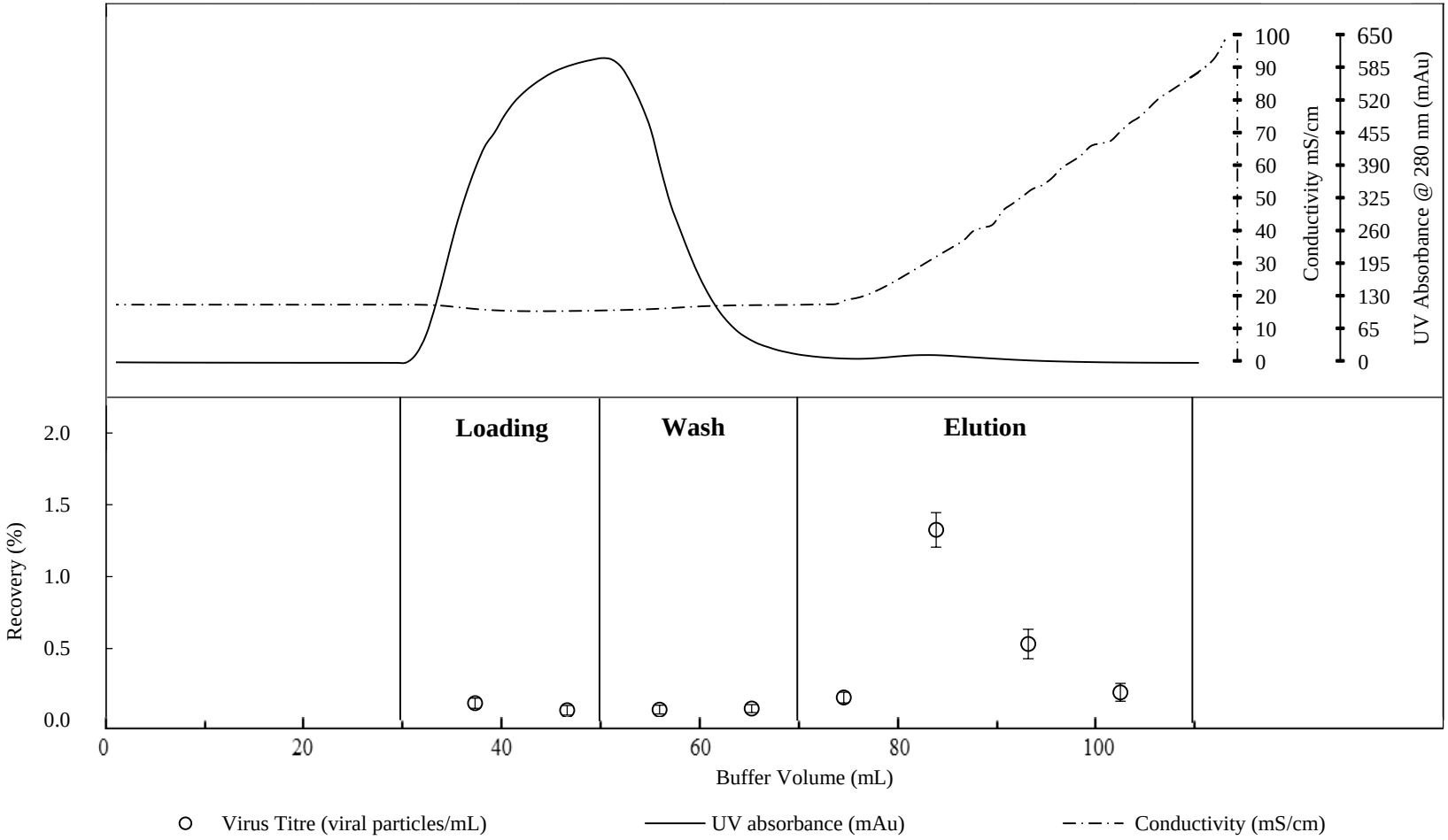

Figure 4-2 UV absorbance and conductivity profile and virus yield. 20 mL 5X diluted virus loading solution followed by 20 mL wash and 40 mL elution with NaCl concentration increasing from 0.2 M to 1.5 M using a 50 mM Natrix *Quantum* Q anion exchange membrane and Äktaprime FPLC system, exported from PrimeView™ 5.0 (GE Health Care, Mississauga, ON, Canada). Data points represent virus recovery (n=2) in individual fractions collected over the course of the process, obtained using BD FACSCalibur flow cytometry, CellQuest Pro and Flowjo software.

4.2.2.3 Loading conductivity

The conductivity of the loading solution was adjusted to 15.4 mS/cm, which was close to those in published data (Gerster et al., 2013; Vicente et al., 2008).

4.2.2.4 Virus breakthrough

In terms of evaluating the feasibility, a question must be asked: is the membrane able to capture viruses from contaminants? To answer this, virus breakthrough was determined by quantifying the virus in the flow-through samples during the loading and wash steps. The results showed that a total of 0.34 ± 0.13 % (n=2) of the loaded virus was lost during the loading and washing steps with host contaminant protein. Compared to generally reported virus breakthrough, which varies from 1% to 10% (Gerster et al., 2013; Grein et al., 2012; Vicente et al., 2009), the low virus breakthrough using the current membrane indicated remarkable selectivity towards the baculovirus.

4.2.2.5 Virus recovery

As shown in Figure 4-2, the total virus recovery in the four elution fractions was 2.21 %. When looking at virus recoveries from individual fractions, fraction #6 reported the highest virus recovery (1.33 ± 0.12 %, n=2), followed by fractions #7 and #8 with 0.53 ± 0.10 % (n=2) and 0.19 ± 0.06 % (n=2), respectively.

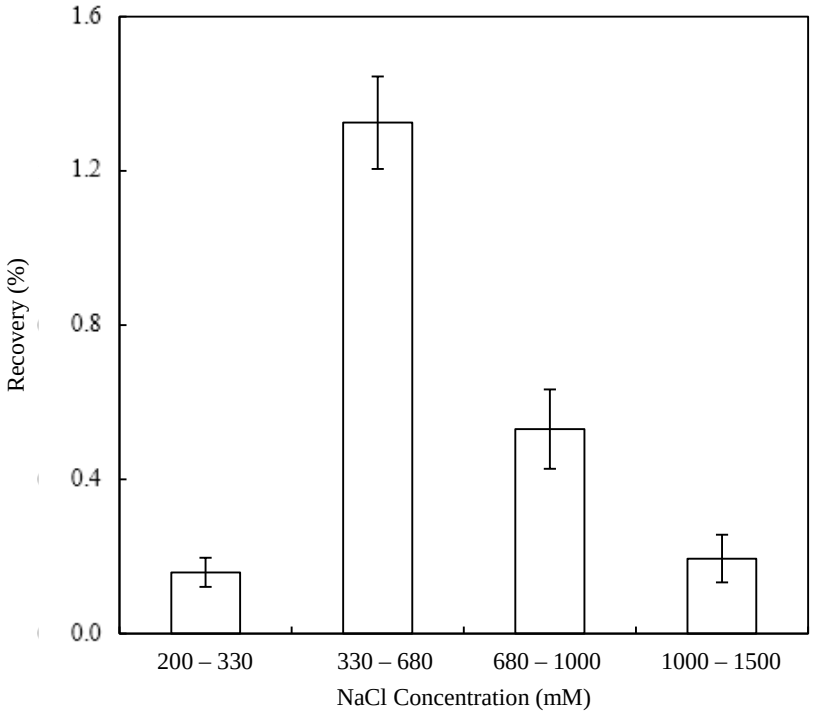

Figure 4-3 Virus recovery (n=2) versus average NaCl concentration over the course of fraction 5 (200 mM to 330 mM), fraction 6 (330 mM to 680 mM NaCl), fraction 7 (680 mM to 1000 mM NaCl) and fraction 8 (1000 mM to 1500 mM NaCl) in elution step of 20mL 5X diluted virus loading purification with linear gradient elution using 50mm Natrix *Quantum* Q anion exchange membrane and Äktaprime FPLC system.

To correlate NaCl concentrations with the effect of virus recovery, the NaCl concentration ranges of the four elution fractions were identified: 200 to 330 mM NaCl (17 – 28 mS/cm), 330 to 680 mM NaCl (28 – 55 mS/cm), 680 mM to 1 M NaCl (55 – 72 mS/cm), and 1 to 1.5 M NaCl (72 – 100 mS/cm). It was expected that stronger NaCl concentrations would result in higher virus recovery, as the higher NaCl concentrations would present enhanced competition to the virus-exchanger interaction. Instead, the profile showed in Figure 4-3 indicates that virus recovery improved when the NaCl concentration increased from 200 mM to 680 mM NaCl and declined when the buffer's NaCl became more concentrated, indicating the higher ionic strength did not promote virus recovery.

4.2.3 Step gradient NaCl operation

To further investigate this system, a step gradient NaCl elution method was also conducted.

4.2.3.1 Step gradient elution

The idea of building up step gradient NaCl elution is to maximize the contact time of the membrane with the NaCl concentrations that favors virus recovery. Therefore, in contrast to linear gradient elution where the eluting buffer's NaCl concentration increased gradually, the step gradient resulted in stepwise changes in buffer NaCl concentration for certain stages.

4.2.3.2 Purification process

Figure 4-4 summarizes the process profile for this trial. 30 mL of equilibration buffer passed the membrane to equilibrate the anion exchange media. Then 20 mL of 5X diluted virus solution were run through the membrane. Conductivity dropped throughout the loading process as the ionic strength of the virus loading solution was lower than that of the equilibration buffer. Two-stage washing with 10 mL wash buffer # 1 and 10 mL of wash buffer # 2 cleared the membrane of any residual supernatant solution, as indicated by the declining portion of UV absorbance following the loading process.

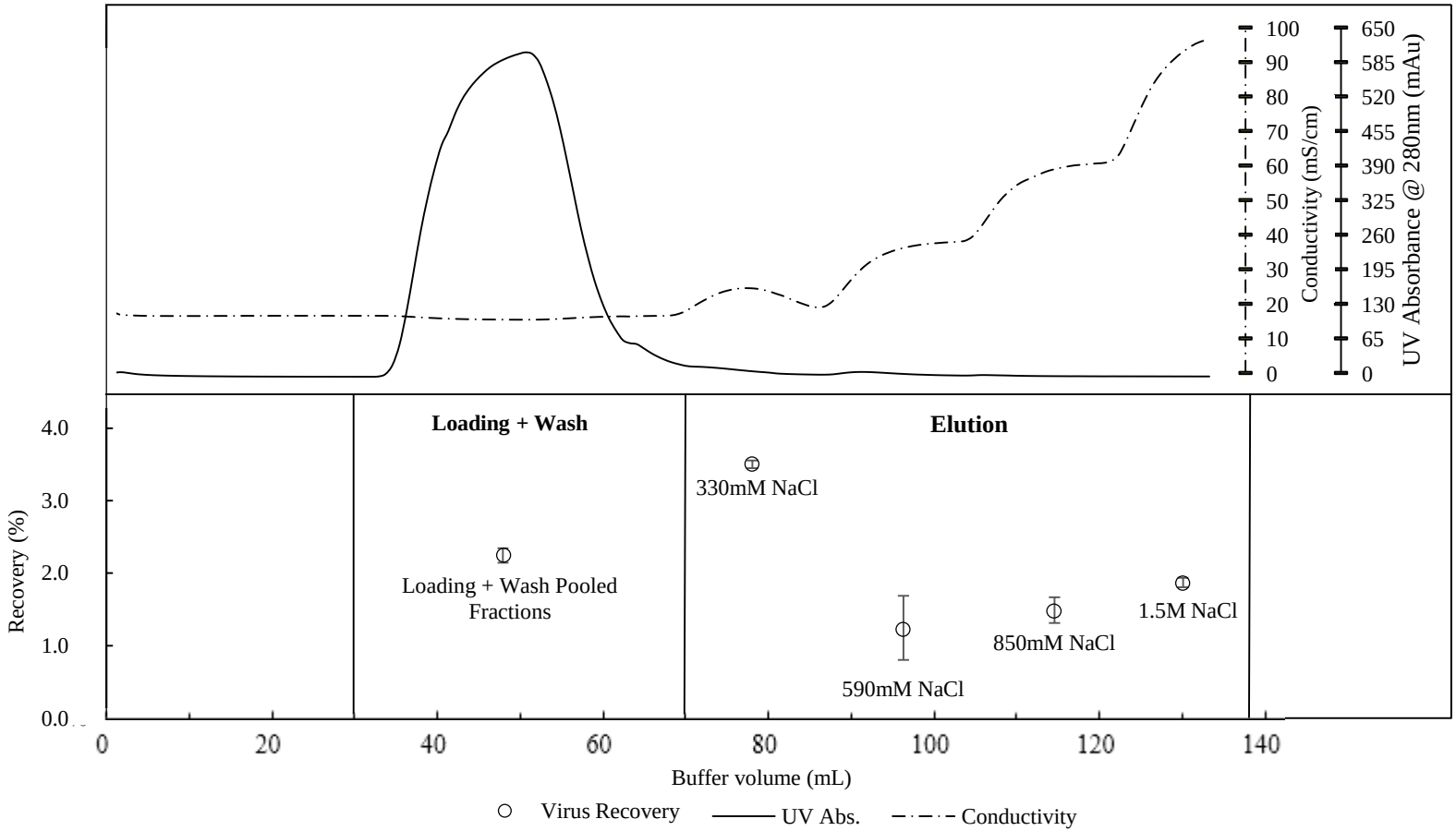

Figure 4-4 Online UV absorbance and conductivity profile of 20 mL 5X diluted virus loading purification with 20 mL wash and 80 mL step gradient elution at 330 mM NaCl, 590 mM NaCl, 850 mM NaCl, and 1500 mM NaCl using a 50mM Natrix *Quantum* Q anion exchange membrane and Äktaprime FPLC system, exported from PrimeView™ 5.0 (GE Health Care, Mississauga, ON, Canada). Data points represent virus recovery (n=2) in pooled fractions during loading and wash, 330 mM NaCl elution step, 590 mM elution step, 850 mM elution step and 1500 mM NaCl, respectively, obtained using BD FACSCalibur flow cytometry, CellQuest Pro and Flowjo software.

Based on linear gradient elution studies, four elution steps were determined at NaCl concentrations of 330 mM (28 mS/cm), 590 mM (49 mS/cm), 850 mM (64 mS/cm) and 1.5 M NaCl (100 mS/cm). The step-like conductivity curve reflects the stepwise changes in NaCl concentration. The length of each step was extended to 25 bed volumes (20 mL), producing an overall process length of 100 bed volumes (80 mL).

4.2.3.3 Virus loss in loading and wash

The total quantity virus recovered during the loading and wash steps was 2.24 %. The anion exchange media showed consistency in successful virus binding and maintained strong interaction with the virus during wash conditions.

4.2.3.4 Virus recovery

Based on the discussion in the previous linear gradient study, the NaCl concentration range of 330 mM – 660 mM NaCl, which resulted in the highest recover, was differentiated into two levels: 330 mM and 590 mM. Further NaCl steps were determined at 850 mM and 1.5 M NaCl. The quantitation by flow cytometry indicated an overall recovery of 8.11 ± 0.68 % (n=2).

There have been studies showing virus recovery from 60 % to 80 % (Gerster et al., 2013; Grein et al., 2012; Vicente et al., 2009) using anion exchange processes, the low virus recovery from the current process needs extensive review. To ensure that those losses were real, a significant study surrounding the quantification of the virus was undertaken (Appendix A).

4.2.3.5 Protein analysis

The samples were also subjected to total protein assays and electrophoresis analysis, to further reveal the process' performance. The samples were prepared in duplicate for Micro BCA assay. The total protein shows that the total protein content in the virus loading solution was 9567 ± 22 μg (n=2).

A total of 8180 ± 100 μg (n=2) protein was removed through the loading and wash processes. The total protein in the 330 mM NaCl elution fraction was 117 ± 8 μg (n=2) while other elution fractions' protein levels were below the detection limit.

The SDS-PAGE results showed that the flow-through samples have a strong band between 60 and 70 kDa but a gp64 protein band is not identifiable in the western blot results, which implied that the baculovirus major gp64 protein was not at significant level in the flow-through (Loading 1, Loading 2, Wash 1, and Wash 2) (Figure 4-5).

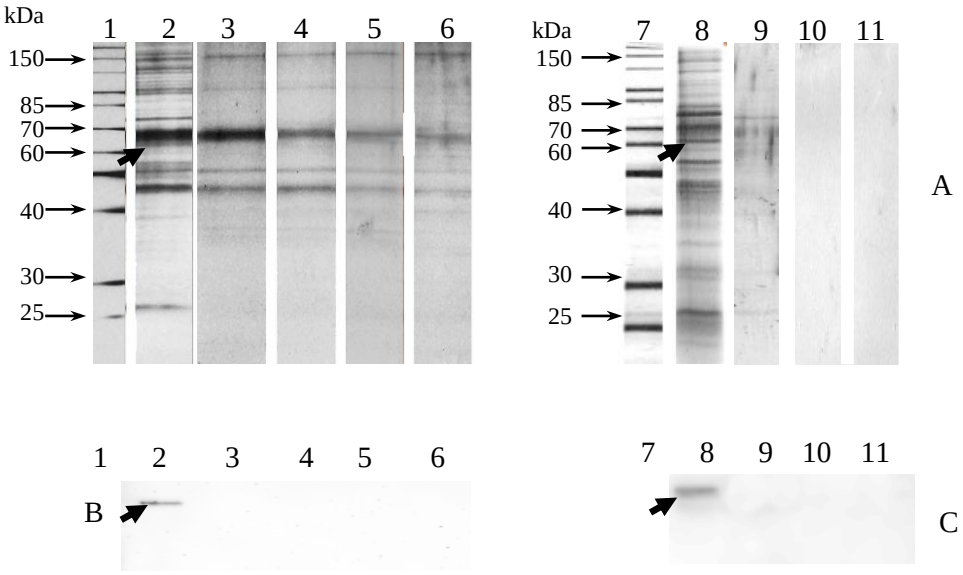

Figure 4-5 A: Silver stained gel after SDS-PAGE, loaded with molecular weight marker (lane 1 and 7), virus loading solution (lane 2), loading fractions (lane 3 and 4), wash fractions (lane 5 and 6), 330 mM, 590 mM, 850 mM, and 1.5 M NaCl Elutions (lane 8 – 11). B: Western blot of virus loading solution and flow-through. C: Western blot of virus loading solution, 330 mM, 590 mM, 850 mM, and 1.5 M NaCl Elutions. The arrows indicate the location of gp64 protein.

The 330 mM NaCl elution lane, compared to the virus solution sample, has a consistent p74 envelope protein (Faulkner, Kuzio, Williams, & Wilson, 1997) band and a weaker impurity band between 60 and 70 kDa, compared to virus solution, while a gp64 protein band became distinct above the 60 kDa marker. Further identification of the gp64 band was done by western blot. Figure 4-5 B and C showed the existence of gp64 envelope proteins in the virus loading solution and 10 % elution, while

the loading permeates did not contain this protein. Though the 30 % elution sample has faint bands in silver staining, due to the low protein concentration in the sample, western blot did not resolve an observable gp64 band.

4.2.4 Membrane cleaning at extreme conditions

Given the low recovery from the current purification process, a membrane cleaning process was investigated to resolve the virus binding issue with this membrane. High NaCl concentrations and low pHs are often used for membrane cleaning procedures. The surface charge of the baculovirus' average protein is positive at pH 5.0. 3 M NaCl is the highest concentration compatible with the membrane material. The cleaning buffer was to ensure least binding interaction between the bound viruses and the membrane ligand and provide strongest electrostatic competitors. Therefore, the 50 mm Natrix *Quantum* Q anion exchange membrane used in the step gradient elution study was subjected to a cleaning process with a cleaning buffer, consisting of 3 M NaCl and 30 mM HEPES at pH 5.0.

4.2.4.1 Cleaning process

30 mL of the cleaning buffer was passed through the used membrane from the step gradient operation at a flow rate of 1 mL/min to ensure sufficient contact time between the buffer and the membrane.

Virus titration has been done to the fractions collected over the course of the process and the results are summarized in Figure 4-6. The fraction-by-fraction virus recovery was declining during the process from 3.75 $\pm$ 0.47 % (n=2) to 0.13 $\pm$ 0.04 % (n=2), respectively. The total recovery from this cleaning process was 6.80 % $\pm$ 1.35 % (n=2). Recall that the step-gradient recovered ~ 8.11 % of the bound viruses, there was still ~ 85 % of the loaded viruses remaining in the membrane.

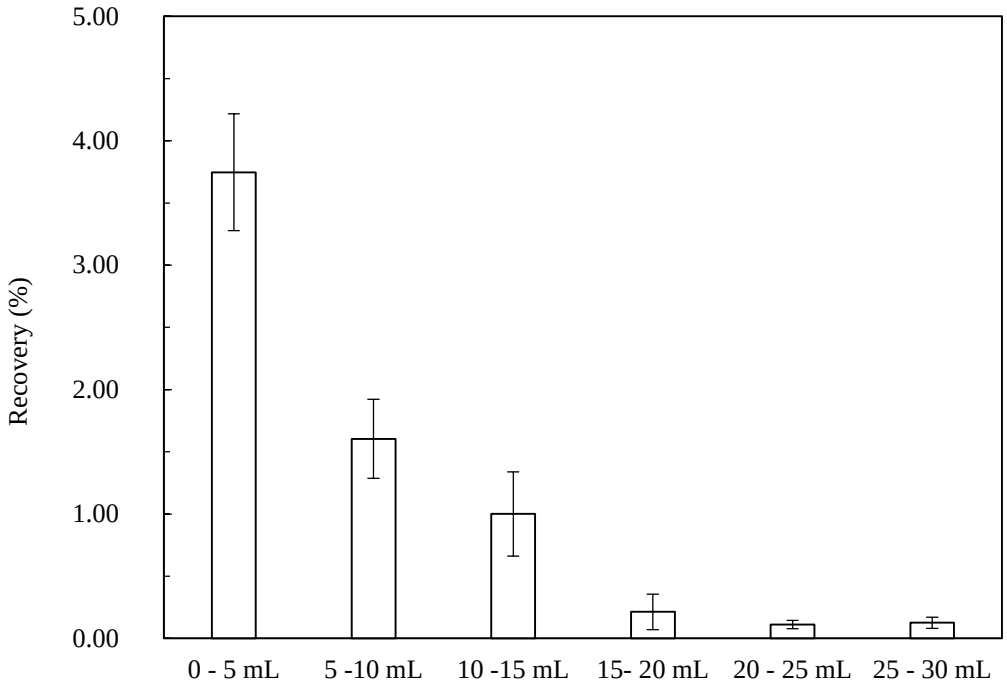

Figure 4-6 Virus titration from fractions collected during the cleaning process using flow cytometric assay. Fractions were collected 5mL each. Error bars indicate standard error for n=2.

It has been reported that anion exchange media (membrane or monolith) can be regenerated with 1.5 M NaCl at most (Gerster et al., 2013; Vicente et al., 2009). At the current cleaning conditions of 3 M NaCl and pH 5.0, any electrostatic binding should be overcome. However, most of viruses were not able to be recovered. Further investigation into the recovery issue is needed regarding the potential physical hindrance using the Natrix *Quantum* Q membranes.

Chapter 5

Reverse-Flow Elution Operations for the Process Development of Baculovirus Purification using a Novel Strong Anion Exchange Membrane Chromatography

5.1 Overview

Investigation of the potential transport hindrance of viral particles during the process was carried out by evaluating virus yields using a reverse-flow elution method. If transport hindrance is associated with the baculovirus particles during the current process, the captured viruses are assumed to be trapped at the near-surface region of the membrane and their transport towards deeper section of the membrane is limited. To recover these particles, the buffer flow is reversed such that NaCl buffer enters the membrane at the outlet and exits at the inlet. It is expected that the reverse-flow elution will boost virus recovery.

5.2 Materials and methods

5.2.1 Reverse-flow

Given that the current chromatography system's flow direction cannot be changed automatically, to achieve reverse-flow elution, the membrane was manually reinstalled in a bottom-up position as shown in Figure 3-2b. Five-fold dilution was applied to the virus supernatant solution by adding the equilibration buffer. Viruses were captured while passing through the membrane by anion exchange ligands. The remaining supernatant solution in the membrane was cleaned by a two-stage wash step using wash buffer #1, consisting of 30 mM HEPES and 200 mM NaCl at pH 6.9 and wash buffer #2 consisting of 30 mM HEPES and 200 mM NaCl at pH 6.0.

At the end of washing process, the system was paused and the membrane was disconnected from the flow path to re-install in the bottom-up position. Then the process was resumed to start the elution process. The membrane position was kept as reversed throughout the rest of the process.

5.3 Results and discussion

5.3.1 Linear gradient reverse-flow elution

5.3.1.1 Purification process

The online monitoring profile is summarized in Figure 5-1. Membrane equilibration was done with consumption of 36 mL of equilibration buffer prior to virus loading. Starting from the 36 mL volume mark in the upper x axis, the UV absorbance curve rose as the protein content became abundant in the permeating flow, when the virus solution was being passed through the membrane until a maximum was reached, at 56 mL.

The increase in UV absorbance corresponded to the volume of loading solution, which was 20 mL. Then UV absorbance began to decline as the wash steps were initiated and gradually removed the remaining contaminant protein in the membrane. After the membrane was washed with roughly 25 mL of wash buffer, UV absorbance reached a baseline indicating minimal protein content in the downstream flow. Then the operation was paused and the membrane was disconnected from the flow path and reinstalled in the position shown in Figure 3-2b, to allow the upstream buffer flow to permeate the membrane from its outlet to inlet. Conductivity increased because of the linear gradient that was being applied for the elution. A local peak appeared in the UV absorbance during the initial portion of the conductivity increase suggests protein being removed from the membrane.

5.3.1.2 Effect of reverse-flow

The influence of modifying the flow direction across the membrane was evaluated in terms of virus recovery. The virus titre of the fractions collected after flow reversion is shown as bar charts in Figure 5-1. As only the procedure for elution was modified from the normal flow operation, the loading process presented consistent minimal virus loss (3.60 % $\pm$ 0.85 %, n=2). Similar to normal flow gradient elution, a local recovery peak occurred in the first 0 % - 10 % conductivity increase of the process, which corresponds to a sodium chloride concentration range of 200 mM to 330 mM. The recovery of the corresponding fraction was 21 $\pm$ 1 % (n=2).

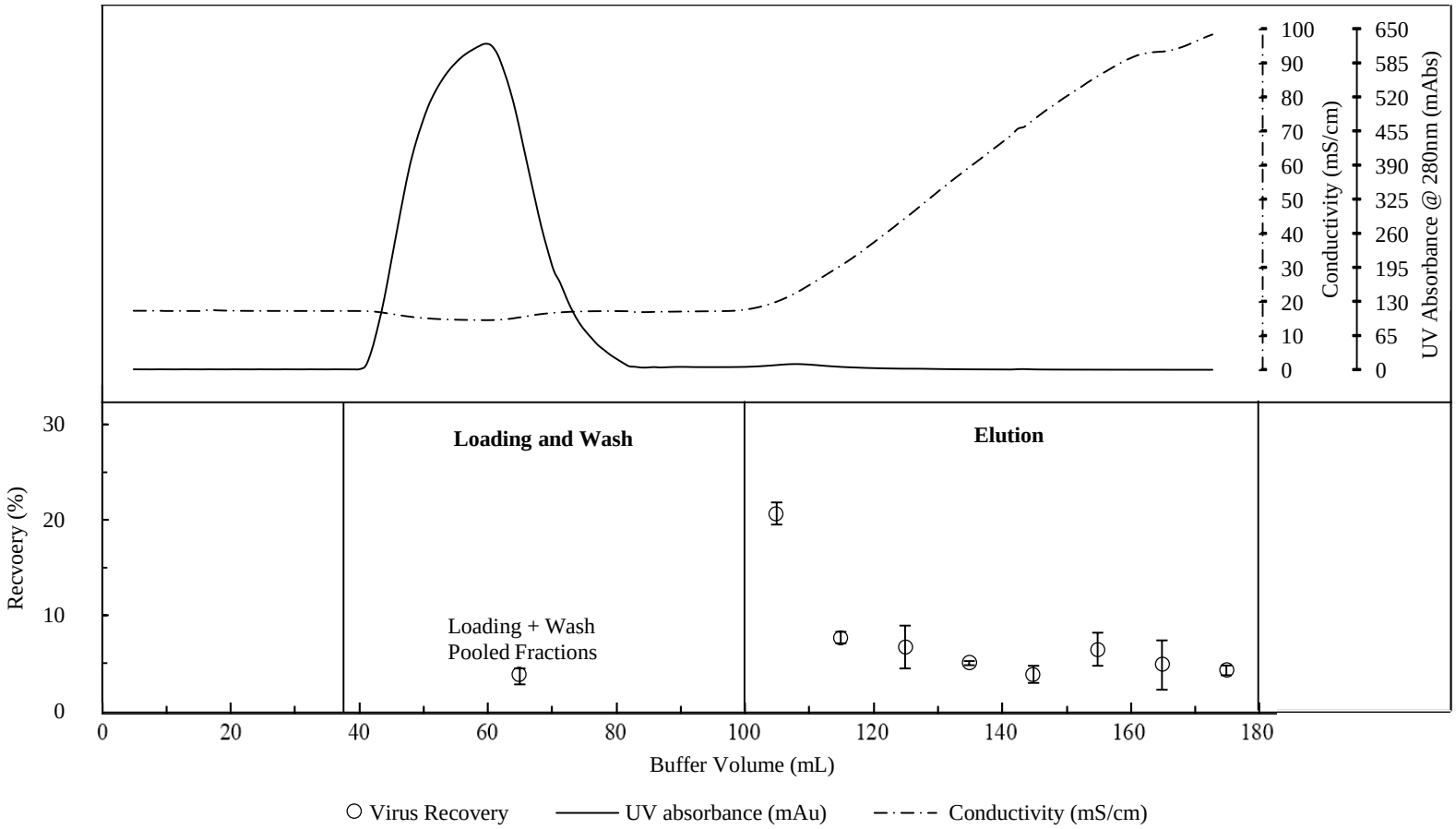

Figure 5-1 UV absorbance and conductivity profile of 20mL 5X diluted virus loading purification process operated with reverse-flow linear gradient NaCl elution from 200mM to 1500mM NaCl over a length of 80mL at flow rate of 4mL/min using 50mM Natrix *Quantum* Q anion exchange membrane with Äktaprime FPLC system exported from PrimeView™ 5.0 (GE Health Care, Mississauga, ON, Canada). Data points reflect virus recovery (n=2) in pooled fraction during loading and wash, and individual fractions during elution, obtained using BD FACSCalibur flow cytometry, CellQuest Pro and Flowjo software.

The overall process recovery was identified as 59 % ± 14 % (n=2), showing a substantial enhancement in recovery compared to the recovery from normal flow linear elution (2 %). The recoveries were higher over the entire process comparing to those from the normal flow operation (Figure 5-2). Moreover, the recovery is also significantly higher than that achieved in the cleaning process. This finding further demonstrated that the virus recovery issue was a result of "fouling" (external accumulation) towards baculoviruses rather than irreversible or extremely strong binding.

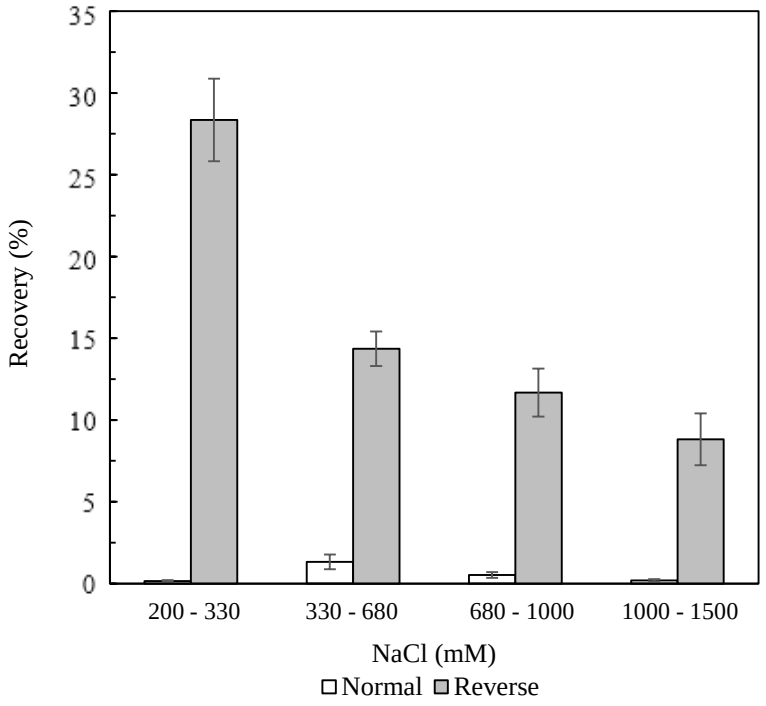

Figure 5-2 "Reverse" represents virus yield achieved in linear gradient NaCl elution during salt ranges of 200 mM NaCl to 330 mM NaCl, 330 mM NaCl to 680 mM NaCl, 680 mM NaCl to 1000 mM NaCl and 1000 mM NaCl to 1500 mM NaCl, respectively, from 20 mL 5 X diluted virus loading purification process using reverse-flow linear gradient elution process. "Normal" represents virus yield achieved in linear gradient NaCl elution during salt ranges of 200 mM NaCl to 330 mM NaCl, 330 mM NaCl to 680 mM NaCl, 680 mM NaCl to 1000 mM NaCl and 1000 mM NaCl to 1500 mM NaCl respectively from the 20 mL 5X diluted virus loading purification process using normal flow linear gradient elution process.Step gradient elution with reverse-flow operation. Error bars indicate standard error for n=2.

5.3.2 Step gradient elution

5.3.2.1 Purification process

The membrane was firstly installed in a normal flow position, as shown in Figure 3-2a. 30 mL of equilibration buffer was driven through the membrane by the ÄKTAPrime™ plus (GE Healthcare, Mississauga, ON, Canada) chromatography system. The process profile is shown in Figure 5-3. The UV absorbance and conductivity remained stable throughout this step. The virus loading was initiated as the virus solution flew through the membrane along with an increase in UV absorbance and a slight reduction in flow conductivity (17.3 mS/cm to 15 mS/cm). The UV absorbance indicated abundant protein content in the downstream. After 20 mL of virus solution was loaded, the wash buffer was introduced through the membrane for cleaning. The decline in UV absorbance reflected the decrease in protein concentration in the buffer flow with the progress of the wash process until the absorbance reached its initial baseline. Then the operation was paused and the membrane was disconnected and reinstalled in a bottom-up position.

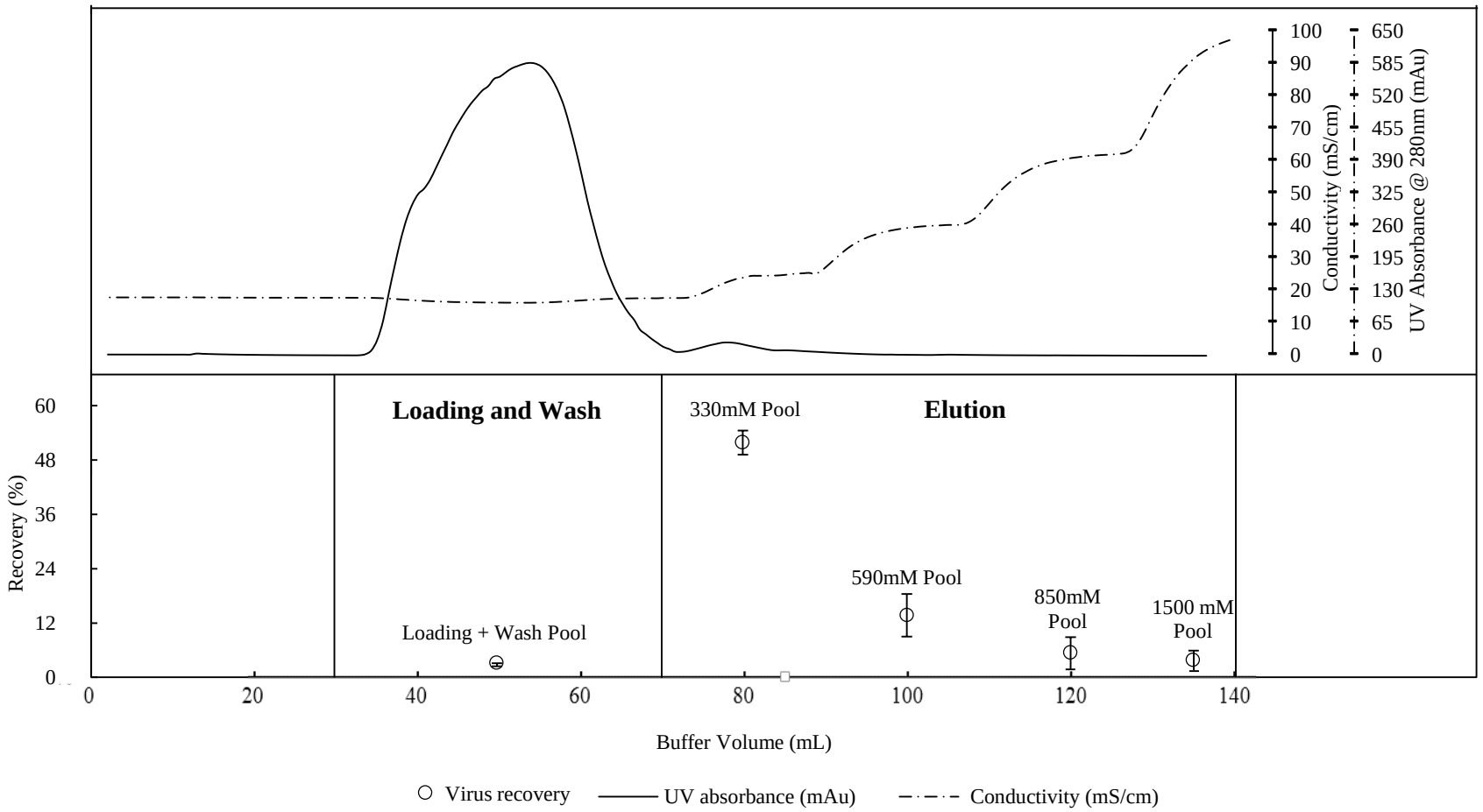

Figure 5-3 UV absorbance and conductivity profile exported by PrimeView 5.0 from 20 mL 5 X diluted virus loading purification process operated with reverse-flow step gradient elution using 50 mm Natrix *Quantum* Q anion exchange membrane and ÄKTAPrime FPLC system. Data points reflect virus recovery from pooled fractions during loading and wash, 330 mM NaCl elution, 590 mM NaCl elution, 850 mM NaCl elution and 1500 mM NaCl elution, respectively (n=2).

A step gradient with pre-established NaCl levels of 330 mM NaCl, 590 mM NaCl, 850 mM NaCl, and 1500 mM NaCl was used in the reverse-flow elution. The conductivity curve reflected the stepwise increase in NaCl concentration. Another UV increase, but one with a much smaller magnitude, appeared during the initial portion of the 330 mM NaCl elution step, implying protein species in the permeating flow. Then the UV curve kept declining until the end of the process. An aliquot was taken from each sample and subjected to flow cytometric virus quantitation (Figure 5-3).

As the reverse-flow operation was conducted at the beginning of the elution process, the loading and wash procedures remained unchanged and similar to those in previous trials. They showed high virus capture efficiency, which agreed with existing results. A virus loss of 2.79 ± 0.35 % (n=2) was determined from the pooled fractions of loading and wash processes.

5.3.2.2 Effect of reverse flow

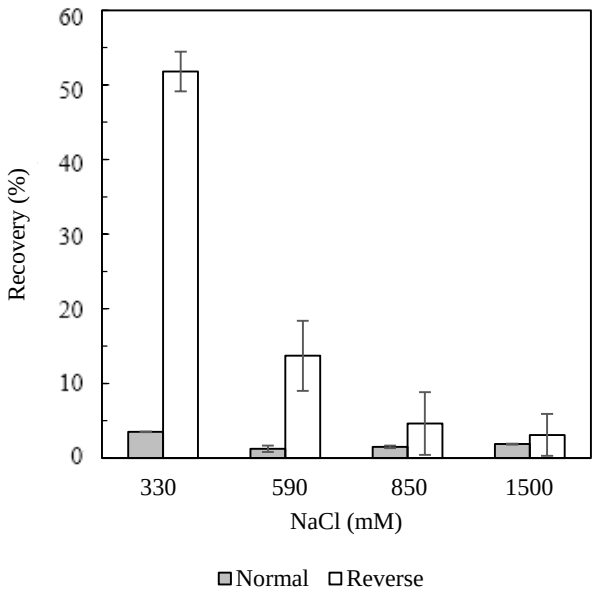

Figure 5-4 “Reverse” represents virus yield achieved in elution step at salt levels of 330 mM, 590 mM, 850 mM and 1500 mM NaCl, respectively, from 20 mL 5 X diluted virus loading purification process using reverse-flow elution process. “Normal” represents virus yield achieved in the elution step at salt levels of 330 mM, 590 mM, 850 mM and 1500 mM NaCl, respectively, from 20 mL 5 X diluted virus-loading purification process using normal flow elution process. Error bars indicate standard error for n=2.

The highest recovery was obtained with an elution of 330 mM NaCl (51 % ± 2 %). At 590 mM NaCl, the recovery was 13 % ± 4 %. At 850 mM NaCl and 1.5M NaCl, 4 % ± 4 % and 3 % ± 2 % were recovered. Compared to normal flow elution results, as shown in Figure 5-4, virus recovery was significantly improved by reversing the flow through the membrane cartridge.

5.3.2.3 Effect of step gradient

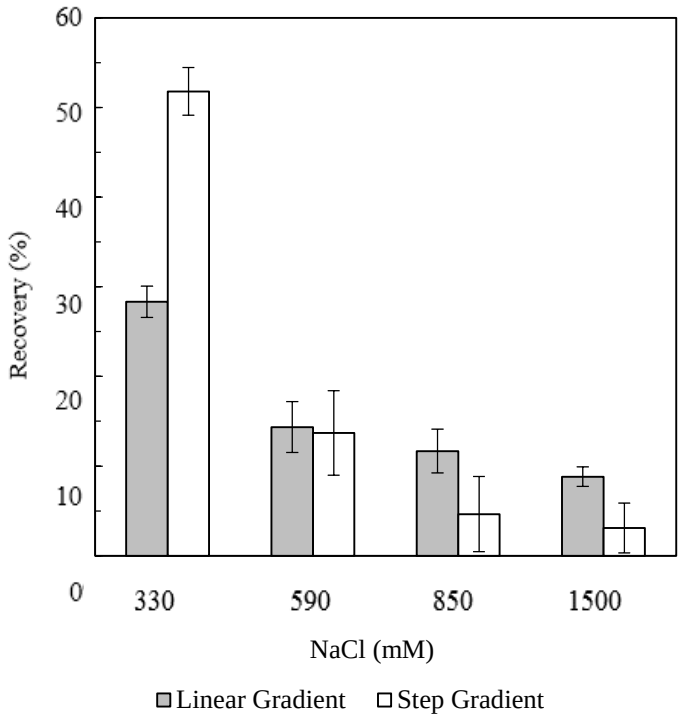

Figure 5-5 Comparison of recoveries at different NaCl levels from linear gradient and step gradient operations (n=2). The recoveries of linear gradient correspond to the fractions collected at salt ranges of 200 – 330 mM, 3330 – 680 mM, 680 – 850 mM, and 850 – 1500 mM. Error bars indicate standard error for n=2.

Through the step gradient operation, the process yield improved to 73 ± 8 % ($p > 0.10$). As shown in Figure 5-5, the virus recovered with 330 mM NaCl in step gradient operation increased 1.8 fold, compared to those recovered from 200 – 330 M NaCl in the linear gradient operation ($p < 0.01$).

5.3.2.4 Protein analysis

The samples collected from the reverse-flow process were analyzed using Micro BCA assay, SDS-PAGE, silver staining, and western blot. The total protein assay showed that 6412 ± 7 μg of protein was removed when the viruses were being loaded onto the membrane. The wash process further removed 1462 ± 71 μg of proteins, together with the loading permeate representing 84 % of the total protein in the virus loading solution (9200 ± 19 μg). The 330 mM elution contained 182 ± 6 μg of protein, which accounted for 2 % of the total protein in the virus loading solution. The fractions collected in higher NaCl concentrations (590 mM, 850 mM, and 1.5M) were below the detection limit.

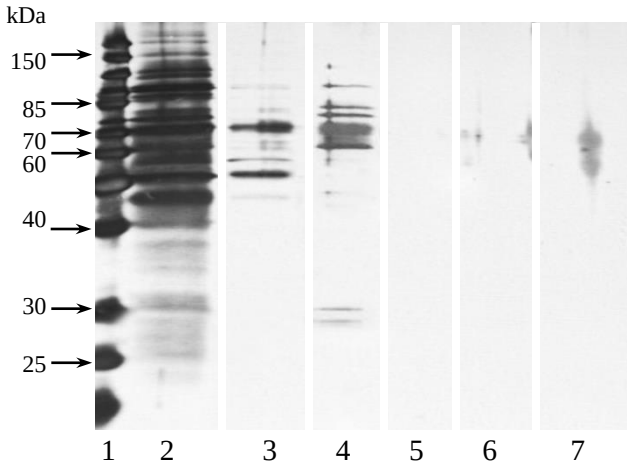

Figure 5-6 Silver-stained SDS-PAGE gel loaded with (from left to right): molecular weight marker (lane 1), virus loading solution (lane 2), loading and wash fractions pool (lane 3), 330 mM NaCl elution fractions pool (lane 4), 590 mM NaCl elution fractions pool (lane 5), 850 mM NaCl elution fractions pool (lane 6), and 1.5 M NaCl elution fractions pool (lane 7).

Figure 5-6 is the silver-stained gel SDS-PAGE, loaded with fraction samples. The loading and wash fractions samples had similar protein composition in reverse and normal flow operation (Figure 4-5). A major strong polypeptide band appeared at 70 kDa and a minor polypeptide band was identified at roughly 50 kDa. The gp64 protein band was absent in the loading + wash fractions pool. In the 330 mM elution sample, several distinct bands were identified: p78 capsid protein, 70 kDa impurities, and

gp64 protein. Compared to the 330 mM NaCl elution from the normal flow operation, the elution process with reversed flow direction reduced impurity compositions in the eluent, as shown in the reduction of protein bands in the 330 mM NaCl. The protein compositions in the fractions collected at higher salt concentrations were below the detecting limit.

Chapter 6

Conclusions and Recommendations

6.1 Conclusions

The Natrix *Quantum* Q anion exchange membranes are not applicable for the purification of baculovirus using regular direct-flow chromatography. There is major physical hindrance that prevents the baculovirus from transferring through the membrane.

This baculovirus-retaining issue can be overcome by introducing buffer flow from the opposite side of the surface where baculovirus was retained. The virus recovery significantly increased when reverse-flow elution was applied for linear gradient elution. The same NaCl steps from the normal flow step gradient operation were applied in the reverse-flow step gradient process. Virus recovery was further improved using the step NaCl gradient elution, which led to a final virus recovery of ~73%.

The protein level of the original virus solution was reduced as 85 % of the initial protein was removed, while baculovirus proteins were well conserved.

6.2 Recommendations

1. Attempt process design with cross flow operation. Given the infeasibility using dead-end operation mode, cross flow operation can potentially circumvent the physical hindrance issue, as cross flow did not necessarily require the target molecule to transport through the entire membrane matrix.
2. Determine binding capacity using free membrane material. The binding capacity and dynamics can be evaluated using free membrane material with stirred cell device and batch adsorption operation.
3. Investigate the activity of purified virus. In addition to virus recovery, the activity of recovered virus is important for future applications. Various infectious assays including TCID50 and plaque assays can be used for evaluation of infectious virus recovery.
4. Evaluate the DNA levels before and after purification. Free DNA species is another major source of contaminant in the initial virus solution. The suspended DNA levels can be determined using SYBR Green I at 488 nm excitation and 528 nm emission wavelength (Grein et al., 2012).

References

Andujar-Sánchez, M., Cámara-Artigas, A., & Jara-Pérez, V. (2003). Purification of angiotensin I converting enzyme from pig lung using concanavalin-A sepharose chromatography. *Journal of chromatography. B, Analytical technologies in the biomedical and life sciences*, *783*(1), 247–252.

Aucoin, M. G., Mena, J. A., & Kamen, A. A. (2010). Bioprocessing of baculovirus vectors: a review. *Current Gene Therapy*, *10*(3), 174–186.

Barsoum, J. (1999). Concentration of recombinant baculovirus by cation-exchange chromatography. *BioTechniques*, *26*(5), 834–6, 838, 840.

Barsoum, J., Brown, R., McKee, M., & Boyce, F. M. (1997). Efficient transduction of mammalian cells by a recombinant baculovirus having the vesicular stomatitis virus G glycoprotein. *Human Gene Therapy*, *8*(17), 2011–2018.

BD Bioscience. (2007). BD FACSCalibur Flow Cytometry System Technical Specifications.

Beckman Coulter. (2011). Flow-Set Pro Fluorospheres, 1–3.

Blissard, G. W., & Wenz, J. R. (1992). Baculovirus gp64 envelope glycoprotein is sufficient to mediate pH-dependent membrane fusion. *Journal of Virology*, *66*(11), 6829–6835.

Bonnerjea, J., Oh, S., Hoare, M., & Dunnill, P. (1986). Protein Purification: The Right Step at the Right Time. *Bio/Technology*, *4*(11), 954–958.

Boyce, F. M., & Bucher, N. L. (1996). Baculovirus-mediated gene transfer into mammalian cells. *Proceedings of the National Academy of Sciences*, *93*(6), 2348–2352.

Brandt, S., Goffe, R. A., Kessler, S. B., O'Connor, J. L., & Zale, S. E. (1988). Membrane-Based Affinity Technology for Commercial Scale Purifications. *Bio/Technology*, *6*(7), 779–782.

Briefs, K.-G., & Kula, M.-R. (1992). Fast protein chromatography on analytical and preparative scale using modified microporous membranes. *Chemical Engineering Science*, *47*(1), 141–149.

Brussaard, C. P. D., Marie, D., & Bratbak, G. (2000). Flow cytometric detection of viruses. *Journal of Virological Methods*, *85*(1-2), 175–182.

Carinhas, N., Bernal, V., Yokomizo, A. Y., Carrondo, M. J. T., Oliveira, R., & Alves, P. M. (2009). Baculovirus production for gene therapy: the role of cell density, multiplicity of infection and medium exchange. *Applied Microbiology and Biotechnology*, *81*(6), 1041–1049.

Caron, A. W., Archambault, J., & Massie, B. (1990). High-level recombinant protein production in bioreactors using the baculovirus-insect cell expression system. *Biotechnology and Bioengineering*, *36*(11), 1133–1140.

Champluvier, B., & Kula, M.-R. (1991). Microfiltration membranes as pseudo-affinity adsorbents: modification and comparison with gel beads. *Journal of Chromatography A*, *539*(2), 315–325.

Chen, G.-Y., Chen, C.-Y., Chang, M. D.-T., Matsuura, Y., & Hu, Y.-C. (2009). Concanavalin A affinity chromatography for efficient baculovirus purification. *Biotechnology Progress*, *25*(6), 1669–1677.

Denizli, A., & Pişkin, E. (2001). Dye-ligand affinity systems. *Journal of Biochemical and Biophysical Methods*, *49*(1-3), 391–416.

Faulkner, P., Kuzio, J., Williams, G. V, & Wilson, J. A. (1997). Analysis of p74, a PDV envelope protein of Autographa californica nucleopolyhedrovirus required for occlusion body infectivity in vivo. *The Journal of general virology*, *78 (Pt 12*, 3091–3100.

Gallagher, S. R. (2006). One-dimensional SDS gel electrophoresis of proteins. *Current Protocols in Molecular Biology / edited by Frederick M. Ausubel ... [et al.]*, *Chapter 10*, Unit 10.2A.

GE Healthcare Bio-Sciences. (2009). *ÄKTAprime™ plus Operating Instructions* (p. 59). Uppsala: GE Healthcare.

Gerster, P., Kopecky, E.-M., Hammerschmidt, N., Klausberger, M., Krammer, F., Grabherr, R., … Jungbauer, A. (2013). Purification of infective baculoviruses by monoliths. *Journal of chromatography. A*, *1290*(null), 36–45.

Ghosh, R. (2002). Protein separation using membrane chromatography: opportunities and challenges. *Journal of Chromatography. A*, *952*(1-2), 13–27.

Grein, T. A., Michalsky, R., Vega López, M., & Czermak, P. (2012). Purification of a recombinant baculovirus of Autographa californica M nucleopolyhedrovirus by ion exchange membrane chromatography. *Journal of Virological Methods*, *183*(2), 117–124.

Guarino, L. (2011). Baculoviruses. In *eLS*. Chichester: John Wiley & Sons, Ltd.

Harrison, R. G., Todd, P., Rudge, S. R., & Petrides, D. P. (2003). *Bioseparations Science and Engineering*. New York: Oxford University Press.

Hensler, W. T., & Agathos, S. N. (1994). Evaluation of monitoring approaches and effects of culture conditions on recombinant protein production in baculovirus-infected insect cells. *Cytotechnology*, *15*(1-3), 177–186.

Hofmann, C. (1995). Efficient Gene Transfer Into Human Hepatocytes by Baculovirus Vectors. *Proceedings of the National Academy of Sciences*, *92*(22), 10099–10103.

Hu, Y. (2005). Baculovirus as a highly efficient expression vector in insect and mammalian cells. *Acta Pharmacologica Sinica*, *26*(4), 405–416.

Ikonomou, L., Schneider, Y.-J., & Agathos, S. N. (2003). Insect cell culture for industrial production of recombinant proteins. *Applied Microbiology and Biotechnology*, *62*(1), 1–20. doi:10.1007/s00253-003-1223-9

Jorio, H., Tran, R., Meghrous, J., Bourget, L., & Kamen, A. (2006). Analysis of baculovirus aggregates using flow cytometry. *Journal of Virological Methods*, *134*(1-2), 8–14.

Klein, E. (2000). Affinity membranes: a 10-year review. *Journal of Membrane Science*, *179*(1-2), 1–27.

Kost, T. A., & Condreay, J. P. (1999). Recombinant baculoviruses as expression vectors for insect and mammalian cells. *Current Opinion in Biotechnology*, *10*(5), 428–433.

Kurien, B. T., & Scofield, R. H. (2006). Western blotting. *Methods (San Diego, Calif.)*, *38*(4), 283–293.

Laemmli, U. K. U. (1970). Cleavage of Structural Proteins during the Assembly of the Head of Bacteriophage T4. *Nature*, *227*(5259), 680–685.

Lesch, H. P., Makkonen, K.-E., Laitinen, A., Määttä, A.-M., Närvänen, O., Airenne, K. J., & Ylä-Herttuala, S. (2011). Requirements for baculoviruses for clinical gene therapy applications. *Journal of Invertebrate Pathology*, *107*, S106–S112.

Maiorella, B., Inlow, D., Shauger, A., & Harano, D. (1988). Large-Scale Insect Cell-Culture for Recombinant Protein Production. *Bio/Technology*, *6*(12), 1406–1410.

McCutchen, B. F., Choudary, P. V., Crenshaw, R., Maddox, D., Kamita, S. G., Palekar, N., … Maeda, S. (1991). Development of a Recombinant Baculovirus Expressing an Insect-Selective Neurotoxin: Potential for Pest Control. *Bio/Technology*, *9*(9), 848–852.

Montgomery, D. C. (2009). Chapter 2 Simple Comparative Experiments. In *Design and Analysis of Experiments* (7th editio., pp. 23–59). Hoboken, NJ: Wiley.

Morenweiser, R. (2005). Downstream processing of viral vectors and vaccines. *Gene Therapy*, *12*, S103–S110.

Moscardi, F. (1999). Assessment of the application of baculoviruses for control of Lepidoptera. *Annual review of entomology*, *44*, 257–289. doi:10.1146/annurev.ento.44.1.257

Natrix Separations. (2008). *50mm Syringe Column Q NX1100 Information Sheet* (p. 2).

Negrete, A., & Kotin, R. M. (2008). Strategies for manufacturing recombinant adeno-associated virus vectors for gene therapy applications exploiting baculovirus technology. *Briefings in Functional Genomics & Proteomics*, *7*(4), 303–311.

O'Reilly, D. R., Miller, L. K., & Luckow, V. A. (1993). *Baculovirus Expression Vectors: A Laboratory Manual* (p. 347). Oxford University Press.

Orr, V., Zhong, L., Moo-Young, M., & Chou, C. P. (2013). Recent advances in bioprocessing application of membrane chromatography. *Biotechnology advances*, *31*(4), 450–465.

Rohrmann, G. F. (1992). Baculovirus structural proteins. *Journal of General Virology*, *73*(4), 749–761.

Roldão, A., Oliveira, R., Carrondo, M. J. T., & Alves, P. M. (2009). Error assessment in recombinant baculovirus titration: evaluation of different methods. *Journal of Virological Methods*, *159*(1), 69–80.

Roldão, A., Vicente, T., Peixoto, C., Carrondo, M. J. T., & Alves, P. M. (2011). Quality control and analytical methods for baculovirus-based products. *Journal of Invertebrate Pathology*, *107*, S94–S105.

Segura, M. M., Kamen, A. A., & Garnier, A. (2011). Overview of current scalable methods for purification of viral vectors. *Methods in Molecular Biology (Clifton, N.J.)*, *737*, 89–116.

Sheehan, D., & O'Sullivan, S. (2004). Fast Protein Liquid Chromatography. In P. Cutler (Ed.), *Protein Purification Protocols SE - 27* (Vol. 244, pp. 253–258). Humana Press.

Shen, C. F. C., Meghrous, J., & Kamen, A. (2002). Quantitation of baculovirus particles by flow cytometry. *Journal of Virological Methods*, *105*(2), 321–330.

Shuler, M. L., Cho, T., Wickham, T., Ogonah, O., Kool, M., Hammer, D. A., … Wood, H. A. (1990). Bioreactor Development for Production of Viral Pesticides or Heterologous Proteins in Insect Cell Cultures. *Annals of the New York Academy of Sciences*, *589*(1 Biochemical E), 399–422.

Striegel, A. M., Yau, W. W., Kirkland, J. J., & Bly, D. D. (2009). Retention. In *Modern Size-Exclusion Liquid Chromatography* (pp. 18–48). John Wiley & Sons, Inc.

Transfiguracion, J., Jorio, H., Meghrous, J., Jacob, D., & Kamen, A. (2007). High yield purification of functional baculovirus vectors by size exclusion chromatography. *Journal of Virological Methods*, *142*(1-2), 21–28.

Transfiguracion, J., Mena, J. A., Aucoin, M. G., & Kamen, A. A. (2011). Development and validation of a HPLC method for the quantification of baculovirus particles. *Journal of chromatography. B, Analytical Technologies in the Biomedical and Life Sciences*, *879*(1), 61–68.

Urh, M., Simpson, D., & Zhao, K. (2009). Affinity chromatography: general methods. *Methods in Enzymology*, *463*, 417–438.

Vicente, T., Fåber, R., Alves, P. M., Carrondo, M. J. T., & Mota, J. P. B. (2011). Impact of ligand density on the optimization of ion-exchange membrane chromatography for viral vector purification. *Biotechnology and Bioengineering*, *108*(6), 1347–1359.

Vicente, T., Mota, J. P. B., Peixoto, C., Alves, P. M., & Carrondo, M. J. T. (2011). Rational design and optimization of downstream processes of virus particles for biopharmaceutical applications: Current advances. *Biotechnology Advances*, *29*(6), 869–878.

Vicente, T., Peixoto, C., Carrondo, M. J. T., & Alves, P. M. (2009). Purification of recombinant baculoviruses for gene therapy using membrane processes. *Gene therapy*, *16*(6), 766–75.

Vicente, T., Peixoto, C., Mota, J. P. B., Carrondo, M. J. T., & Alves, P. M. (2011). Optimizing Downstream Processing of Enveloped Viruses. *Genetic Engineering & Biotechnology News*, *31*(2), 34–35.

Vicente, T., Sousa, M. F. Q., Peixoto, C., Mota, J. P. B., Alves, P. M., & Carrondo, M. J. T. (2008). Anion-exchange membrane chromatography for purification of rotavirus-like particles. *Journal of Membrane Science*, *311*(1-2), 270–283.

Wickham, T. J., & Nemerow, G. R. (1993). Optimization of growth methods and recombinant protein production in BTI-Tn-5B1-4 insect cells using the baculovirus expression system. *Biotechnology Progress*, *9*(1), 25–30.

Wood, H. A., & Granados, R. R. (1991). Genetically engineered baculoviruses as agents for pest control. *Annual Review of Microbiology*, *45*, 69–87.

Wu, C., Soh, K. Y., & Wang, S. (2007). Ion-exchange membrane chromatography method for rapid and efficient purification of recombinant baculovirus and baculovirus gp64 protein. *Human Gene Therapy*, *18*(7), 665–672.

Yang, Y., Lo, S.-L., Yang, J., Yang, J., Goh, S. S. L., Wu, C., … Wang, S. (2009). Polyethylenimine coating to produce serum-resistant baculoviral vectors for in vivo gene delivery. *Biomaterials*, *30*(29), 5767–5774.

Zhong, L., Scharer, J., Moo-Young, M., Fenner, D., Crossley, L., Honeyman, C. H., … Chou, C. P. (2011). Potential application of hydrogel-based strong anion-exchange membrane for plasmid DNA purification. *Journal of chromatography. B, Analytical Technologies in the Biomedical and Life sciences*, *879*(9-10), 564–572.

Appendix A

Calibration and Optimization of BD FACSCalibur Flow Cytometer for In-House Virus Quantitation

A.1 Overview

Flow cytometric virus assays offer a labor-saving, low-variability, and process-efficient way to generate reliable virus titration results (Roldão, Oliveira, Carrondo, & Alves, 2009). A specific flow cytometric method for baculovirus quantitation has been published by Shen et al. (2002). This latter method, however, was developed using an EPICS XL-MCL flow cytometer (Beckman Coulter, Miami, FL) with EXPO™ 32 software, which brings into question how generic is the protocol? Can this method be used with other instruments? In this thesis, the method developed by Shen et al. is used, but particles are analyzed using a BD FACSCalibur Flow Cytometer (BD Biosciences, Mississauga, ON, Canada).

A.2 Materials and methods

A.2.1 Flow cytometry

Baculovirus samples were analyzed using a FACSCalibur Flow Cytometer (BD Biosciences, Mississauga, ON, Canada) equipped with a 15 milli watt 488 nm argon-ion laser.

A.2.1.1 Standardization reagent

Flow-Set™ Pro 3 μm (nomial diameter) Fluorospheres (Beckman Coulter Canada, Missisauga, ON, Canada) were used for day-to-day instrument calibration. The fluorosphere emits fluorescence between 515-800 nm when excited at 488 nm.

A.2.1.2 Flow cytometry analysis

Samples were treated for SYBR Green I staining and then transferred to 5 mL non-sterile disposable BD Falcon™ Polystyrene Round-Bottom Tubes (BD Biosciences, Mississauga, ON, Canada) and analyzed using the flow cytometer (BD Biosciences, Mississauga, ON, Canada). All the samples were prepared in duplicate and measured for 30 s at a flow rate of 12 μL/min. The instrument settings were optimized for consistent quantitation and appropriate resolution, as described in the following section. Flow cytmetry readings were collected using CellQuest Pro (BD Biosciences, Mississauga, ON, Canada), and subsequently processed and analyzed using Flowjo (Treestar Inc., Ashland, OR, United States).

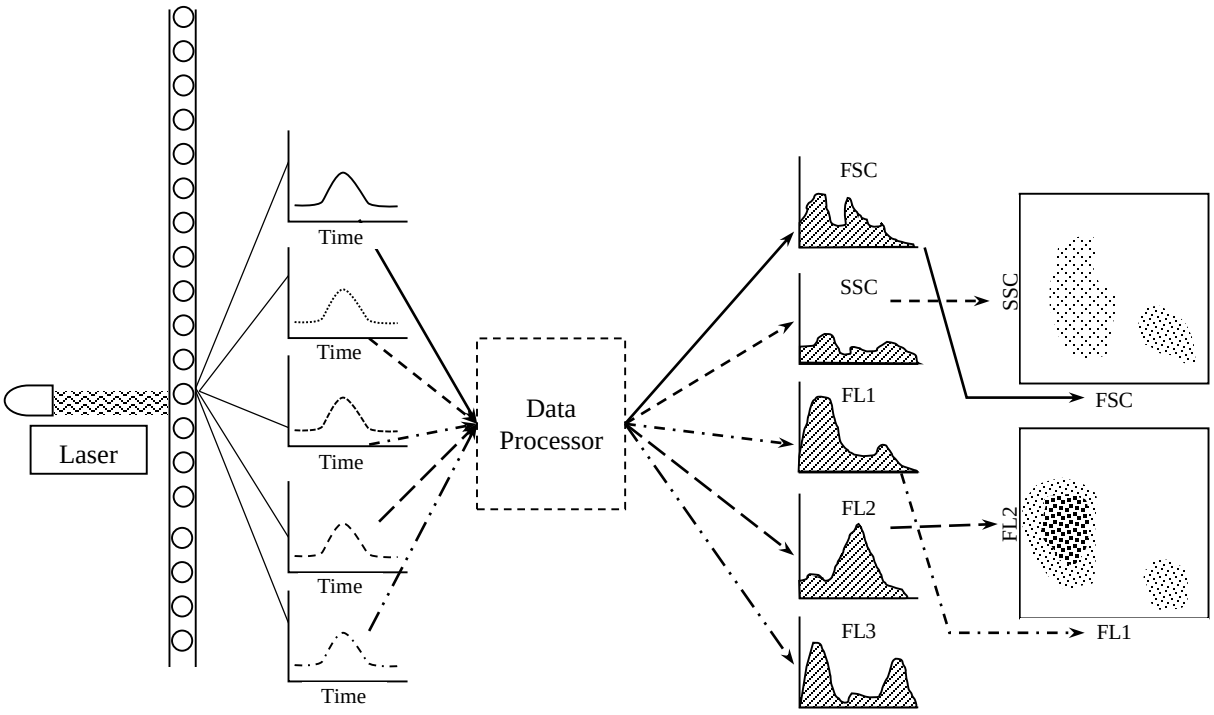

Figure A-1 Data processing of flow cytometer. The laser strikes single partcles to generate emissions at different wavelenghts. The emitted lights are directed by bypass band filters into corresponding detectors and coverted into voltage pulses. Then data processor transforms the voltage signals into digital values and plots the particles as a point with its singal values.

A.3 Results and discussion

A.3.1 Instrument parameters

Instrument settings are critical for the successful application of flow cytometry to virus detection. When a particle is interrogated by the instrument, a number of signals are collected from it, including forward-scatter (FSC), side-scatter (SSC), and laser channels (FL1, FL2, and FL3) (Figure A-1). These parameters are discussed in this section.

A.3.1.1 Scatters

When the laser beam strikes a cell, two kinds of scatters are detected by the sensors (Figure A-2A): forward scatter, which correlates to the relative size of the particle, and side scatter, which refers to granularity or density of the particle. When dealing with viruses, there is little to no forward scatters; however, there is a significant amount of side scatter (Figure A-2B). This side scatter can sometimes be a unique identification of different viruses (Brussaard, Marie, & Bratbak, 2000).

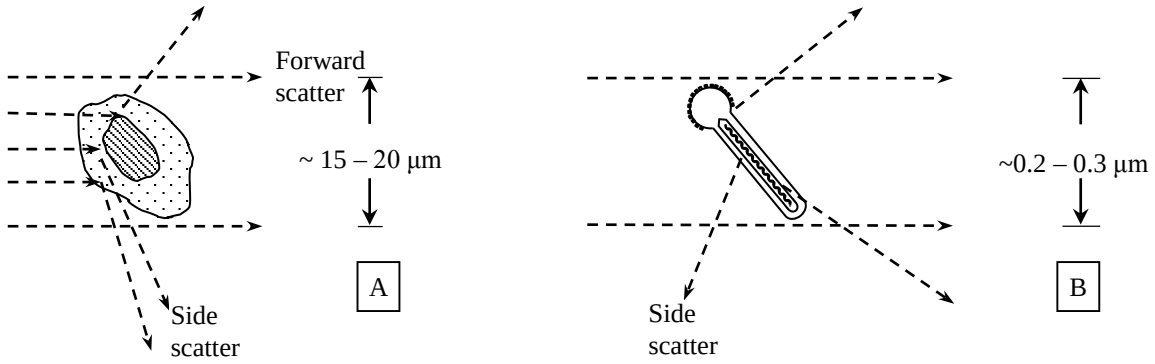

Figure A-2 A. Forward scatter and side scatter generated from a typical cell. B. Forward scatter and side scatter from a baculovirus.

A.3.1.2 Fluorescence

When a fluorochrome absorbs light at certain wavelengths, it is excited and emits fluorescence. The SYBR® green I fluorescent dye used in virus detection emits fluorescence at 520 nm when it binds to DNA and is excited at 488 nm. The emission is collected in the FL1 channel (through a 530 nm bandpass filter).

A.3.1.3 Threshold and voltage

When a sensor receives a light signal, it generates a pulse based on the light intensity and time and converts this pulse into an electric voltage, which will be processed by the electronics system. The electric voltage can be linearly amplified by increasing the detector amplifying voltage.

To eliminate unwanted low voltage noises, the system uses thresholds to screen any possible interference. Basically, any particles, generating signals that below the major threshold, are excluded from data acquisition. A major threshold can be assigned to any one of the parameters. Since the FL1 channel collects most of the viruses' emission, it is therefore set as the major threshold in the study.

A.3.1.4 Data display

As shown in Figure A-1, when a single particle passes the laser beam, a number of light signals are detected, and converted to voltage values by the correspondent sensors and data-processing system, in terms of FSC, SSC, and FL1 to FL3. When a particle suspension is subjected to flow cytometry analysis, the distribution of signals under various types (FSC, SSC, FL1, FL2, and FL3) from the population is obtained as a histogram. By correlating any two of the parameters, a particle is transformed into a point using its parameter values as its position. Therefore, using a two-dimensional dot plot, one can differentiate multiple species within a solution. Additionally, the software's gating function can further extract detailed information for each population such as particle number, fluorescence distribution, scatter distribution, etc.

A.3.2 Detection of fluorospheres

Standardized fluorospheres are important to flow cytometry based methods. It is a calibrating regent that can reflect minor fluctuations in the flow cytometer's flow rates when they are put through the instrument. Due to good uniformity in terms of fluorescent intensity, density and size, a Flow-Set™ Pro Fluorospheres (Beckman Coulter Canada, LP., Mississauga, ON, Canada) solution has been used as a reference to determine instrument settings for baculovirus quantification (Brussaard et al., 2000; Shen et al., 2002).

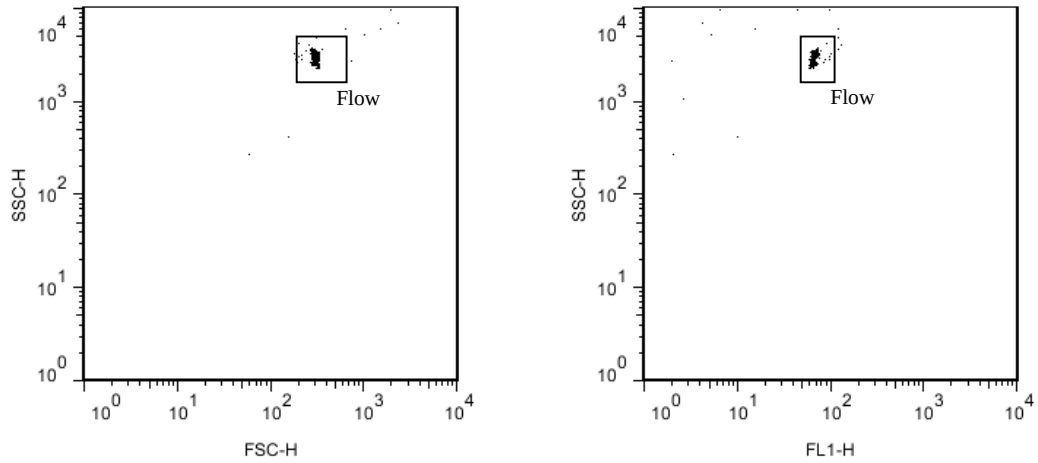

Figure A-3 2-D dot plots during detection of Flow Set in SSC vs. FSC and SSC vs. FL1 scales

The Flow-Set fluorospheres were diluted 20 times and put through the flow cytometer at a flow rate of 12 μL/min (instrument settings given in Table A-1). The major threshold was set to FL1 to eliminate background noise when high FL1 amplifying voltages were used. Upon acquisition, a distinct group of particles was observed. The group can be seen in Figure A-3 as a population of 330 particles from both FSC vs. SSC and SSC vs. FL1 scales. This number was converted with Equation (3-1) to obtain the actual particle concentration in the initial solution. A resulting concentration of 1.1×10^6 particles/mL reflected excellent consistency with the reported concentration of the control (1.0×10^6 particles/mL).

Table A-1 Instrument settings for fluorosphere detection.

Parameter	Value	Threshold
Flow rate	12 μL/min	n/a
FSC	E00	n/a
SSC	330	n/a
FL1	480	52

A.3.3 Finding baculovirus using the flow cytometer

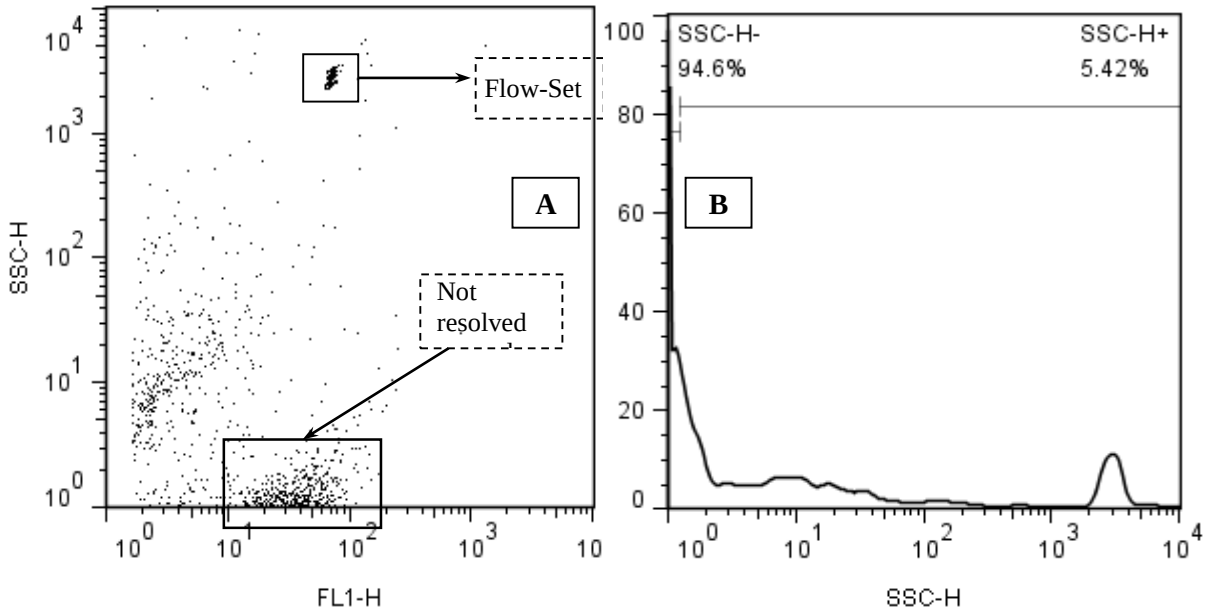

Figure A-4 A. 2-D dot plot at SSC and FL1 scale. An aliquote of 900X diluted baculovirus stock solution was subjected to sample preparation procedure and put through the flow cytometry for 30s. B. Histogram of particle count versus SSC form the same sample in A. "SSC-H^{-}" is the gate covering the particles with a fluorescence intensity less than 1. "SSC-H^{+}" is the gate that summrizes the total particle number outside "SSC-H^{-}".

Using the instrument settings for the fluorospheres as a starting point, the detection of baculovirus began with testing a baculovirus sample mixed with fluorospheres (Figure A-4). The fluorospheres were added to a 900 × diluted baculovirus stock to a final concentration of 2 % (v/v). After the mixture was put through the flow cytometry, the fluorescent beads appeared within the region of SSC: 50-100 and FL1: 2000-3600, which is consistent with the Flow-Set region in Figure A-4A.

In the lower SSC region, a group of particles occurred between FL1 values 10 to 100 (Fig. A-4A). This could be the potential baculovirus group. However, in the FL1 histogram (Fig. A-4B), there is a peak between the FL1 values of 1 to 10, which does not agree with the potential virus group in the 2-D scale. Further analysis based on the SSC histogram pointed out that over 94.6%

of the total particles in the plot exist near the x-axis. This result means that the majority of the detected particles had a very small SSC signal (less than 2), which hampered the overall resolution of the particles. Given that the same protocol was followed as described in Shen et al. (2002), the differences in instrument sensitivity or software resolving power might lead to the difference in data display.

Shen et al. (2002) reported an SSC scale ranging from 0.1 to 1000, while the current instrument plots the data at an SSC scale of 1 to 10000. The major viral group in Shen et al. (2002) appeared in the lower-than-10^0 SSC region, which exceeded the lower SSC limitaton with the BD Calibur Flow Cytoemter. Therefore, to properly resolve the baculoviruses, further instrument optimization is needed.

A.3.3.1 Improving resolution by higher amplifying SSC voltage

Based the analysis in the previous section, the same 900 × diluted virus sample was analyzed again with a new set of new voltages given below (Table A-2).

Table A-2 Instrument settings for virus detection.

Parameter	Value	Threshold
Flow rate	12 μL/min	
FSC	E00	n/a
SSC	390	n/a
FL1	480	52

While the SSC voltage increased, the side scatter signals of the particles were strengthened, resulting in an elevation of the particles' position in the y direction (SSC) (Fig. A-5). The group near the bottom axis moved upwards, revealing a denser particle region in the FL1 region of 0-50. However, quantification results still indicated roughly 90 % of the total particles remaining near the plot bottom, with SSC values lower than 2. It should be noted that the increase in SSC also elevated the position of

the Flow-Set. By further enhancement in the SSC voltage, the Flow-Set group was no longer well-resolved, as its position exceeded the maximum y-axis value.

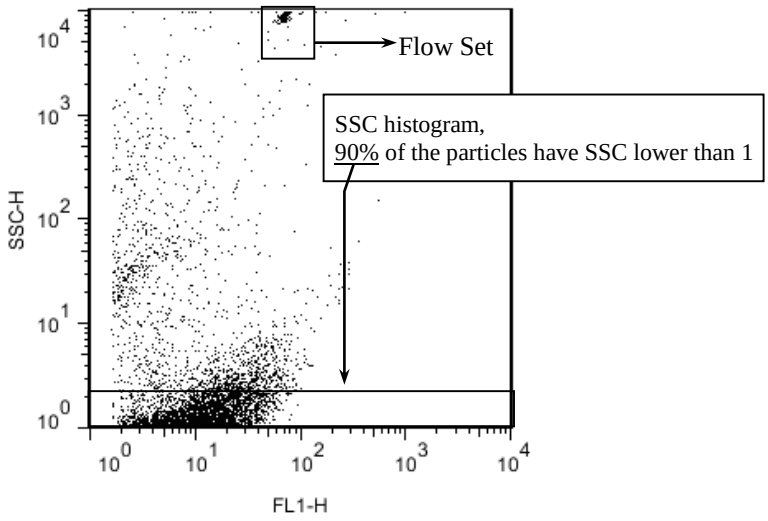

Figure A-5 2-D dot plot at SSC vs. FL1 scale of an aliquote of 900 X diluted baculovirus stock solution. The fluorospheres were mixted with the aliquote.

Figure A-6 shows a 2-D dot plot with SSC vs. FSC scale at instrument settings of SSC 660 and FL1 480 (Table A-3). Proper resolution of the major potential baculovirus group was finally obtained. A tail-shaped secondary virus group occurs in the FL1 region of 10 to 100, which corresponds to virus aggregation (Jorio, Tran, Meghrous, Bourget, & Kamen, 2006).

Table A-3 Instrument settings

Parameter	Value	Threshold
Flow rate	12 μL/min	
FSC	E00	n/a
SSC	660	n/a
FL1	480	52

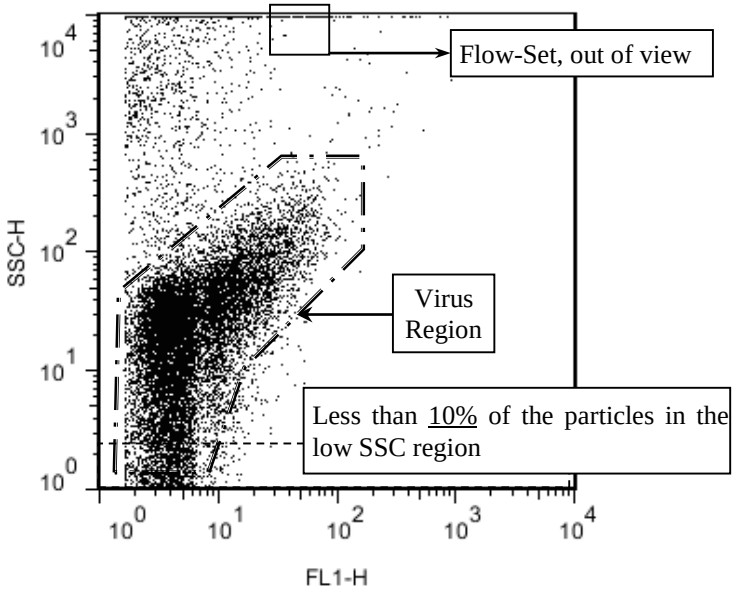

Figure A-6 2-D dot plot with SSC vs. FSC scale at instrument setting of SSC 660 and FL1 480 of the stock recombinant baculovirus.

A.3.4 Negative control

In addition to the identification of the major virus population, it is also necessary to consider the interference from the other species' particles that can potentially overlap with this preliminary virus region. An experiment was carried out to identify any background noises from reagents in the protocol. A blank solution was prepared as described by Shen et al. (2002), with the virus solution replaced by a PBS buffer.

As depicted in Figure A-7, the particles detected in the blank solution present little overlay over the major virus region in Figure A-6. By proper gating analysis, the particle count from the reagents can be removed from the true virus count.

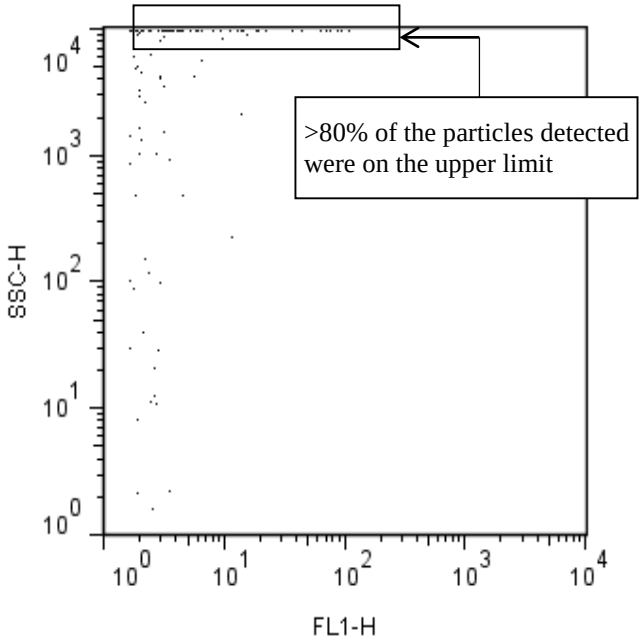

Figure A-7 2-D dot plot of a blank solution: a mixture of 20 μL of 2 % (v/v) paraformaldehyde, 10 μL of 10 % (v/v) Triton-X 100, 20 μL of 200 X diluted SYBR Green I, and 950 μL of PBS.

A.3.5 Dilution test

To further validate the established gating analysis for baculovirus (shown as the "virus region" in Figure A-6), a set of virus solutions was prepared with serial dilutions of 300× and 900×. Therefore, when subjected to flow cytometry testing, the counts of particles in the virus region should reflect the dilution factor applied to the virus solution, while the number of background noises should remain roughly constant. The results are summarized in Figure A-8. The gated count significantly declines when the dilution factor increased from 300 to 900, while the counts of the background noise region are relatively stable. The limited effect of dilution on background noises suggests that the noises are reflective of the constant fraction of the reagents. The ratio of the count in the 300 × diluted sample to the count in the 900× sample is 2.93, which agreed with the change in the dilution factors and demonstrates the reliability of the flow cytometry measurement.

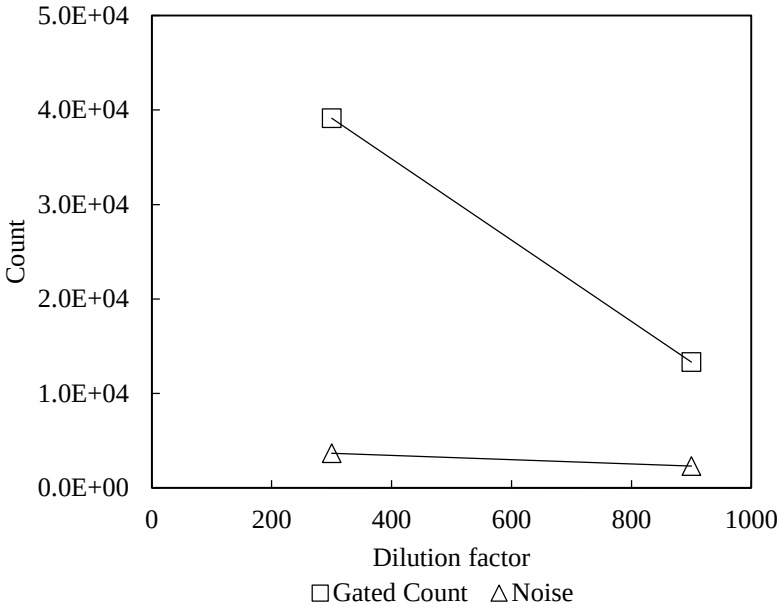

Figure A-8 Particle count of gated regions of diluted baculovirus samples. “Gated Count” refers to the particle number in the virus region and “Noise” refers to the total partcle number outside the virus region.

A.3.6 RT-PCR vs. Flow Cytometry Linearity Validation

A series of virus stock dilutions were prepared for validation test of flow cytometry acquired virus titres. RT-PCR method has been used for linearity examination of the flow cytometry data.

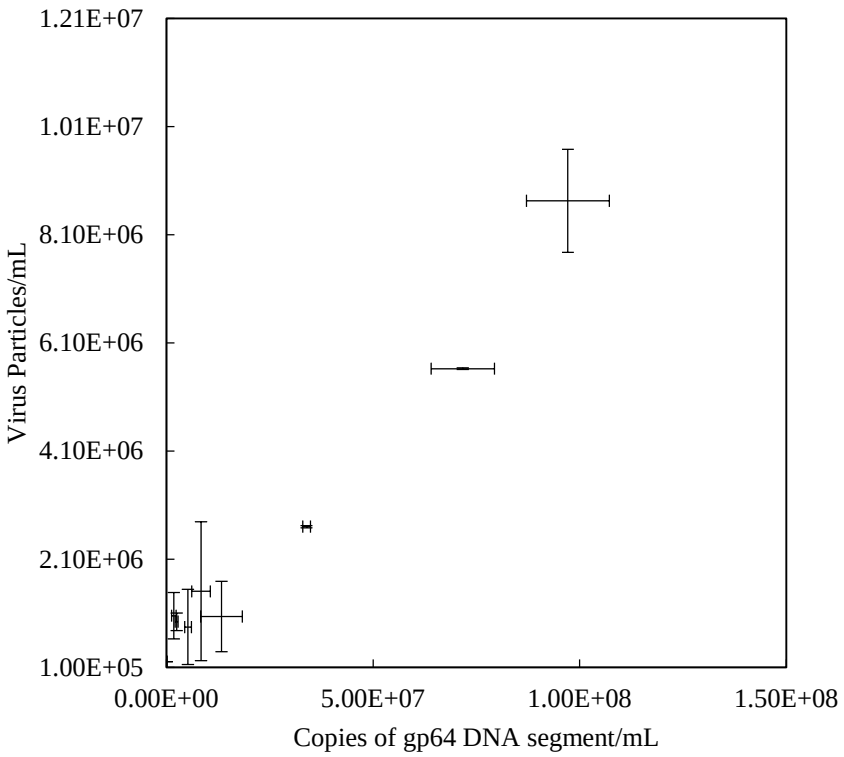

Figure A-9 Comparison analysis of RT-PCR and flow cytometry acquired data. (n=4 for RT-PCR; n=2 for flow cytometry)

Based on Figure A-9, consistent trend in virus titres was reflected both with flow cytometry and RT-PCR. The virus titres based on gp64 DNA segments are generally 12.6 times higher than those based on virus particles.

A.3.7 Virus production

An insect cell culture at a cell density of 2×10^6 cells/mL in Gibco® Sf-900™ III serum-free media was infected with a MOI of 1. Then 1 mL aliquot of the culture was taken for flow cytometry analysis at 24 hours, 48 hours, and 96 hours post infection (hpi). Based on the flow cytometry resuts, a virus production curve was plotted (Figure A-10). The baculovirus production kinetics agreed with published results (Shen et al., 2002).

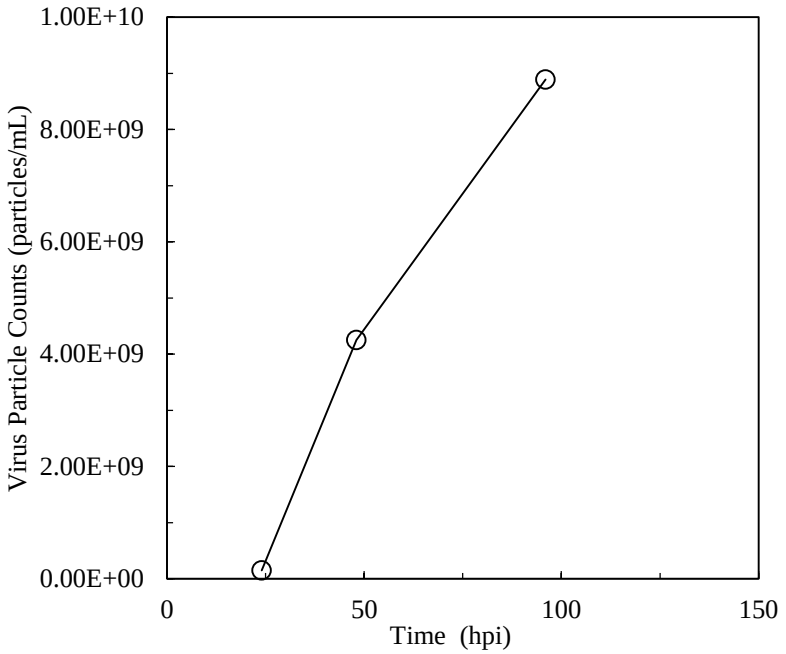

Figure A-10 Production kinetics of the recombinant baculoviru in Sf9 cells and Gibco® Sf-900™ III serum free media in a 30 mL shake-flask experiment.

A.3.8 Benzonase® Digestion Study

Benzonase® Nuclease (EMD Millipore, MA, USA) is a genetically engineered endonuclease. It degrades all forms of DNA and RNA. Since the flow cytometric detection of baculovirus depends on the use of SYBR Green I, which stains double stranded DNA, the existing free DNA in the virus solution can produce considerable amount of error in the results. To obtain reliable baculovirus titres, this study investigated the influence of Benzonase® on the baculovirus quantitation.

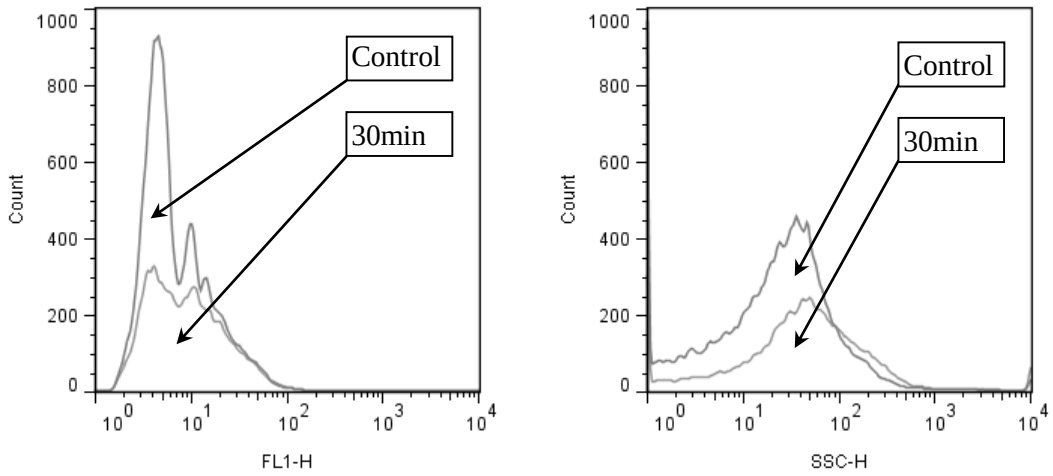

Figure A-11 The effect of Benzonase® treatment on flow cytomtric data acquisition. The left graph depicts the distribution change in FL1 scale and the right graph shows the distribution change in SSC scale.

The Benzonase® treatment procedures were carried out according to (Jorio et al., 2006). Three aliquots were taken from the original baculovirus stock. Two of the stock samples were treated with the Benzonase® procedures for 30 min and 60 min, respectively, while the other stock sample was the control. Then, all of these samples were subjected to flow cytometric assay to acquire virus titres. The histograms above (Figure A-11) show the distribution of particle numbers against their relative fluorescence intensities and their side scatters. In the green fluoresce histogram, two distinct populations are identified. In the results of the the control sample, between the fluorescence values 1 and 7, there is a major particle peak which contains 65.5% of the total particles. A secondary group, with 34.6% of the total particles, was identified between the fluorescence values 7 and 1000. For the sample treated with the Benzonase® for 30 min, two distinct populations appeared as well, which were located at the same fluorescence ranges as the untreated the samples. Meanwhile, the peak height of the lower fluorescence group was significantly reduced. The secondary population peak, which represents the population of higher fluorescence, was only slightly reduced, compared to the huge change in lower

fluorescence population. Extended nuclease treatment did not reduce the population further, as shown in Figure A-12.

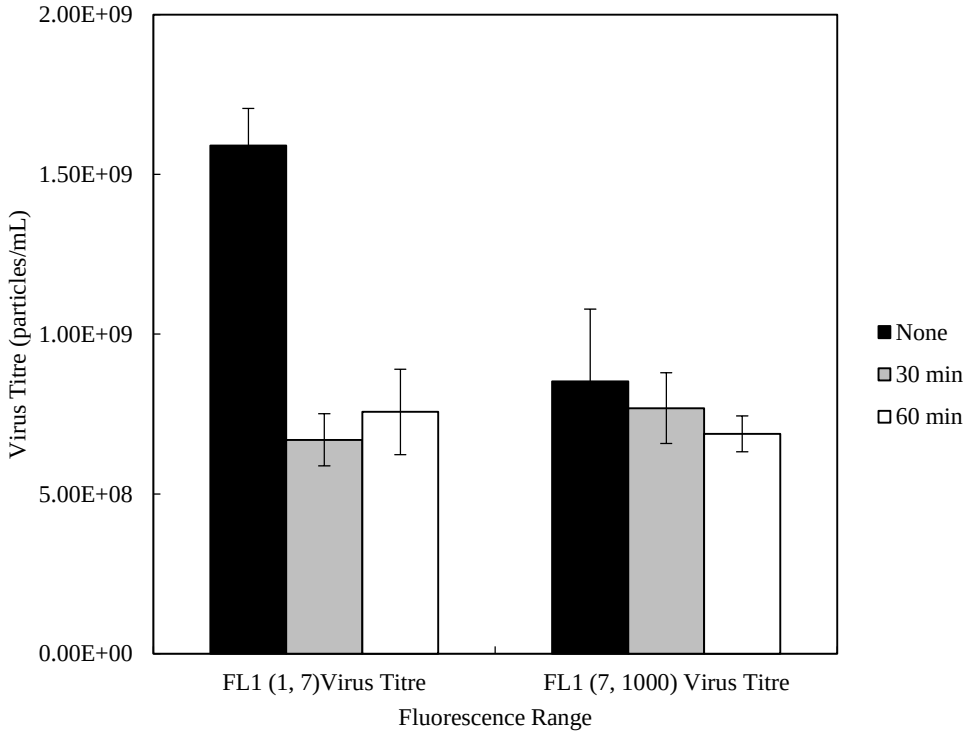

Figure A-12 Effect of Benzonase® treatment on stock virus samples for different incubation times in two fluorescnece regions.

The nuclease treatment decreased 41% of the total virus titre. The reduction in the lower fluorescence region is 58% while the higher fluorescence region lost 10% of the population. Jorio et al. suggested that the population with higher green fluorescence is virus aggregate, which are dense group of intact virus particles. Because Benzonase® only degrades double-stranded DNA, the virus count in the aggregation was not affected as the reagent cannot access to the encapsulated DNA within the virus. At the same time, the reduction of count in the lower fluorescence region was due to the digestion of free DNA by the nuclease. Meanwhile, the remaining population in the low fluorescence region was singular virus particles, as longer Benzonase® incubation had limited influence on these particles.

In the histogram of Side Scatter distribution, only a single population was found. In contrast to the fluorescent histogram, the SSC plot did not provide additional information on the nature of the two groups found in fluorescence graph. With 30 min Benzonase® treatment, the reduction of population with regard to SSC scale did not suggest any local trend but overall decline in the count.

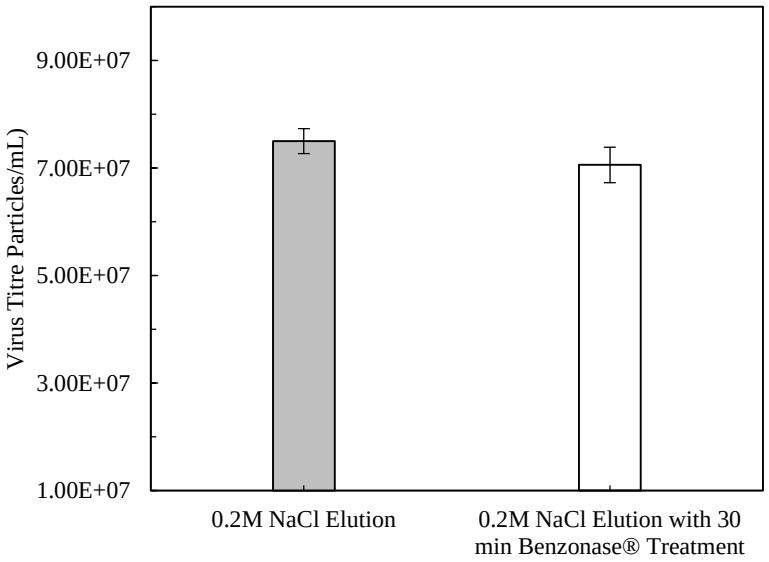

Figure A-13 Effect of Benzonase® treatment in eluted samples (n=2).

The effect of Benzonase® addition was also evaluated for eluted samples. An aliquot from the permeating flow, during a 0.2 M NaCl elution process, was treated according the reaction protocol and was prepared for flow cytometric assays together with an untreated aliquot, which was the control. The flow cytometry procedure was done at the same operating parameters as the virus stock samples.

The results indicated that the nuclease had minimal impact on the virus titre of the elution samples, as shown in Figure A-13. This finding suggested the low free double-stranded DNA content in the eluted samples, which did not cause significant overestimation to the titration, compared to the error in the quantitation of the stock virus samples. An explanation to this is the dsDNA's charge property. Double-stranded DNA is negatively charged and irreversible bound to anion exchangers at

baculovirus' pI, so the free DNA in the virus loading samples did not come to the permeate flow while the virus particles were being eluted. The consistent titres of the eluted sample before and after nuclease digestion also illustrate the potential to simultaneously remove genetic contaminants in a single process with the anion exchange chromatography.

This chapter pointed out that the Benzonase® treatment is essential to virus loading solution for reducing free-DNA-induced errors in further quantitation analysis using a flow cytometry. For all the existent results obtained in the past, an adjustment to the virus titres of positive control samples at a 40% reduction has been made to the works in this thesis.

A.4 Summary

By investigating the compatibility of the published protocol with the commercial flow cytometer, the appropriate operating parameters were identified: FSC: E00, SSC: 660 and FL1: 480. The dilution tests proved good linearity with this instrument. Negative control experiments further improved the accuracy of gating analysis for the baculovirus. The comparison analysis over a series of diluted samples using both RT-PCR and flow cytometry presented consistent correlation between the data from these two methods. The kinetics concluded from flow cytometric results during baculovirus production provided strong evidence that the results were reliable. And finally, the Benzonase® digestion study implied the DNA interference, and provided essential correction to flow cytometry data. Therefore, given all the adjustment in this appendix, the flow cytometry is therefore used for baculovirus quantitation.

Appendix B

Characterization of the hydrogel material's microstructure using scanning electron microscopy

To further investigate the physical hindrance occurred in baculovirus purification process using the current anion exchange membrane, the columns were disassembled and the membranes were subjected to SEM imaging.

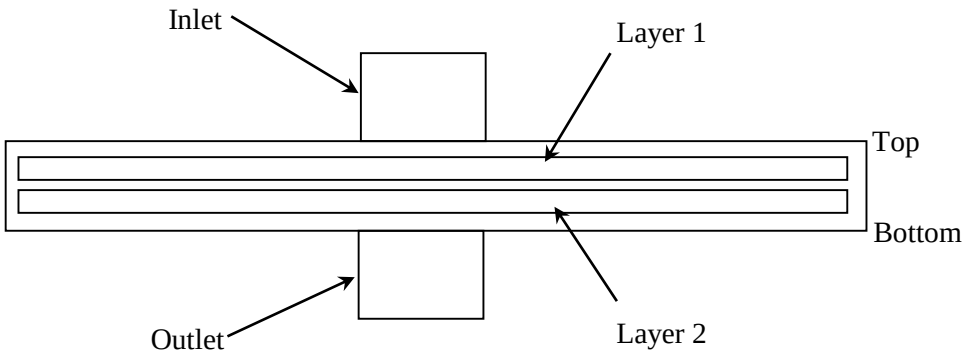

Figure B-1 Membrane column assembly.

As seen in B-1, the column contains two layers of membranes. Here, the upper side of the two layers is denoted as "top" while the other side is denoted as "bottom". Both of the two sides were scanned using SEM.

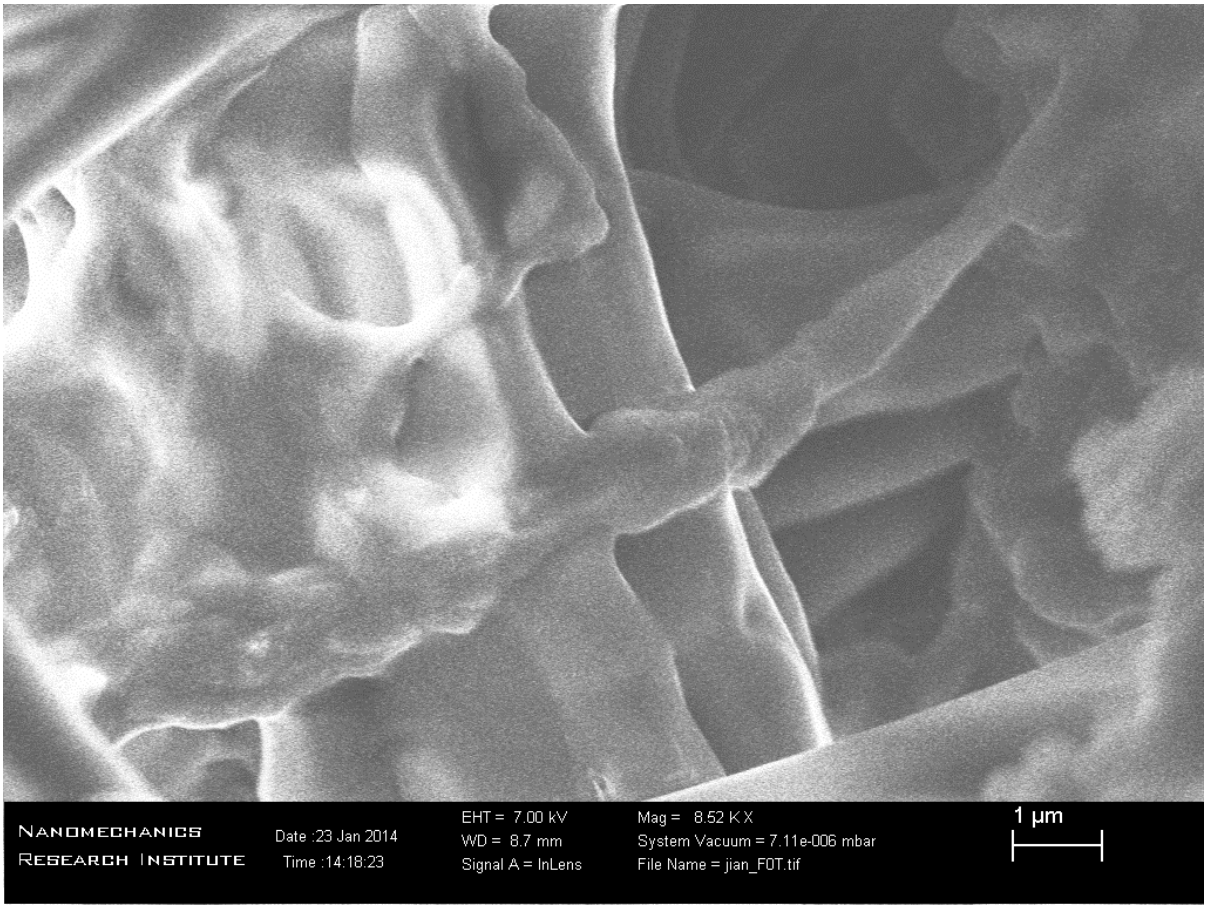

Figure B-2 SEM image of "top" side of a untreated membrane.

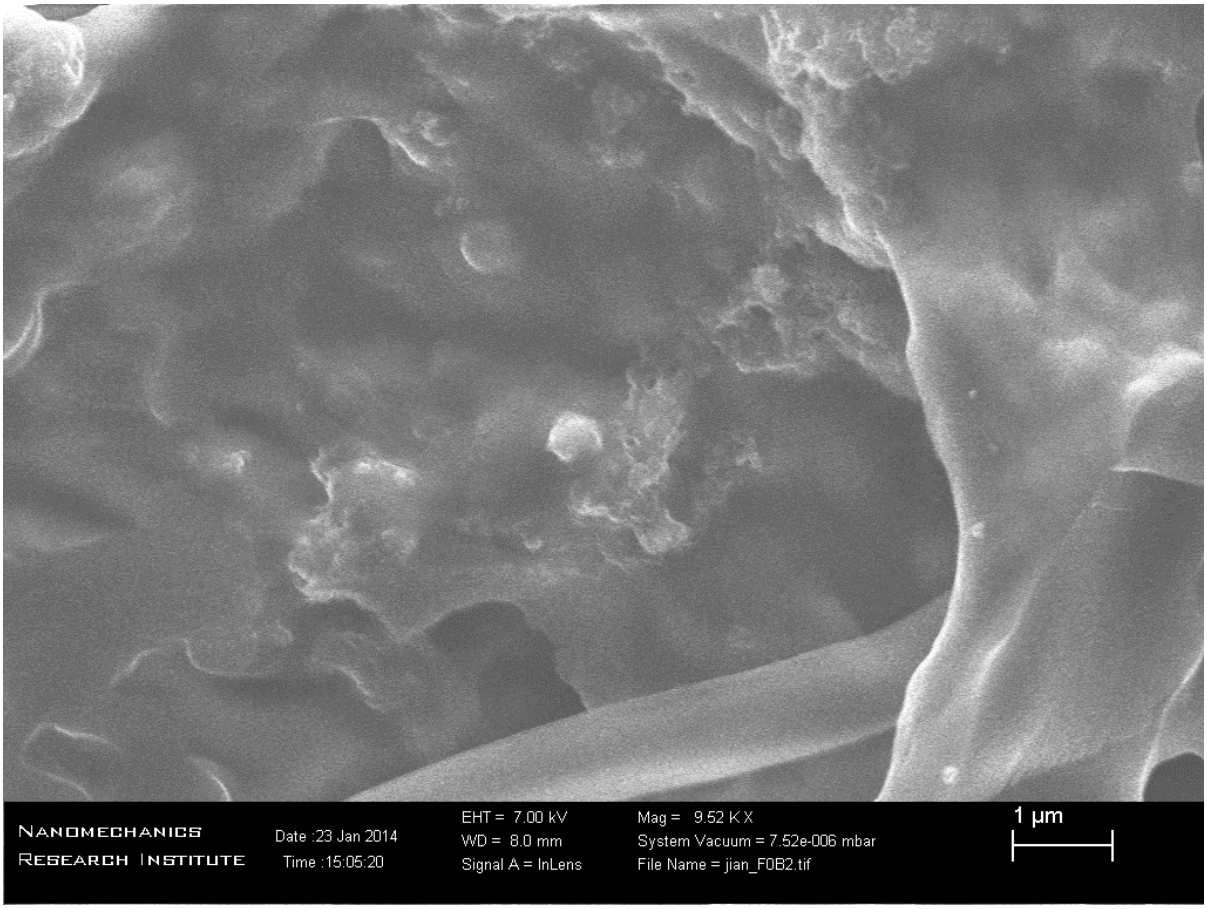

Figure B-3 SEM image of the "bottom" side of a untreated membrane.

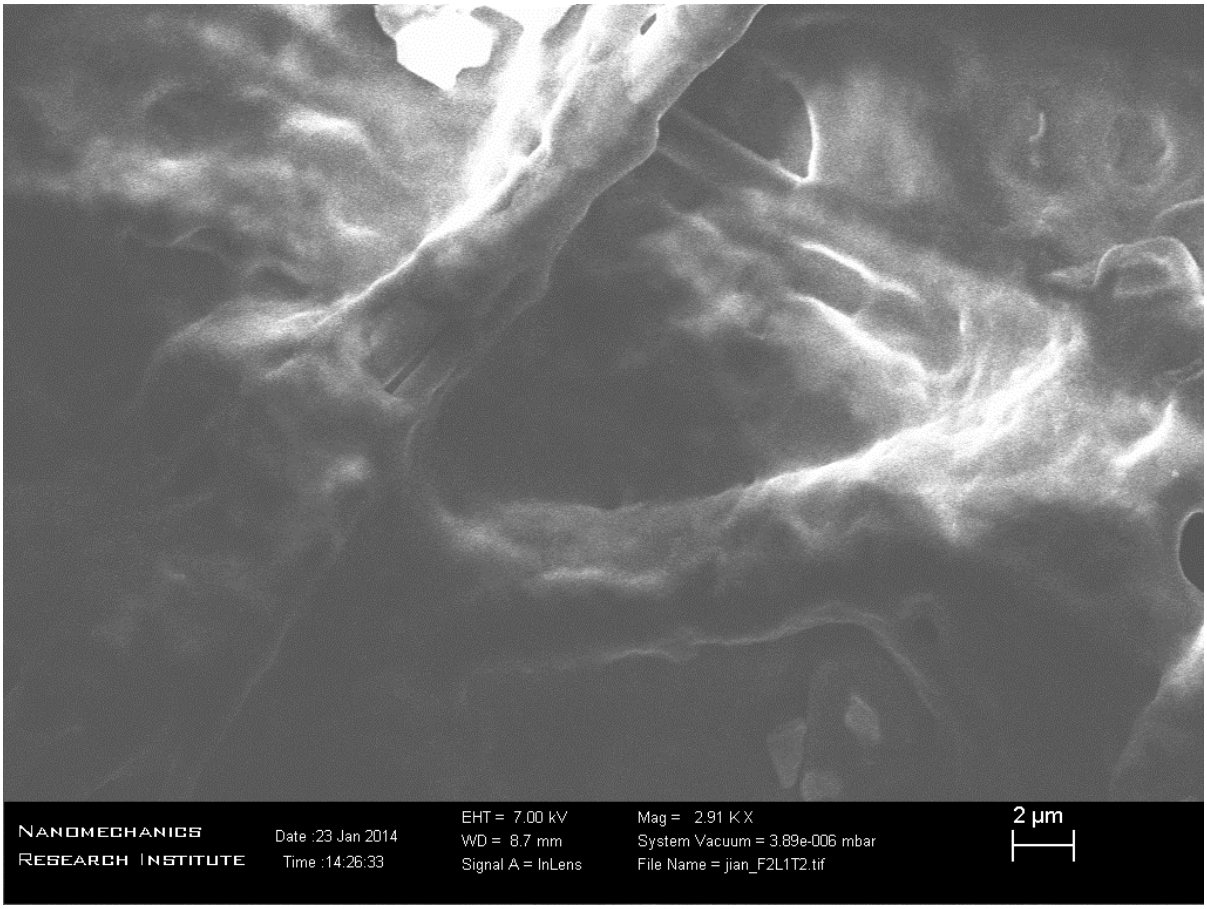

Figure B-4 SEM image of the "top" side of layer 1 from a membrane used in normal flow purifcation.

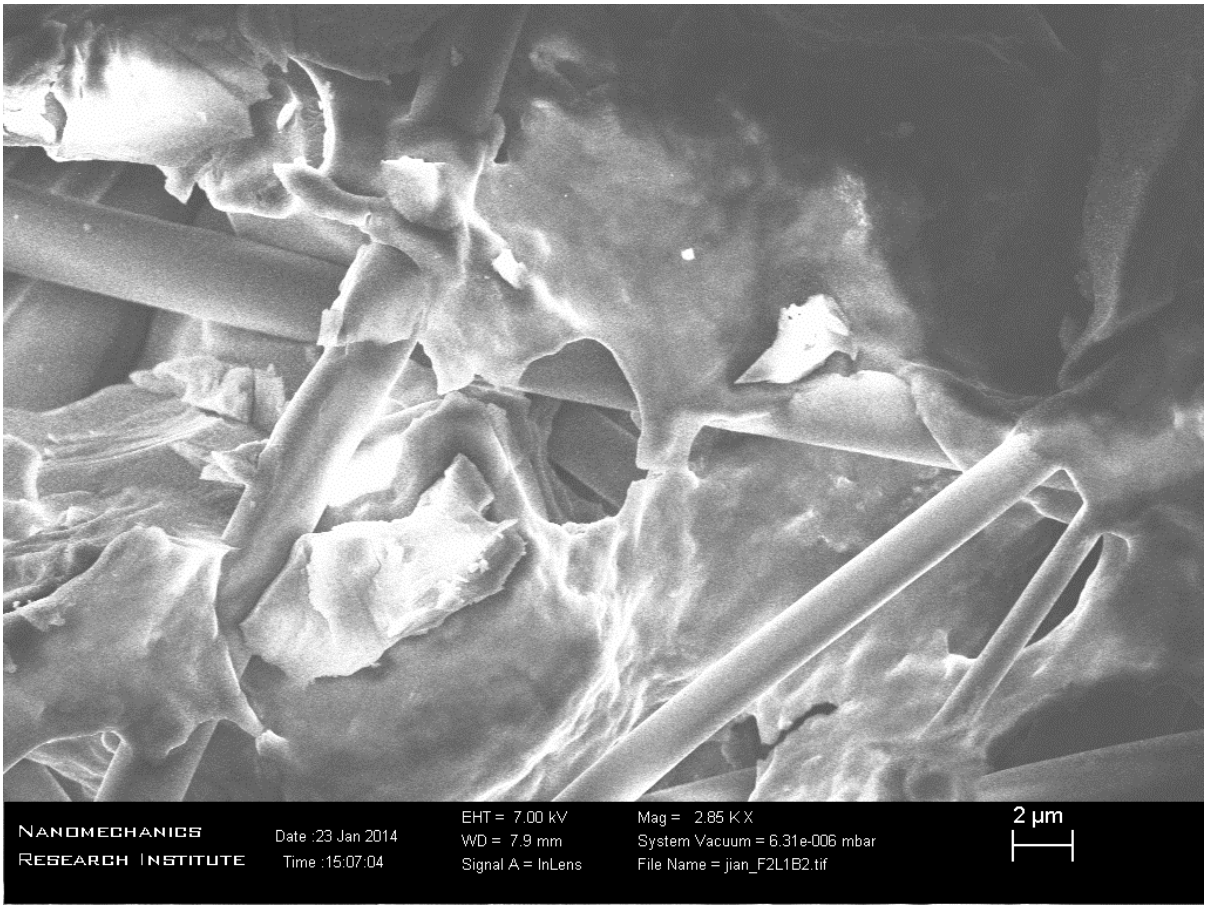

Figure B-5 SEM image of the "bottom" side of layer 1 from a membrane used in normal flow purifcation.

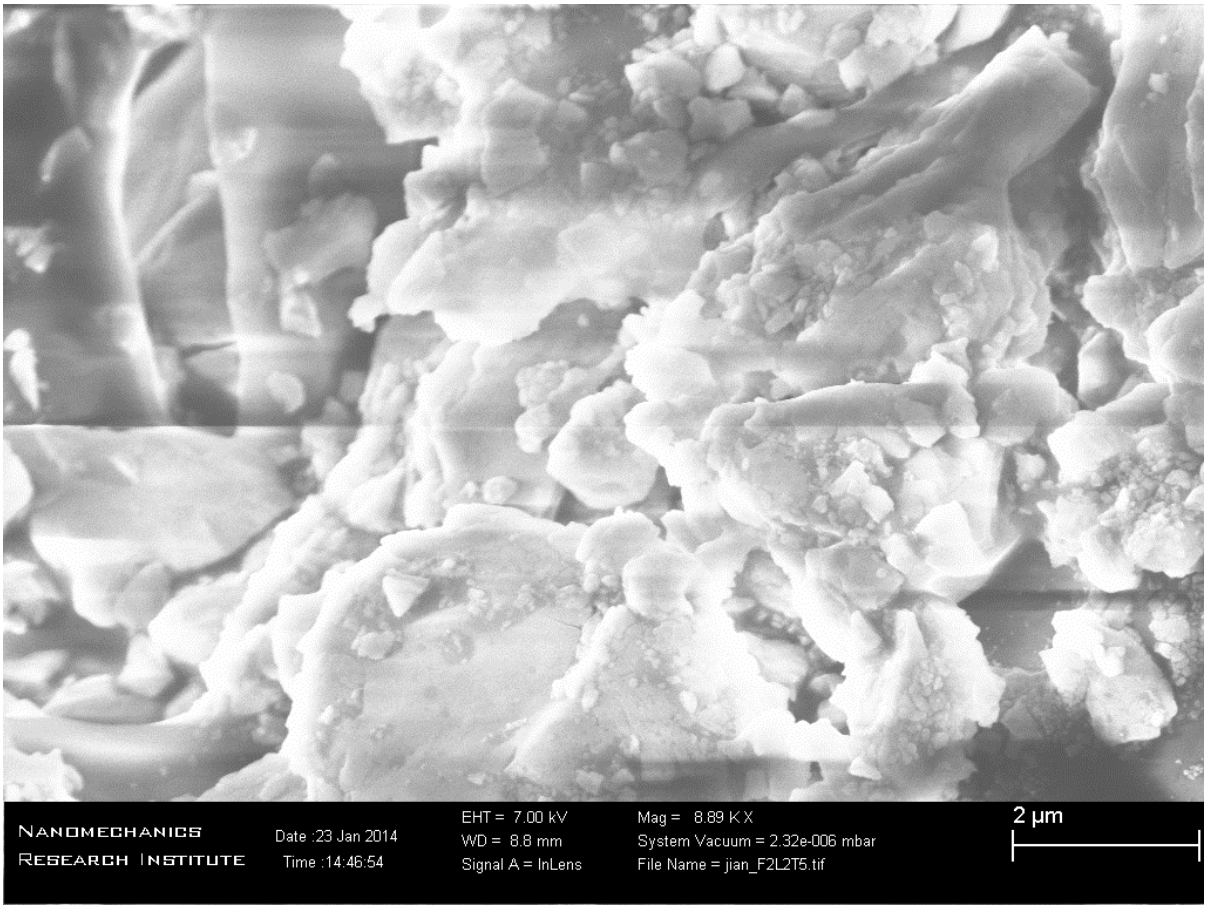

Figure B-6 SEM image of the "top" side of layer 2 from a membrane used in normal flow purifcation.

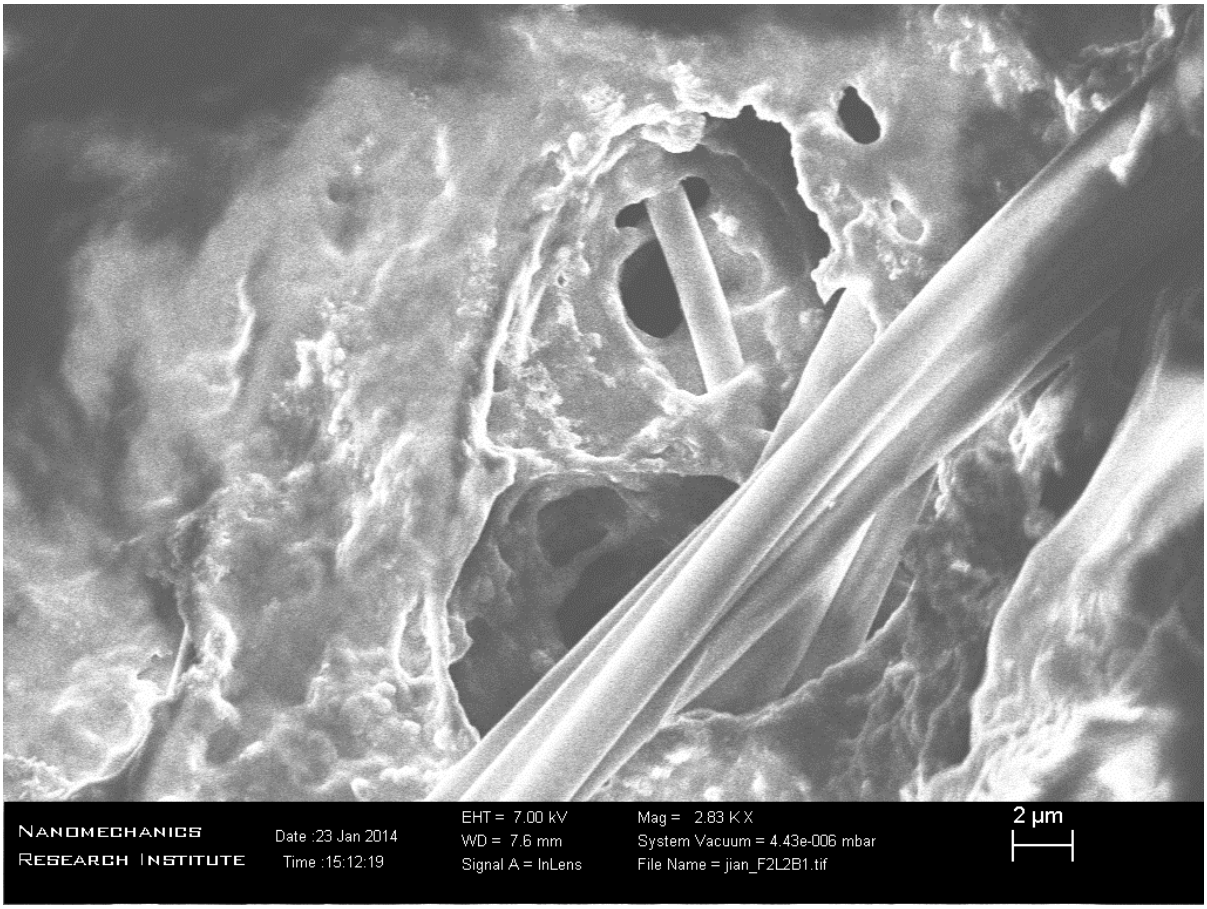

Figure B-7 SEM image of the "bottom" side of layer 2 from a membrane used in normal flow purifcation.

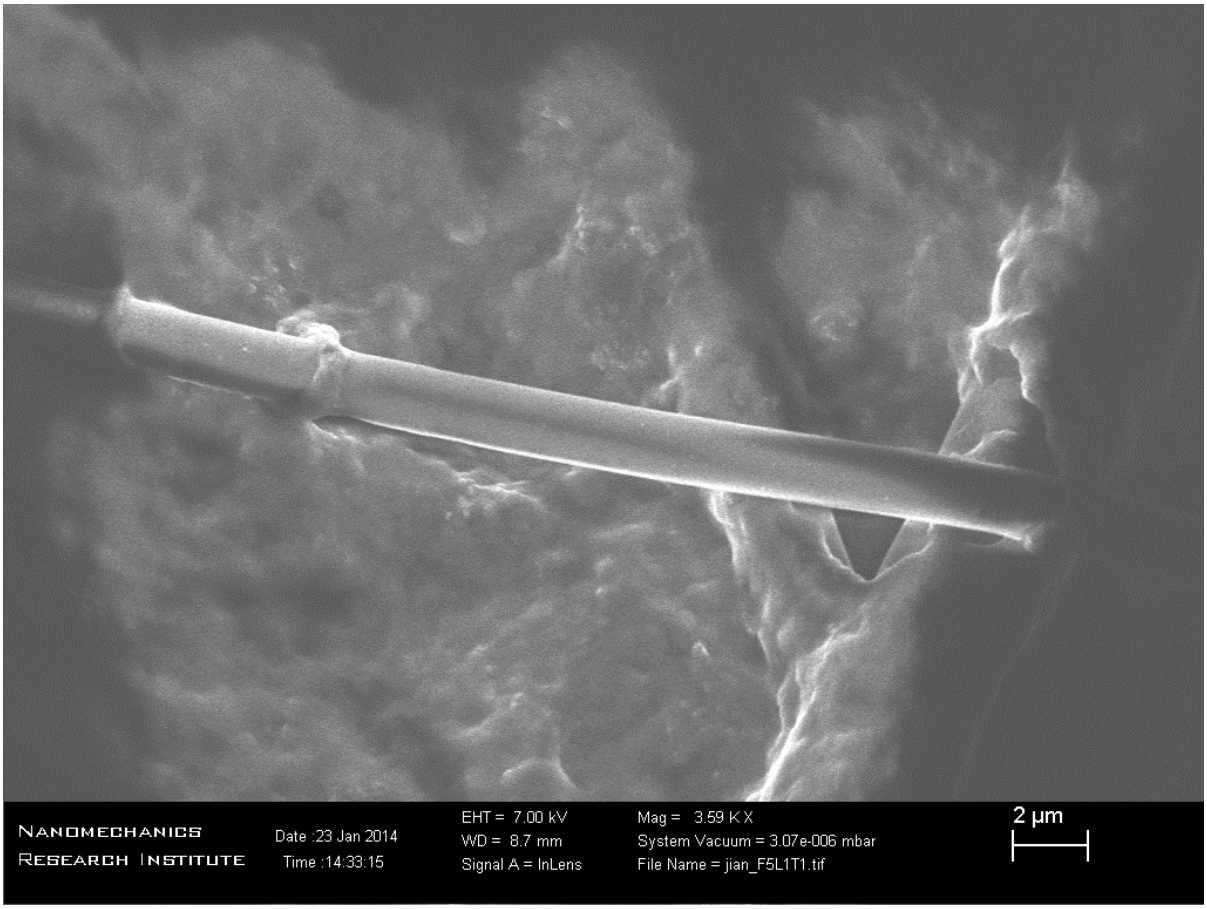

Figure B-8 SEM image of the "top" side of layer 1 from a membrane used in reverse flow purifcation.

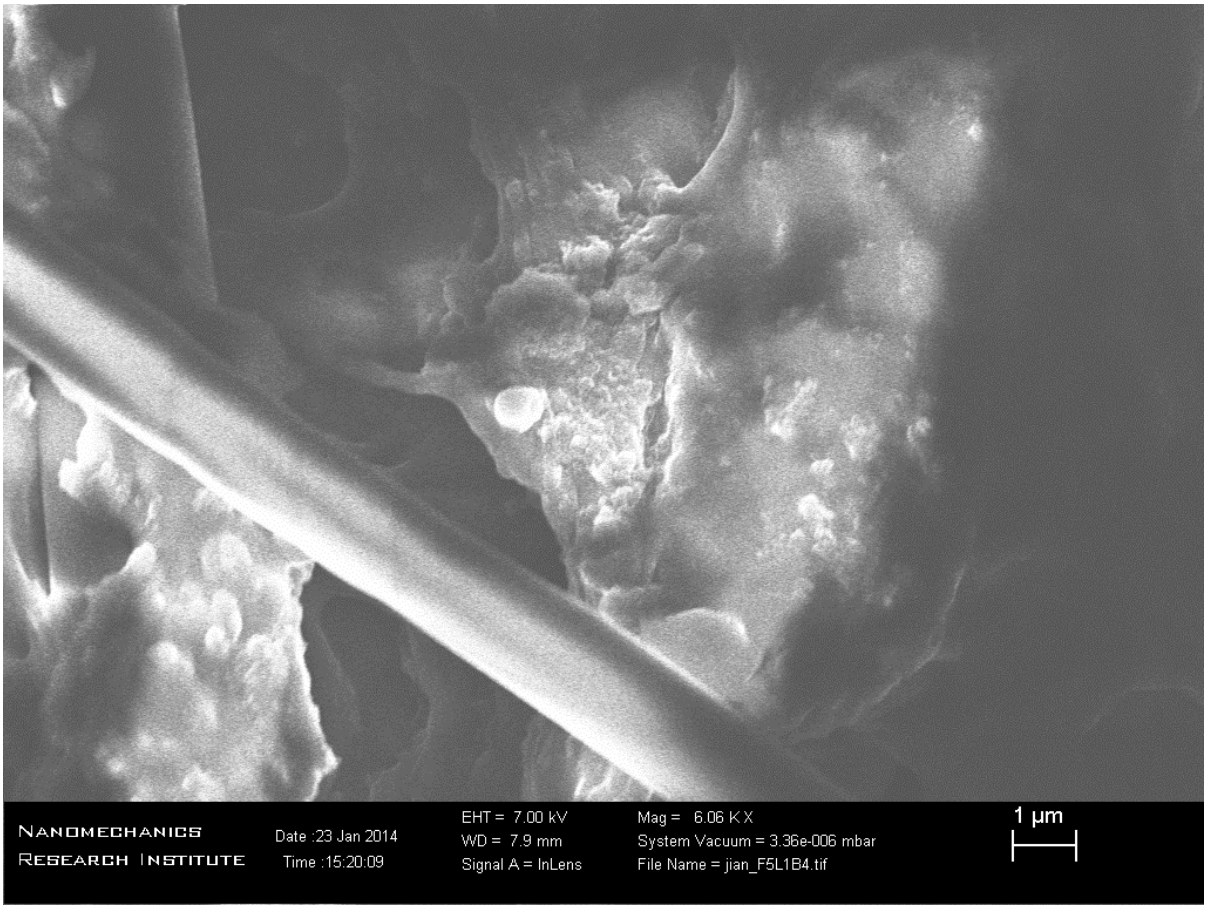

Figure B-9 SEM image of the "bottom" side of layer 1 from a membrane used in reverse flow purifcation.

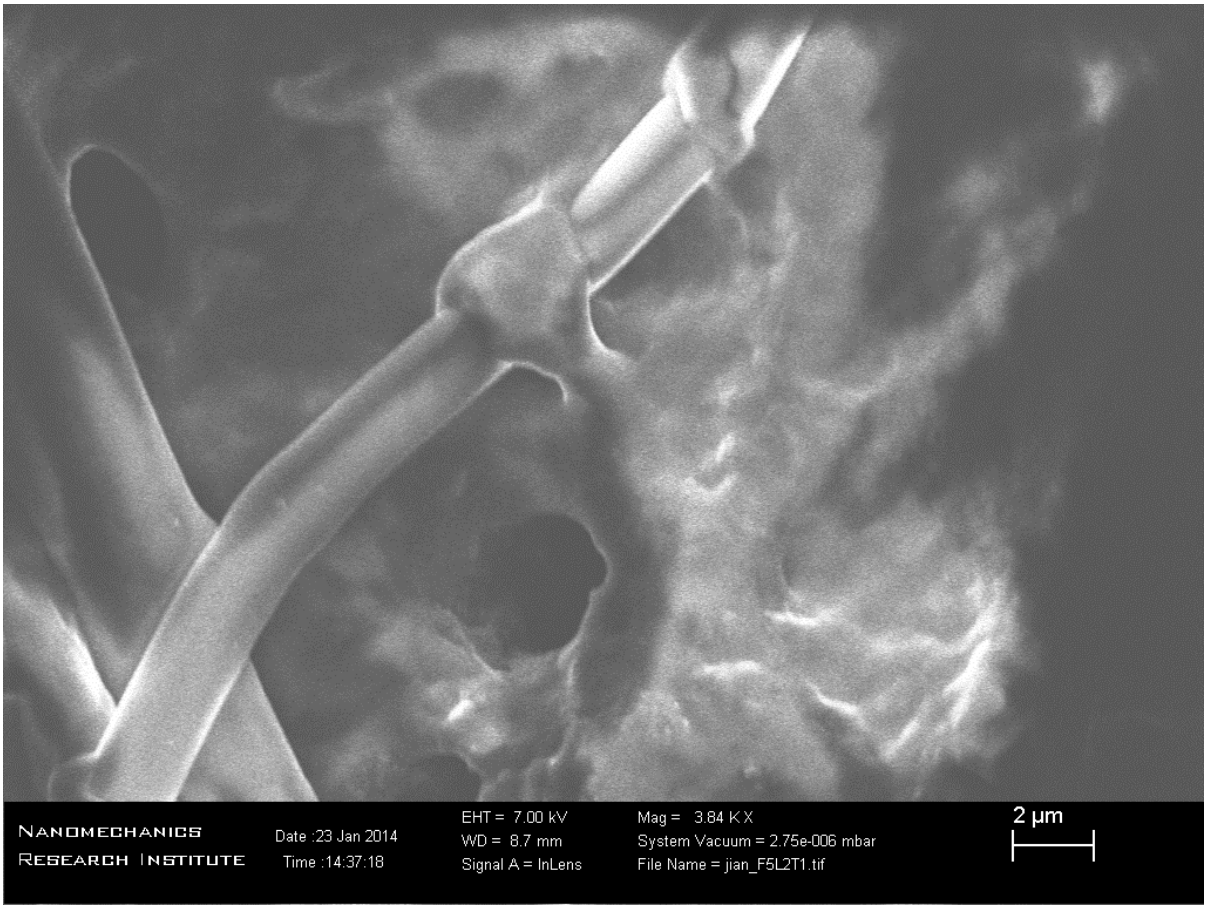

Figure B-10 SEM image of the "top" side of layer 2 from a membrane used in reverse flow purifcation.

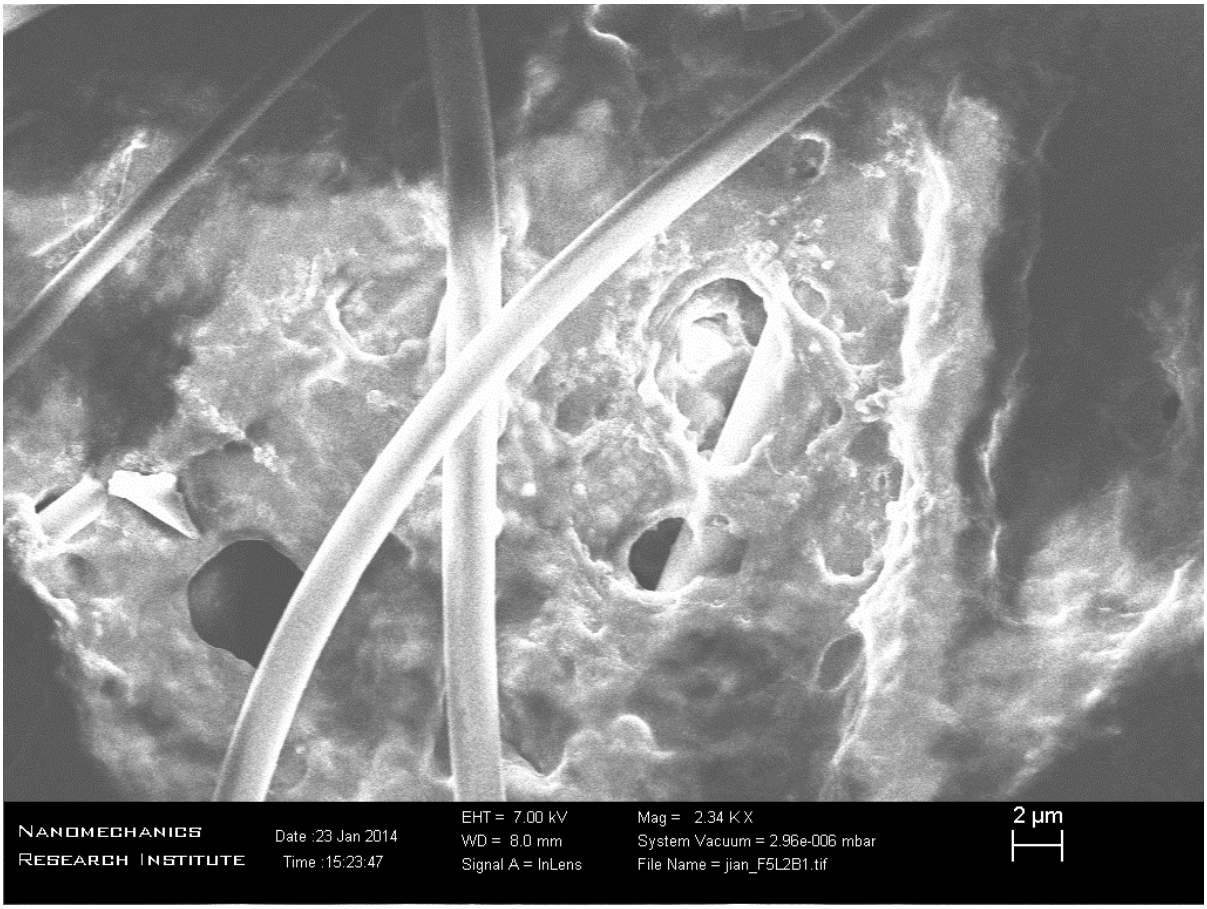

Figure B-11 SEM image of the “bottom” side of layer 2 from a membrane used in reverse flow purifcation.

Appendix C

Sample calculation for Micro BCA assay

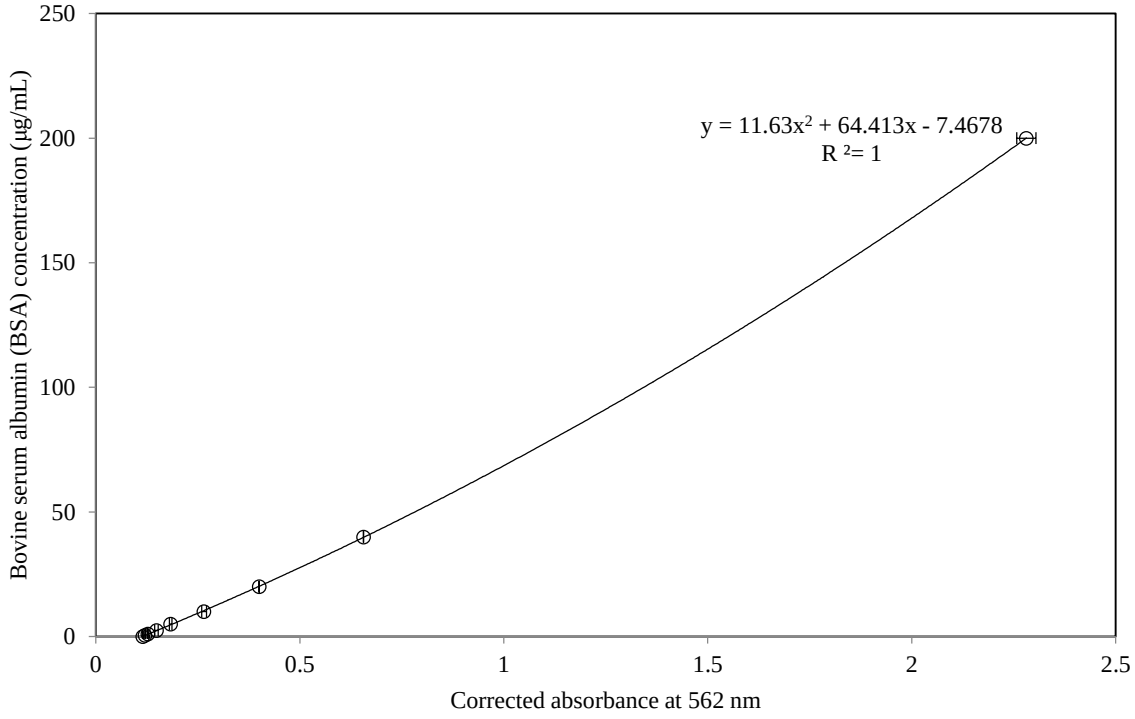

Figure C-1 Caliburation curve for absorbance at 562 nm. BSA samples over a linearge range from 2.5 – 200 µg/mL. the trendline shows a second order polynomial approximation to the date point. Error bars indicate standard error at n=2.

The sample calculation for total protein is based on a standard curve, generated by absorbance of serial dilutions of BSA samples. A second order polynomial approximation was used to evaluate the correlation between sample absorbance at 562 nm and its protein content.

The absorbance of samples collected in purification processes are converted to protein concentration using the polynomial equation, where y is the protein concentration and x is the corrected absorbance.0